

## Precambrian evolution of the Sirwa Window, Anti-Atlas Orogen, Morocco

R.J. Thomas<sup>a,\*</sup>, L.P. Chevallier<sup>a</sup>, P.G. Gresse<sup>a</sup>, R.E. Harmer<sup>b</sup>,  
B.M. Eglinton<sup>b</sup>, R.A. Armstrong<sup>c</sup>, C.H. de Beer<sup>a</sup>, J.E.J. Martini<sup>b</sup>,  
G.S. de Kock<sup>b</sup>, P.H. Macey<sup>d</sup>, B.A. Ingram<sup>b</sup>

<sup>a</sup> Council for Geoscience, P.O. Box 572, Bellville 7535, South Africa

<sup>b</sup> Council for Geoscience, P. Bag X112, Pretoria 0001, South Africa

<sup>c</sup> PRISE, Australian National University, Canberra, Australia

<sup>d</sup> Council for Geoscience, P.O. Box 775, Uppington 8800, South Africa

Received 14 June 2001; accepted 18 April 2002

### Abstract

We present the results of a field, geochemical and geochronological study of a  $\sim 5000$  km<sup>2</sup> area of the Sirwa Window of the Anti-Atlas Orogen of Morocco. The region includes the northern edge of the Palaeoproterozoic (Eburnean) West African Craton (Zenaga Complex) and the southern margin of the Neoproterozoic (Pan-African) Anti-Atlas Orogen. The Zenaga Complex comprises medium grade supracrustal schists and intrusive granitoid orthogneisses, three of which gave within-error U–Pb SHRIMP zircon dates of  $\sim 2035$  Ma. The Anti-Atlas Orogen contains a vast thickness of volcano-sedimentary rocks known collectively as the Anti-Atlas Supergroup. The oldest of these comprises three, probably coeval, sequences collectively known as the Bleida Group. The Bleida Group includes tectonic inliers of schists and orthogneisses which gave a SHRIMP date of  $743 \pm 14$  Ma; medium-grade ophiolitic rocks in the central part of the area (Khzama and Nqob fragments) and a low-grade clastic-chemical volcano-sedimentary sequence (Taghdout Subgroup) along the northern margin of the Zenaga Complex. These rocks are interpreted as representing island-arc, fore-arc basin ocean-floor, and rifted continental margin sequences, respectively. The rocks developed north of the West African Craton during Neoproterozoic subduction of oceanic crust and the development of an arc/fore-arc complex.

The Bleida Group is overlain by the thick flysch-like volcano-sedimentary rocks of the Sarhro Group which were deposited before 615 Ma, according to the SHRIMP dates obtained from the oldest granitic bodies intruding them. The presence of glaciogenic diamictite units suggests a possible depositional age of  $\sim 700$  Ma. It is thought that the Sarhro Group was deposited in the fore-arc basin which developed between the island arc and the cratonic continental margin to the south. A reversal of plate movement vectors during Sarhro Group times led to a change from turbidite to coarse clastic deltaic deposition. This culminated in closure of the fore-arc basin and collision of the island arc with the Craton margin, ophiolite emplacement and deformation of the Sarhro Group and older rocks during the Pan-African Orogeny,

\* Corresponding author. Tel.: +27-21-9484754; fax: +27-21-9488788

E-mail address: [bob@geobell.org.za](mailto:bob@geobell.org.za) (R.J. Thomas).

which is probably dated at  $\sim 660$  Ma, the SHRIMP age given by metamorphic overgrowths on zircons from the arc rocks.

The Pan-African collision event was associated with widespread late- to post-orogenic magmatism, including granitoids intruded at  $\sim 614$  Ma (Mzil Granite, Ida-ou-Iloun batholith) and a huge gabbro-diorite-granodiorite-granite I-type granitoid batholith at  $\sim 580$  Ma (Askaoun batholith). The granitoids are post-dated by the extensive post-orogenic volcano-sedimentary molasse sequences of the Ouarzazate Group and coeval polyphase granite plutons between 575 and 560 Ma. The Ouarzazate Group comprises immature, coarse clastic sedimentary rocks (conglomerates, arkoses, reworked volcanic rocks) acid to intermediate volcanoclastic rocks (lapilli and crystal tuffs, volcanic breccias, ignimbrites, etc.) and lavas (minor basalt, andesite and voluminous rhyolite). The volcanic component of this extensive succession was extruded from at least five separate interfingering volcanic centres, each with characteristic stratigraphies (designated subgroups), typically in fault-bound settings. The volcanic centres include calderas containing coeval high-level granites and quartz porphyry bodies, along with rhyolitic plugs, domes and dykes. Post-orogenic magmatism terminated with the emplacement of a number of potassic leucogranite bodies, one of which has been dated at  $\sim 560$  Ma. This plutonic phase is recorded in the Zenaga Complex by Rb–Sr mica ages of  $\sim 580$ –525 Ma.

The Ouarzazate Group is conformably to disconformably overlain by a typical foreland basin succession (Tata Group). A sporadically-developed basal conglomerate unit is overlain by two marine carbonate-clastic/shale cycles. Stable isotope studies have indicated that the base of the Cambrian Era ( $\sim 544$  Ma) lies near the top of the lowermost dolomitic unit.

The evolution of the Sirwa Window may serve as a model for the entire Anti-Atlas Orogen, recording a cycle of cratonic rifting and ocean basin formation ( $\sim 800$  Ma), subduction and island-arc formation ( $\sim 750$  Ma), flysch deposition and volcanism in a fore-arc basin. Plate movement reversal from extension to convergence in Sarhro Group times led to eventual arc-continent collision and ophiolite obduction ( $\sim 660$  Ma), late- to post-orogenic plutonism ( $\sim 615$ –580 Ma), post-orogenic extension, collapse, exhumation and molasse sedimentation, volcanism and plutonism (580–560 Ma) and marine foreland basin deposition (550 Ma to Palaeozoic).

© 2002 Elsevier Science B.V. All rights reserved.

*Keywords:* Morocco; Anti-Atlas; Sirwa; Pan-African; Eburnean

## 1. Introduction and geological setting of the Sirwa Window

The Sirwa Window is one of the largest and best-exposed of a number of Precambrian inliers ('Boutonnieres'), surrounded by Palaeozoic to younger rocks, which trend SW–NE behind (SE of) the High Atlas mountain range in Morocco (Fig. 1). The inliers form a lower, sub-parallel mountain chain known as the Anti-Atlas range. The Precambrian rocks within the Anti-Atlas belt comprise the northern margin of the West African Craton (Reguibat Shield), known to be broadly Palaeoproterozoic in age (Charlot, 1976), and the southern margin of a Neoproterozoic/lower Palaeozoic ('Pan-African') collision belt named here the 'Anti-Atlas Orogen'. The Anti-Atlas Orogen,

including the Sirwa Window has been the subject of a number of recent articles, including Fekkak et al. (1999), Hefferan et al. (2000), and Ennih and Liégeois (2001). The Anti-Atlas Orogen forms part of the Africa-wide network of Pan-African mobile belts associated with the amalgamation of Gondwana.

The erosional windows of Precambrian rocks are the result of large-scale updoming and cross-folding during the Hercynian or Alpine Orogenies. The Sirwa Window covers a total of some 6000 km<sup>2</sup> west of Ouarzazate (Fig. 1). It is an important inlier in that it contains good outcrops of the northern margin of the West African Craton (locally known as the Zenaga Complex), an almost complete succession of the Anti-Atlas Orogen (from the early rift–drift phase to the development

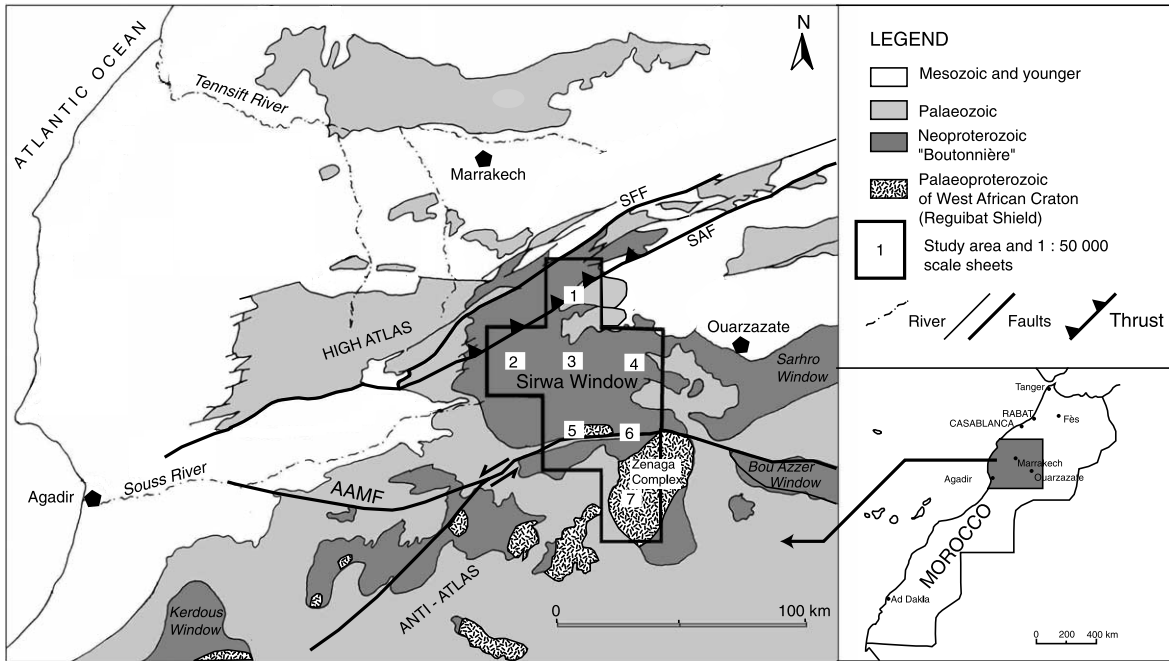


Fig. 1. Location of the Anti-Atlas Orogen in NW Africa.

of a post-orogenic foreland basin) along with ophiolitic and arc fragments in the suture between basement and mobile belt.

The present study was carried out under the auspices of DG-MEM (Direction de la Géologie et des Mines) geological mapping contracts with the Council for Geoscience (CGS), South Africa, between 1997 and 2000. In all, seven 1:50 000 scale sheets (Douar Çour, Assarag, Tachoukacht, Tamallakout, Sirwa, Taghdout and Açdif) were mapped, an area of nearly 5000 km<sup>2</sup>, or some 90% of the surface area of the Sirwa Window and encompassing all the main Precambrian lithostratigraphic subdivisions. The work included detailed geological mapping, petrographic, geochemical and geochronological studies, and the creation of a lithostratigraphic framework. The maps illustrating the distribution of the various units of the Sirwa Window are taken from a combined seven-sheet GIS dataset on *Arc Info*, and published by the Moroccan Geological Survey. In this paper, we detail the lithostratigraphy of the Sirwa Window, and present new isotope and geochemical data, in order to provide a complete geological history of the inlier.

## 2. Analytical techniques, data reduction and presentation

This article is structured so as to introduce analytical data at various points within the text. This section gives reference to the various standard techniques which were employed. Major and trace element geochemistry was completed on fused disks of over 250 samples by XRF, at the CGS laboratories in Pretoria. H<sub>2</sub>O<sup>+</sup> and H<sub>2</sub>O<sup>–</sup> were determined on a Leco RMC100 infra-red spectrometer, while S and CO<sub>2</sub> analyses were obtained from a Leco CS244 infra-red spectrometer. Rb–Sr and Sm–Nd isotopes were also performed at the CGS, Pretoria using conventional techniques as described in Harmer et al. (1998).

As the geochronology of the area had previously been restricted mainly to Rb–Sr dating, which proved difficult to interpret, and given the preponderance of acid plutonic and volcanic rocks throughout the stratigraphic record, the emplacement ages of which were very poorly constrained, we employed U–Pb–Th SHRIMP dating on zircons as the main dating technique. Sample

preparation and zircon extraction were undertaken by the CGS laboratories in Pretoria. Fully representative aliquots of the zircons were mounted in epoxy resin and analysed at the Research School of Earth Sciences, Australian National University, Canberra on either SHRIMP I or II, after zircon characterisation using transmitted and reflected light, back-scatter electron imaging and cathodoluminescence (CL) imaging. Spots for analysis were selected on the basis of the images obtained. Analysis on SHRIMP, decay constants, subsequent data reduction, etc. were performed following previously documented techniques (e.g. Compston et al., 1984; Williams and Claesson, 1987; Compston et al., 1992; Claoue-Long et al., 1995; Tera and Wasserburg, 1972; Steiger and Jäger, 1977). U/Pb in the unknowns was normalised to a  $^{206}\text{Pb}^*/^{238}\text{U}$  value of 0.1859, equivalent to an age of 1099.1 Ma (Paces and Miller, 1993), for As3. U and Th concentrations were determined relative to those measured in the SL 13 standard.

Dates and model ratios have been calculated using Geodate for Windows (Eglington and Harmer, 1999) and following Ludwig (1999). Uncertainties in the SHRIMP U–Pb results tables and plots are at 1 sigma, whilst weighted averages and interpreted dates are quoted with 95% confidence uncertainties.

Typical zircon morphologies are illustrated by CL images and the dates obtained are shown on concordia and Tera–Wasserburg plots. The full analytical SHRIMP dataset, along with over 250 whole-rock major and trace element geochemical analyses is available on the journal's website.

Model Rb–Sr and Sm–Nd dates and epsilon values are quoted at 95% confidence levels. Epsilon values were calculated at the time of formation of each unit, using the following values for the present-day composition of CHUR:  $^{147}\text{Sm}/^{144}\text{Nd} = 0.1967$  and  $^{143}\text{Nd}/^{144}\text{Nd} = 0.51264$ . Errors in epsilon values were calculated assuming no error in age.  $T_{\text{DM}}$  ages were calculated using the depleted mantle model of Michard et al. (1985) which has the present-day parameters:  $^{147}\text{Sm}/^{144}\text{Nd} = 0.222$  and  $^{143}\text{Nd}/^{144}\text{Nd} = 0.513114$ .

### 3. Lithostratigraphy

It is only possible in a single article to describe the broad Precambrian lithostratigraphy of the Sirwa Window with its 5000 km<sup>2</sup> of complex geology. Hence, although mapping was carried out at formation and member level in the volcano-sedimentary rocks, and we detailed the various phases of individual plutons, only the main lithostratigraphic groups and suites are described here. In total, 7 subgroups, 31 formations, 47 members and 34 plutonic units, within the nine or so major groupings, and a wide variety of minor intrusive rocks of various compositions, such as dyke swarms of various ages are described and formalised. In all, 132 new formal stratigraphic names had to be introduced for the Precambrian rocks, but in this paper these have been limited to the bare minimum. However, this detailed information, including many measured stratigraphic sections through all of the important units, is published in sheet explanations which accompany the 1:50 000 scale geological sheets (Thomas et al., 2000a,b, 2001; Gresse et al., 2000; Chevallier et al., 2001; De Beer et al., 2000; De Kock et al., 2000). Table 1 is a simplification of the lithostratigraphy of the Sirwa Window, while Fig. 2 is a simplified geological map of the study area. In the following account, the main features of the major rock groupings are described in stratigraphic order from oldest to youngest.

#### 3.1. Palaeoproterozoic Zenaga Complex

The Palaeoproterozoic Zenaga Complex represents the oldest metamorphic and igneous rocks in the Sirwa Window, occupying an elevated (~1500 m a.s.l.) flat plateau known as the Zenaga Plain (Fig. 3). Small tectonic slivers of the rocks are locally exposed north of the main outcrop in a major E–W dislocation ('Accident Majeur'), translated by Ennih and Liégeois (2001) to 'Anti-Atlas Major Fault' (AAMF). These authors suggested that the cratonic rocks extend northwards as far as the South Atlas Fault (SAF, Fig. 2). The Zenaga Complex forms the crystalline basement onto which some of the Neoproterozoic Pan-African successions were deposited. While the

Table 1  
Simplified lithostratigraphy of the Precambrian of the Sirwa Window

| Group (old nomenclature in brackets)   | Sub-group  | Number of formations   | Members |
|--|--|--|---------|
| <i>TATA</i> (Ad–Tw)  | –  | 4  | 3       |
| <i>Intrusive rocks</i> (PIII)  | Broadly syn-Ouarzazate Group intrusive rocks- <i>Toufghrane Suite</i> comprising a total of 13 named granites (many poly-phase) and various minor intrusive rhyolitic necks, plugs and dykes                               |  |         |
| <i>Ouarzazate</i> (PIII)   | <i>Achkoukchi Complex</i>  | 1  | 3       |
|  | <i>Bouljama</i>  | 6  | 18      |
|  | <i>Tafrant</i>   | 3  | 3       |
|  | <i>Tiouin</i>  | 4  | 11      |
|  | <i>Aghbar Formation</i>  | –  | –       |
| <i>Intrusive rocks</i> (PII <sup>3</sup> )   | Late syn to post-tectonic plutonic igneous rocks ( <i>Assarag Suite</i> ), comprising various named granitoids, diorites, gabbros, forming two extensive batholiths ( <i>Askaoun</i> and <i>Ida-ou-Ilouin batholiths</i> ) |  |         |
| <i>Bou Salda Formation</i> (with 4 members), <i>Tadmant</i> and <i>Tamrivine Rhyolites</i> (PII <sup>3</sup> -PIII)  |  |  |         |
| <i>Sarhro</i> (PII <sup>3</sup> )  | –  | 7  | 7       |
| <i>Ifzwane Suite dolerites</i> (PII <sup>3</sup> )   |  |  |         |
| <i>Bleïda</i> (PII <sup>1–2</sup> )  | <i>Taghdout</i><br><i>Khzama</i>   | 3  | 2       |
|  |  | 5 named units <i>Tasriwine</i> and <i>Nqob Ophiolites</i> , <i>Tachoukacht Schist</i> , <i>Iriri Migmatite</i> and the <i>Ourika Complex</i> |         |
| Basement <i>Zenaga Complex</i> (PI) comprising older schists and 5 intrusive units ( <i>Tamazzarra</i> , <i>Azguemerzi</i> , <i>Tikhsa Granites</i> , <i>Assourg Tonalite</i> , <i>Timzicht mafic/ultramafic Suite</i> ) |  |  |         |

Previous chronostratigraphic nomenclature of PI, PII...etc. for the Precambrian is given in brackets, with Ad–Tw = Eocambrian Adoudonien and Taliwininen (e.g. after [Serv. Geol. Maroc., 1990](#)).

complex is poorly exposed and typified by low, flat-lying outcrops on the plain itself, notable basement highs occur (e.g. the Kourkda high), preserved in the marginal escarpment. The Zenaga Complex rocks are deeply altered and ferruginised as a result of the later volcanic rocks which passed through and buried them during Neoproterozoic times. The complex can be subdivided into an older sequence of supracrustal rocks and the orthogneisses which intrude them.

### 3.1.1. Supracrustal rocks—Zenaga schists

The oldest rocks are medium to high grade schists, gneisses and migmatites. The most typical

lithology comprises grey, well foliated, and in places banded, *semi-pelitic gneisses*. The layering is in places complexly deformed by tight to isoclinal, small-scale ductile folds, with variable plunges. Evidence of partial melting is common, with deformed leucosomes of several generations apparent. The gneisses are composed of quartz, K-feldspar, plagioclase, biotite and muscovite ± garnet ± sillimanite, typical amphibolite facies parageneses. In many outcrops, these gneisses contain pods and lenses of light greyish-green, mottled, fine- to medium-grained, granular, foliated *calc-silicate rocks* ranging up to a few metres in size and typically zoned, with garnet-rich cores.

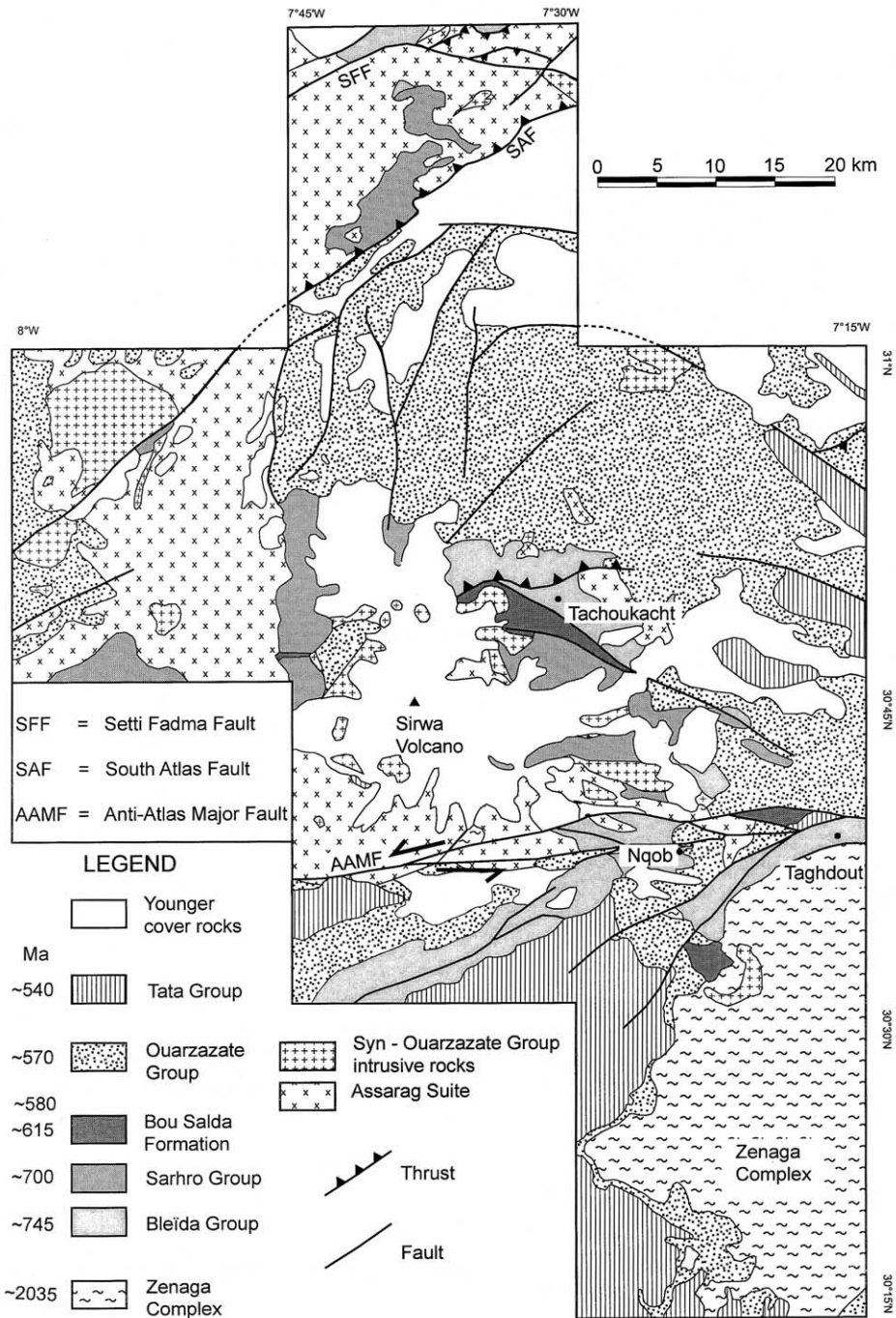


Fig. 2. Simplified geological map of the Sirwa Window.

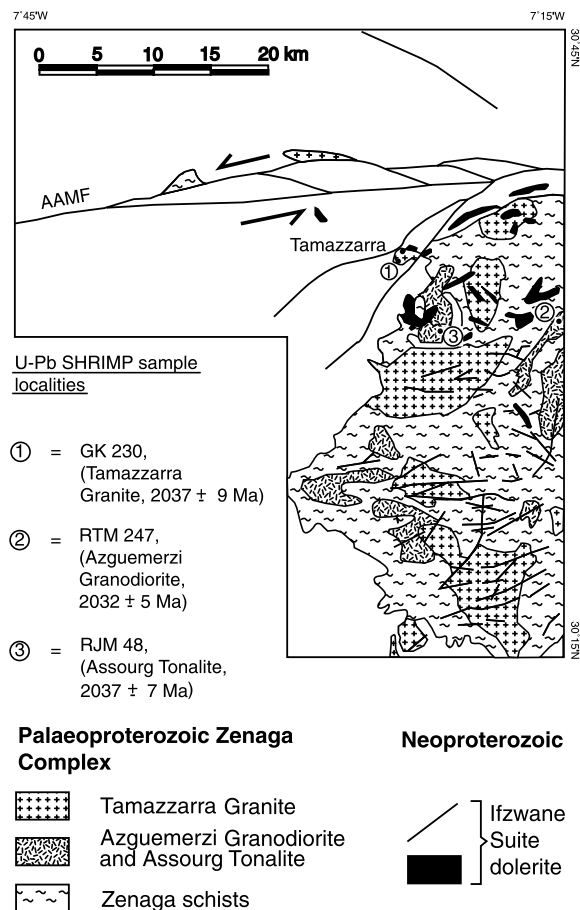


Fig. 3. Geological map of the Zenaga Complex, Sirwa Window.

Typical samples are composed of quartz, calcic plagioclase, garnet, carbonate, accessory apatite, opaques and zircon, with secondary epidote and muscovite.

The semi-pelitic gneisses are locally interleaved with fine-grained granoblastic, grey *psammitic gneisses*, made up of ~40% quartz, ~50% plagioclase and biotite ± muscovite. *Biotite-rich schists* are also common, usually forming pods and layers up to a few metres in thickness and displaying small-scale chevron-type folds. These commonly contain fibrous talc but little or no feldspar, indicating an ultramafic composition. *Quartz–muscovite ± chlorite schists* with over 60% quartz are a minor component of the Zenaga

schists, as are rare lenses of *quartzite* and impure *marble*.

The older gneiss sequence is interpreted as representing a package of paragneisses of metasedimentary origin. In addition, small (metres to tens of metres) pods and lenses of layered *amphibolite* are locally present within the Zenaga gneisses. These are typified by hornblende ± plagioclase ± biotite ± quartz assemblages, typical of amphibolite facies basic igneous rocks. These rocks probably represent meta-basic volcanic or intrusive rocks within the predominantly metasedimentary pile.

### 3.1.2. Intrusive orthogneisses

The Zenaga schists are intruded by four major plutonic igneous units (Fig. 3). The *Azguemerzi Granodiorite*, which forms up to 20% of the exposed area of the complex, is a grey, coarse-grained feldspar-megacrystic granitic augen-gneiss, forming a number of thick sheet-like bodies that intruded sub-parallel to the foliation in the Zenaga schists. It is characterised by quartz, K-spar and oligoclase (both as augen up to 4 cm in length and in the groundmass), biotite (partly altered to chlorite) ± hornblende ± muscovite ± garnet with accessory zircon, apatite and opaques. The possibly related *Assourg Tonalite* is a dark grey, coarse-grained mesocratic tonalitic orthogneiss which crops out at a number of localities in close proximity to the Azguemerzi Granite. The Tonalite is strongly foliated, with margins and fabric parallel to that of the country-rock Zenaga gneisses. In some places it is weakly megacrystic, with greenish plagioclase porphyroblasts up to 1 cm in size. Relationships with the other Zenaga orthogneisses are unclear, although in some places it shows increasing feldspar megacryst content and appears to be gradational with the Azguemerzi Granodiorite. The Assourg Tonalite tends to be highly altered, typically consisting of quartz, sericitised plagioclase, olive biotite, ± hornblende ± garnet. In some samples, the mafic minerals are completely pseudomorphed by chlorite, opaque mineral and epidote. The texture is foliated, reticulate and locally cataclastic with polycrystalline quartz augen and ribbons of fine-grained recrystallised quartz.

The *Timzicht mafic/ultramafic Suite* is a minor group of intrusive rocks, forming a few irregular pods and lenses, typically a few hundreds of metres in length, and cannot be shown on Fig. 3. The largest bodies, elongated along the strike of the country rock gneisses, are made up of coarse-grained diorite, strongly foliated at their margins, but with relatively undeformed cores. In one area, gabbroic and pyroxenitic varieties occur in podiform bodies oriented SW–NE, parallel to the local regional metamorphic fabric. The ultramafic *mica pyroxenites* are coarse-grained (2–6 mm grain size), poorly foliated, very dark grey to black rocks, made up of < 5% interstitial calcic plagioclase, 70% variably uraltised clinopyroxene, ~ 10% primary foxy-brown biotite, up to 5% opaque minerals and as much as 20% late phlogopite which forms large interstitial flakes with pyroxene and biotite inclusions. Fibrous mats of weakly-coloured amphibole may represent pseudomorphs after primary orthopyroxene. The composition grades through *gabbroic* rocks with increasing feldspar content to dark-grey, coarse-grained, foliated *diorites* and *quartz diorites*.

The youngest of the Zenaga granites (it demonstrably cuts the Azguemerzi Granodiorite), the extensive (~ 20% by area of the complex) *Tamazzarra Granite* is a pale grey to pink, well-foliated, muscovite leucogranite with a remarkably consistent mineralogy of quartz, sericitised perthitic K-spar, plagioclase, primary and secondary muscovite, along with traces of accessory opaque mineral, apatite, zircon and secondary carbonate. The granite is ubiquitously associated with coarse-grained, poorly- to unfoliated-tourmaline pegmatite, forming sheets, dykes and irregular masses on all scales, some of which have been exploited for mica, beryl and feldspar. The similar *Tiksha Granite* crops out in the east of the Zenaga Complex.

### 3.1.3. Geochemistry of the Zenaga Complex

Only a few analyses were made of the older Zenaga schists (De Kock et al., 2000; Thomas et al., 2001), but analyses of the various intrusive orthogneisses are plotted on the total alkalis—

SiO<sub>2</sub> diagram (TAS—as utilised for the classification of volcanic rocks: after Le Maitre et al., 1989) in Fig. 4a and on a MgO–FeO–Alkalis (FMA) diagram in Fig. 4b. These diagrams indicate that the intrusives are sub-alkaline in character with a trend on the FMA diagram typical of calc-alkaline series as defined by Irvine and Barager (1971). The Tamazzarra and Tiksha Granites are clearly granites *sensu stricto* whereas the Azguemerzi and Assourg bodies are granodioritic/tonalitic and the Timzicht gabbroic to dioritic.

Alumina saturation indices (ASI = molar Al<sub>2</sub>O<sub>3</sub>/[Na<sub>2</sub>O + K<sub>2</sub>O + CaO]) are significantly above unity for all the granitoids indicating that these granitoids are peraluminous. While peraluminous character can result from alkali loss during alteration, the recognition of primary muscovite in the Azguemerzi and Tamazzarra bodies suggests that this is a primary magmatic feature. There is a coherent trend between SiO<sub>2</sub> and alkalis which also argues that the elevated ASI values are not an artefact of alteration.

The Assourg and Azguemerzi analyses have overlapping ranges of SiO<sub>2</sub> contents, the Assourg being more silica-rich. The low-SiO<sub>2</sub> Azguemerzi Granodiorite samples have higher Fe<sub>2</sub>O<sub>3</sub>, MgO and CaO contents but lower Na<sub>2</sub>O than the Assourg Tonalite samples. This is not consistent with the Assourg Tonalite being a feldspar megacryst-poor fraction of the Azguemerzi Granodiorite, so despite the age correlation and field association between the two units, the geochemistry does not wholly support a direct evolutionary relationship. The high degree of variability of the concentration of trace elements in the high-SiO<sub>2</sub> Tamazzarra Granite, particularly the levels of Nb and Zr, is noteworthy. Contents of Nb are generally low in these intrusives—mostly 6–10 ppm—whereas Zr varies widely from 12 to over 200 ppm.

### 3.1.4. Geochronology of the Zenaga Complex

The zircons in the 15 dated samples from the Sirwa Window have quite different characteristics, the main points of which are given in Table 2. Three intrusive granitoid units of the Zenaga Complex were dated (*Tamazzarra Granite*, *Assourg Tonalite* and *Azguemerzi Granodiorite*). CL

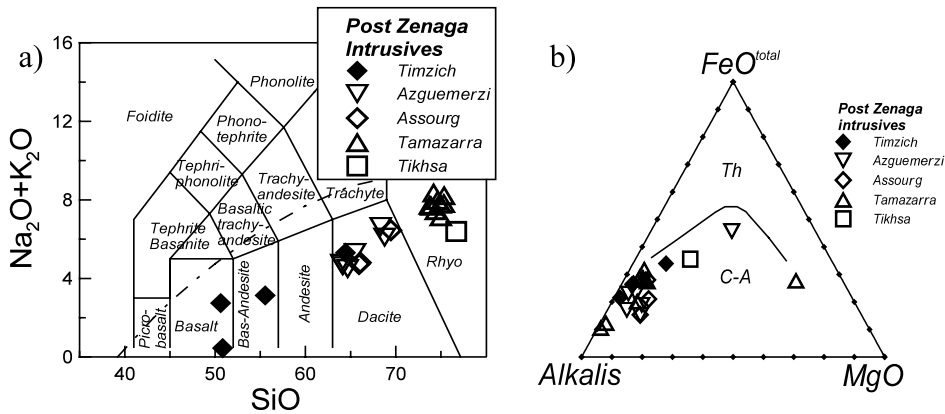


Fig. 4. Geochemical plots of the Zenaga Complex intrusive rocks. (a) Silica-alkalis (TAS) plot-fields for volcanic rocks from Le Maitre et al. (1989). Dashed line = alkaline and sub-alkaline boundary, after Irvine and Barager (1971); (b) FMA ternary diagram-tholeiitic (Th) and calc-alkaline (C-A) fields from Irvine and Barager (1971).

images of zircons are shown in Fig. 5. The granitoids gave identical within-error ages of  $2037 \pm 9$ ,  $2037 \pm 7$ , and  $2032 \pm 5$  Ma, respectively (Fig. 6) and these dates are taken to represent timing of emplacement of the granites and hence that of deformation and amphibolite grade metamorphism during the Eburnean Orogeny. The dates are comparable with recent U–Pb zircon data from other basement inliers at Ighrem and Bas Draa ( $1987 \pm 20$  and  $2050 \pm 6$  Ma; Aït Malek et al., 1998). A minimum age for the supracrustal Zenaga schists and gneisses is thus also constrained. The data for the Tamazzarra Granite and Azguemerzi Granodiorite show some evidence of older dates of  $\sim 2170$  Ma (Fig. 6), possibly representing inherited components from the Zenaga schists. Involvement of these schists is consistent with the peraluminous character of the granitoids. This suggests that the Zenaga schists are also probably products of the Eburnean cycle and are thus broad correlates of major sequences in Africa such as the Birrimian of West Africa and the Kheis-Magondi of southern Africa. The new dates are significantly older than the  $\sim 1800$  Ma Rb–Sr whole-rock dates for the same lithologies (Charlot, 1976; Cahen et al., 1984) and provide a precise estimate for the age of initial crustal development in the area. The lower intercept date of  $571 \pm 103$  Ma on the Tamazzarra Granite possibly reflects Pb-loss during late Pan-African (Ouarzazate Group) times.

### 3.2. Neoproterozoic Anti-Atlas Orogen (Anti-Atlas Supergroup)

#### 3.2.1. Bleïda Group

The *Bleïda Group* encompasses the oldest sedimentary and volcanic successions deposited along the northern margin of the West African Craton. These deposits are represented by three parallel facies, with varying metamorphism, ranging from cratonic to rifted margin to an oceanic environment (Fig. 7).

**3.2.1.1. Low grade volcano-sedimentary rocks.** The continental margin facies of the *Bleïda Group* are exposed in a narrow ( $\sim 3$  km wide) belt along the northern margin of the Zenaga Complex, and in highly deformed and metamorphosed tectonic slices in the AAMF. All the rocks in the Sirwa Window belong within the *Taghdout Subgroup*, in which three formations and number of members are recognised. The broad succession is basalt, dolomite–jaspilite and quartzite, together several kilometres thick.

The lowermost *Agouniy Formation*, restricted to the eastern part of the outcrop, is made up of dark grey, locally plagioclase–porphyritic homogenous to nodular ophitic basalts with characteristic green epidote–chlorite filled amygdales common in some flows. The basalts are strongly altered with pyroxene converted to epidote and chlorite and the plagioclase saussuritised.

Table 2  
Brief morphological descriptions of typical zircons analysed

| Sample  | Group                         | Unit        | Zircon morphology  |
|---------|-------------------------------|-------------|--|
| RTM 247 | Zenaga Complex                | Azguemerzi  | Brown, translucent, elongate, length/breadth ratios ( <i>l/b</i> ) ~ 1.5–2.5), multifaceted with wedge-shaped terminations. Rare inclusions  |
| RJM 48  |                               | Assourg     | Subhedral, elongate to acicular ( <i>l/b</i> ~ 2.5–5), some metamorphic rounding. Some CL-dark zones and embayments  |
| GK 230  | Bleida                        | Tamazzarra  | Pink, multifaceted, <i>l/b</i> ratios ~ 1.5, inclusions present  |
| GM 119  |                               | Iriri       | Colourless to pale yellow, transparent, stubby to elongate ( <i>l/b</i> ratios ~ 1.5), multifaceted, inclusions very rare  |
| GM 73   | Bou Salda Formation           | Tadmant     | Colourless to very pale pink, transparent. Most are fragments of originally elongate to tabular larger crystals. Some grains elongate with square cross-sections and blunt pyramidal terminations. Some inclusions present |
| GM 191  |                               | Tamriwine   | Euhedral, pale brown, transparent to translucent. Stubby to elongate with blunt pyramidal terminations. Some multifaceting, some inclusions present  |
| CBM 68  | Assarag Suite                 | Mzil        | Pale brown, transparent to translucent, acicular with square cross-sections ( <i>l/b</i> ~ 2–5). Short pyramidal terminations  |
| RTM 87  |                               | Askaoun     | Euhedral, multifaceted, <i>l/b</i> ~ 2, strong growth zoning   |
| RJM 1   |                               | Amlouggui   | Purple, anhedral to subhedral, resorbed, elongate to acicular ( <i>l/b</i> ~ 5), square cross-sections, blunt terminations. CL-dark, some lower U zoning, no cores. Some metamorphic reworking of grain margins            |
| GM 58   | Ouarzazate                    | Tourcht     | Pale pink to colourless, euhedral and fragmented grains ~ 100 µm, acicular ( <i>l/b</i> ~ 3), square to wedge-shaped cross-sections. Some growth zoning, some narrow rims, fairly high reflectance                         |
| GK 313  |                               | Tikhfist    | Euhedral, elongate to acicular, strongly zoned, well-developed pyramidal terminations  |
| CM7     |                               | Tawzzart    | Pale pink, < 100 µm, fragmented, elongate ( <i>l/b</i> ~ 1.5). Inclusions, concentric growth zoning present  |
| GM 220  | Syn-Ouarzazate Group Granites | Tilsakht    | Euhedral, elongate to acicular, strongly zoned, well-developed pyramidal terminations  |
| RTM 154 |                               | Tazoult     | Pale brown, translucent, euhedral with rectangular cross-sections, elongate to acicular ( <i>l/b</i> ~ 3–5). Short pyramidal terminations, sometimes wedge-shaped. Various inclusions present                              |
| GM 51   |                               | Imourkhsane | Euhedral, very strongly zoned, some inclusions, <i>l/b</i> ~ 2   |

The basalt is succeeded by the *Tirsal Formation*, a mixed, predominantly sedimentary package including purple quartzite, dolomite, shale, banded jaspilite and cinerite in the low-grade continental margin and green quartzite, cordierite sandstone, marble and phyllite in the AAMF. Some of these form highly distinctive packages have been formalised as members. In the classic section near Taghdout, the following sequence is recognised: The section starts with a 50 m thick purple sandstone, succeeded by a dolomitic member made up of a distinctive laterally consistent package of ~ 100 m of alternating brown sandy

dolomite with herringbone cross-bedding and subordinate calcareous shale on a ~ 5–10 cm scale. The shales have commonly been sheared out in high-strain zones. The dolomite is light brown, with chert lenses and lamellae with stromatolites in the lower beds. Towards the top, the dolomite beds have increasing silica content and lenses of reworked oolites, which define prominent trough cross-bedding, are seen in places.

The dolomitic member is succeeded by a layered succession (10–20 cm scale) of jaspilites and cinerites interbedded with grey arkoses and sandy dolomites about 50–100 m thick. Within these

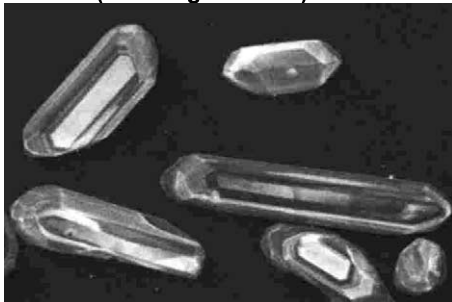
**RJM 48 (Assourg Tonalite)****GK 230 (Tamazzarra Granite)****RTM 247 (Azguemerzi Granodiorite)**

Fig. 5. CL images of typical zircons from dated samples of the Zenaga Complex granitoids.

exhalative rocks, red haematite–jaspilites developed in the east. Near Taghdout, the exhalative rocks are interbedded with ( $\sim 2$  cm) layers of cream, to pale greenish, very fine-grained chert, and medium-grained arkose.

The uppermost *Mimount Formation* comprises quartzitic clastic sedimentary rocks. It forms a sub-vertical, prominent E–W mountain range rising up to 400 m above the Zenaga Plain. The formation consists predominantly of white quartzite, with iron-rich, reddish-brown quartzites and sandstones, quartz conglomerates and minor shales, with a total thickness of  $\sim 1000$  m. In the SW part of the Sirwa Window a series of flat-lying imbricate thrust slices, entirely within the *Mimount quartzite*, has given rise to an extraordinary apparent thickness of over 5 km. The quartzites form upward-fining packages. Sedimentary structures such as cross-bedding, desiccation cracks, interference ripples and rain-drop impressions, consistently indicate northward-younging. In some areas, ripple-marked quartzites were de-

formed into sedimentary megabreccias. These rippled megabreccias are a useful marker and serve to identify the otherwise featureless quartzite imbricate slivers in the AAMF as *Mimount Formation*. A white conglomerate facies of the *Mimount Formation* occurs as small lenses in the ripple-marked quartzites. These are matrix-supported, with a feldspathic matrix of poorly sorted and sub-rounded granule-sized material.

In the AAMF, the Taghdout Subgroup rocks occur as highly tectonised imbricate slivers with higher metamorphic grade. The basalts are intensely altered and hornblende-bearing; the sandstones contain cordierite; quartzites are totally recrystallised and the dolomitic rocks are metamorphosed to fine-grained granoblastic, deformed talc-serpentine marbles.

**3.2.1.2. Medium- to high-grade metamorphic rocks.** Tectonostratigraphically, the *Tachoukacht Schist* forms the lowermost unit of the metamorphosed part of the *Bleïda Group*. It outcrops in the central

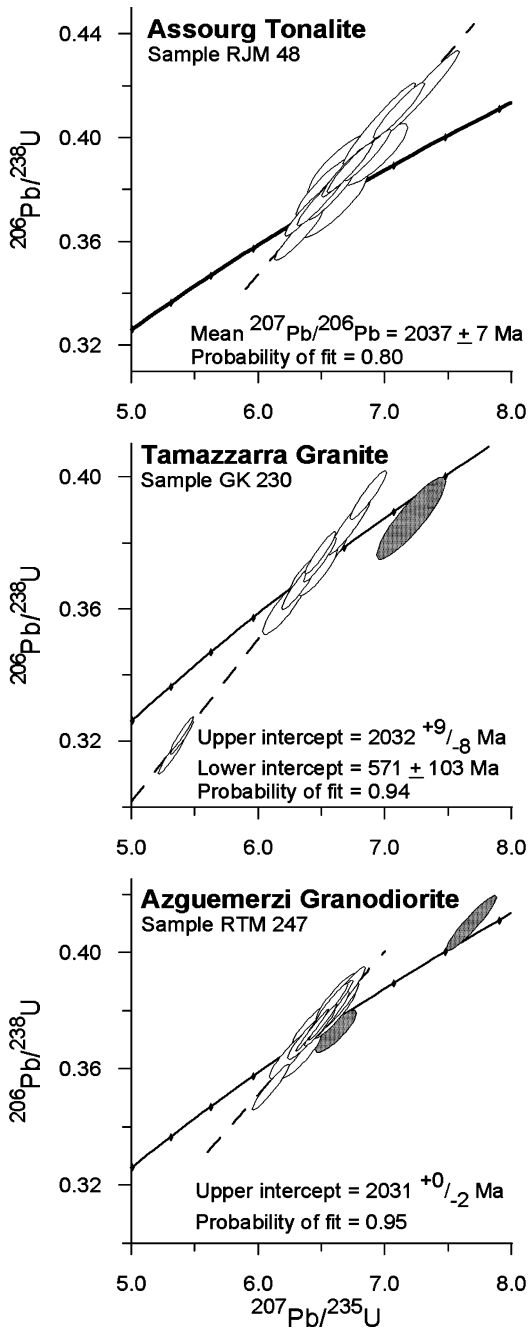


Fig. 6. Concordia plots of zircon data from the Zenaga Complex granitoids.

part of the Sirwa Window in the vicinity of Tachoukacht, where it appears to be overthrust from the north consecutively by the Iriiri migmatite

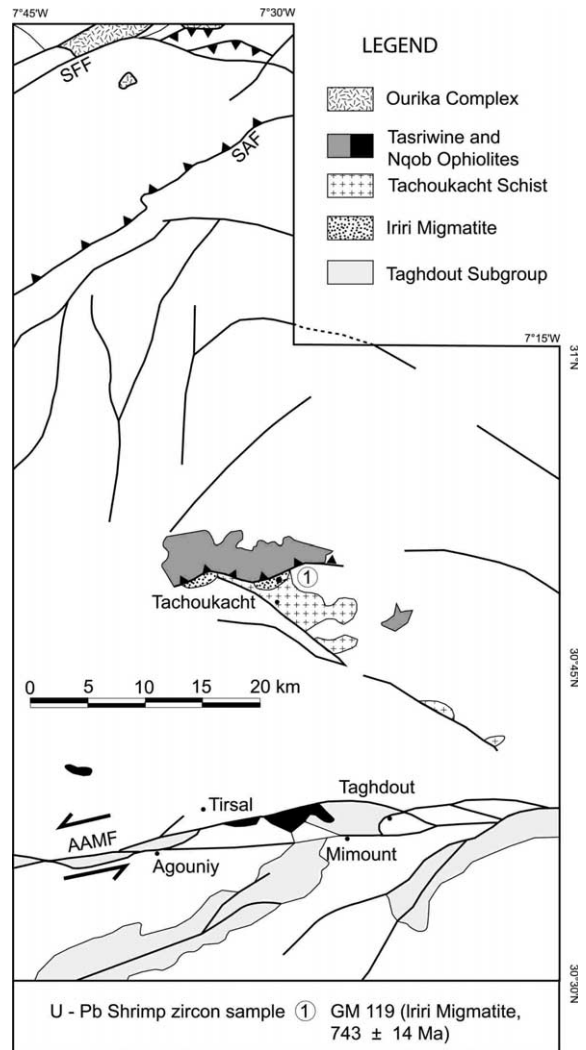


Fig. 7. Distribution of the Bleïda Group, showing the three parallel depositional facies.

and the Tasriwine ophiolite (Fig. 7). This unit was formerly described as the ‘Tachoukacht Gneiss Formation’ by Huch (1988) and Schermerhorn et al. (1986) and as ‘prasinites and ovardites’ by Chabane (1991). Our studies indicate that the rocks are not true anatectic gneisses as they are not pervasively banded, nor do they show pervasive leucosome development. They are a number of different schistose rock types representing different degrees of shearing, mylonitization and medium grade metamorphism.

The sequence is typically composed of quartz–feldspar–mica– and quartz–amphibole schists with abundant disrupted intrafolial quartz veins. Mafic layers are common, composed of dark green hornblende+actinolite. Alteration of amphibole to chlorite is evident, whilst plagioclase is invariably strongly saussuritised. Tourmaline, apatite, titanite and ilmenite are present as accessory minerals. In some low-strain zones, the rocks are recognisable as meta-andesite, reflecting the primary composition of the original sequence.

The regional E–W schistosity planes ( $S_2$ ) are characteristically spaced about 2 mm apart and have been folded, refoliated and crenulated during subsequent deformation. Evidence of an earlier ductile tectono-metamorphic event, leading to the formation of a first planar foliation  $S_1$ , is locally preserved. This event produced the paragenesis:

Quartz + plagioclase + biotite + garnet  
+ amphibole

A subsequent brittle deformation, parallel to  $S_1$ , caused cataclasis and rotation of garnets, retrogressive metamorphism and produced the paragenesis:

Quartz + albite + epidote + chlorite + sericite

The second schistosity ( $S_2$ ) is defined by the parallel alignment of chlorite, sericite and muscovite, along with actinolite in some quartz-rich layers. A still younger crenulation and refoliation event deformed and reorientated chlorite and sericite parallel to a third ( $S_3$ ) crenulation cleavage.

The *Irii Migmatite*, as defined here, differs from the Irii migmatite of Huch (1988) and does not form part of the Tachoukacht gneisses as described by Wallbrecher (1988) and Bassias et al. (1988). Our field observations show that this succession of high grade banded gneiss was thrust over the Tachoukacht Schist from the north. It occurs as two thrust slivers below the basal thrust of the Tasriwine Ophiolite, each about 3 km long and 500 m wide (Fig. 7). The eastern sliver trends north-easterly, at a discordant angle to the generally east–west trending schists and is well exposed in the Irii River 1 km north of Tachoukacht.

The Irii Migmatite consists of grey tonalitic gneisses with coarse-grained pink quartzo-feldspathic leucosomes which are typically interleaved with dark amphibolitic bands or coarsely crystalline hornblendites. Ductile deformation and migmatization gave rise to the pervasive banding ( $S_1$ ), which was followed by a co-planar brittle deformation event ( $S_2$ ) as in the Tachoukacht Schist. In pink leucosomes, the banding consists of strongly elongated quartz ribbons with low-angle grain boundaries, alternating with plagioclase-rich zones. Subsequent brittle deformation caused cataclasis, retrogression and the formation of chlorite, epidote and zoisite/clinozoisite replacing biotite and garnet. Garnets were rotated during the low-grade shearing event, also manifested by synkinematic albite blastesis. Bassias et al. (1988) recognised two phases of garnet crystallization (pre-tectonic and syntectonic) that occur as overgrowths and contain rotated inclusion trains. More mafic zones are composed of highly saussuritised feldspar with elongated lenses of chlorite replacing hornblende. Retrograde metamorphism is also seen as the replacement of primary brown hornblende which occurs as cores surrounded by secondary green actinolite. Further retrogression led to amphibole replacement by chlorite and the exsolution of ilmenite/rutile along cleavage planes. Zircon, apatite and ore minerals are elongated along foliation surfaces. A much younger epidote crystallization event is related to fracture-filling and occurred at a very late stage under pumpellyite-prehnite grade conditions (Bassias et al., 1988).

On the northern flank of the High Atlas massif, in the Setti Fadma region, some 45 km north of Tachoukacht, three tectonically-bounded inliers of schist, gneiss and migmatite are known as the *Ourika Complex* (Fig. 7). The complex was mapped and described as the ‘Série de l’Ourika’ by Proust (1973) and Vogel et al. (1980). Nefly (1998) made a detailed structural investigation of the gneissic complex and described it as a diapiric gneiss dome, with a NNW–trending long axis. He described a central biotite–hornblende–gneiss core, surrounded concentrically by fine-grained biotite gneiss and migmatite, augen gneiss and a peripheral amphibolitic gneiss.

The northern boundary fault of the Ourika Complex is the Meltsen Thrust, a major structure which forms the northern boundary of the Sirwa Window in the High Atlas. Its southern boundary is a major normal fault (the Setti Fadma Fault), parallel to the Meltsen Thrust, which juxtaposed granitoids of the Assarag Suite (which contain Ourika Complex xenoliths in this area) against the Ourika Complex. A small inlier occurs in the High Atlas watershed, in thrust contact with the Neoproterozoic Sarhro Group.

The most abundant lithology in the Ourika Complex is amphibolite-grade, homogeneous grey gneiss, composed of quartz, intermediate plagioclase, hornblende and biotite with accessory ilmeno–magnetite, zircon, apatite, rutile, titanite and secondary epidote, calcite, leucoxene and haematite. A banded (migmatitic) gneiss phase, characterized by a strong ductile planar fabric and folding occurs interlayered with biotite schist, fine-grained biotite–garnet gneiss and amphibolite. A range of leucocratic to tonalitic bands composed of quartz + plagioclase; quartz + plagioclase + biotite; quartz + plagioclase + hornblende have been distinguished. Many of the gneissose rocks are comparable with the Iriwi Migmatite, while some outcrops consist of crenulated schists akin to the Tachoukacht Schist.

*3.2.1.3. Ophiolitic rocks.* The Neoproterozoic ophiolites of the Anti-Atlas, including the famous, and economically important, Bou Azzer Ophiolite have attracted considerable attention over the years. The Sirwa Window contains two small highly tectonised ophiolite fragments (e.g. the Tasriwine and Nqob Ophiolites), grouped within the *Khzama Complex* of the Bleïda Group. During the course of our study, we revised the spatial distribution of these fragments (Fig. 7) but, owing to the considerable volume of available published literature concerning their geochemistry and origin as ophiolite fragments, we did not repeat these detailed investigations. For more information, the reader is referred to Chabane (1991), El Boukhari et al. (1991), Huch (1988), Wallbrecher (1988), Hoffmeister (1988) and Schermerhorn et al. (1986), who have conclusively demonstrated the ophiolitic nature.

The *Tasriwine ophiolite* forms a 4 km wide, east–west striking outcrop, north of the Iriwi migmatite in the central part of the Sirwa Window (Fig. 7). The fragment is partly bounded by normal faults and partly overlain by younger rocks. The ophiolite is highly sheared and banded, with the main ductile foliation generally dipping to the south, although steepening by refolding and refoliation during a late low-grade tectonometamorphic event has occurred. Metamorphosed ultramafic rocks include serpentinite and talc schist, derived from harzburgite; hornblende and tremolite schist representing original pyroxene cumulates. Mafic rocks make up the larger part of the ophiolite, comprising strongly foliated amphibolites of variable grain size, representing metamorphosed gabbro plutons, dolerite dykes and basaltic lava.

The ophiolite contains small quantities of acid volcanic and plutonic rocks. Fine-grained meta-quartz keratophyres and medium- to coarse-grained trondhjemites are regarded as being related to the ‘plagiogranite’ phase of acid magmatism of the ophiolite, based on their geochemistry (Huch, 1988). These quartz–plagioclase rocks occur as lenses, dykes and irregular masses in the amphibolite, especially in the northern half. Large masses of coarse amphibole-rock are locally intruded by anastomosing networks of white albite granite which may be interpreted as plagiogranite. A small lensoid intrusion, the Tourtit Granite, measuring some 5 by 0.5 km with an E–W orientation occurs within the Tasriwine ophiolite. The granite is very strongly sheared and altered. It is considered to be a minor syntectonic granite within the ophiolite.

Chabane (1991) described a complex, idealized complete ophiolite succession composed of meta-ultramafic rocks, gabbros, dolerite dykes, pillow basalts, volcanoclastic and conglomerates as well as keratophyres. Many of the rock types were identified geochemically and could not be mapped accurately in the field. During the course of our study, however, convincing outcrops of the typically ophiolitic features such as sheeted dykes, pillow lavas, described in the literature, could not be found in the field.

The *Nqob ophiolite* is represented by a number of tectonically-bounded slices which occur within the major E–W trending AAMF. This highly complex *mélange* comprises huge dismembered and rotated blocks of numerous lithologies. Within the *mélange*, a number of fairly large (> 1 km) ophiolitic bodies have been recognised. El Boukhari et al. (1991) mapped and described in detail three relatively small, fault-bounded bodies of cumulate mafic and ultramafic rocks in the AAMF. From their study, along with detailed whole-rock and mineral chemical analyses, El Boukhari et al. (1991) showed that the rocks are typical of those produced at mid-ocean spreading ridges, confirming their ophiolitic nature. Hypabyssal, intrusive bodies and dykes of dolerite, diabase, ferro-dolerite and amphibolite (metadolerite), as well as magmatic breccia occur in the ophiolitic complex.

### 3.2.2. Geochronology of the Bleïda Group

Excluding the Zenaga Complex, all the other SHRIMP dates obtained from the Sirwa Window are Neoproterozoic, demonstrating the long period during which no major felsic crust-forming events occurred in this part of Africa—in particular no trace of the widespread Mesoproterozoic (1.4–1.0 Ga) Kibaran-Namaquan cycle of central

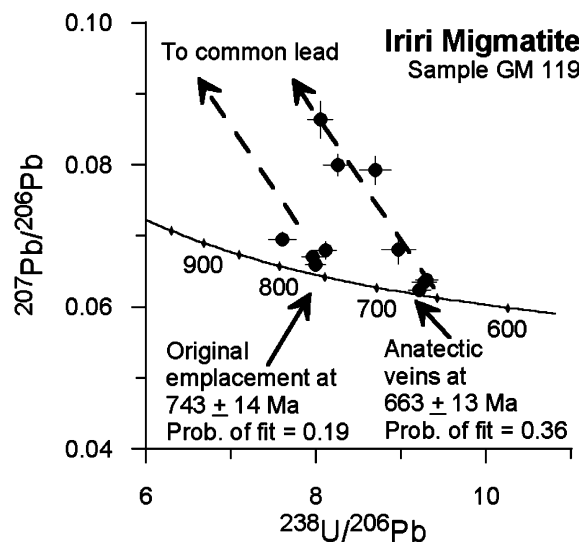


Fig. 8. Tera-Wasserburg plot of zircon data from the Iriiri Migmatite.

### GM 119 (Iriiri Migmatite)

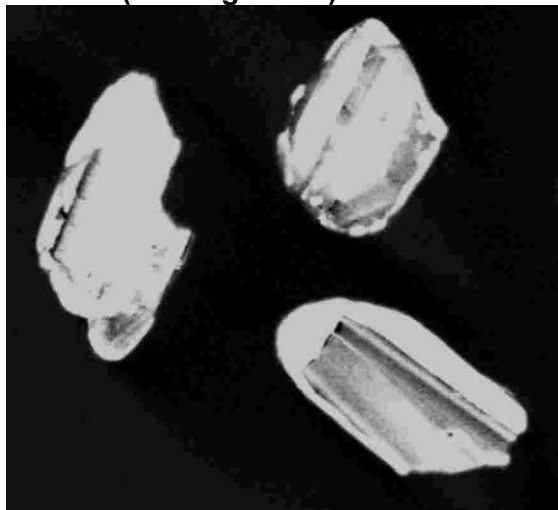


Fig. 9. CL images of typical zircons from the dated sample of the Iriiri Migmatite. Note cores and metamorphic overgrowths.

and southern Africa has been recorded. The oldest Neoproterozoic dates obtained were from zircons from a tonalitic gneiss from the Iriiri Migmatite. The rock contains two zircon populations, an older dated at  $743 \pm 14$  Ma and a younger dated at  $663 \pm 13$  Ma (Fig. 8). The younger dates are found in discrete grains and in metamorphic rims on older grains (see CL images, Fig. 9). The older zircons are considered to date emplacement of the precursor rock, whilst the younger date probably reflects the period of melt formation which generated the acid veining evident in outcrop. As such, this younger date is interpreted as the age of metamorphism and is the best direct estimate of the timing of Pan-African island-arc accretion in the Sirwa Window. This is in broad agreement with the estimate of  $\sim 685$  Ma for collision suggested by Villeneuve and Corneé (1991) and for obduction of the Bou Azzer Ophiolite (Leblanc, 1981). Given the absence of dateable lithologies for the other components of the Bleïda Group (the ophiolitic rocks and the rifted margin sedimentary sequence), 743 Ma is taken as a best estimate of the age of their formation also.

A Sm–Nd isotopic study was carried out to constrain the age and nature of the Bleïda Group protolith. Samples chosen concentrated on the

Table 3  
Sm–Nd data from various lithologies of the Sirwa Window

| Sample  | Unit                                | Age (Ma) | Sm    | Nd    | $^{147}\text{Sm}/^{144}\text{Nd}$ | $^{143}\text{Nd}/^{144}\text{Nd}$ | $^{143}\text{Nd}/^{144}\text{Nd}_{(\text{o})}$ | $\varepsilon_{\text{Nd}}$ | $T_{(\text{CHUR})}$    | $T_{(\text{DM})}$ |
|---------|-------------------------------------|----------|-------|-------|-----------------------------------|-----------------------------------|--|---------------------------|------------------------|-------------------|
| RTM-154 | Tazoult Quartz Porphyry             | 559      | 12.08 | 60.76 | 0.1202                            | $0.51237 \pm 912$                 | 0.511939                                       | $+0.37 \pm 1.4$           | $521 \pm 197$          | $1100 \pm 127$    |
| GM-171  | Upper Ouarzazate rhyolite           | 562      | 2.833 | 18.53 | 0.0924                            | $0.512403 \pm 21$                 | 0.512063                                       | $\pm 2.87 \pm 1.4$        | $347 \pm > 1\text{Ga}$ | $837 \pm 107$     |
| GK-295  | Lower Ouarzazate rhyolite           | 577      | 7.844 | 36.81 | 0.1288                            | $0.512485 \pm 17$                 | 0.511998                                       | $\pm 1.98 \pm 1.4$        | $349 \pm 223$          | $1029 \pm 139$    |
| CBM-100 | Quartz keratophyre (Nqob ophiolite) | 743      | 4.927 | 15.16 | 0.1965                            | $0.513013 \pm 18$                 | 0.512056                                       | $\pm 7.31 \pm 1.4$        | undef                  | $604 \pm 524$     |
| GK-195  | Pyroxenite (Nqob ophiolite)         | 743      | 3.111 | 13.61 | 0.1382                            | $0.512363 \pm 19$                 | 0.511690                                       | $\pm 0.16 \pm 1.4$        | $722 \pm 257$          | $1364 \pm 143$    |
| GM-119  | Iririr Migmatite                    | 743      | 2.372 | 9.466 | 0.1515                            | $0.512676 \pm 13$                 | 0.511938                                       | $\pm 5.00 \pm 1.4$        | undef                  | $947 \pm 181$     |
| GM-122  | Khzama ophiolite                    | 743      | 2.853 | 13.86 | 0.1245                            | $0.512493 \pm 23$                 | 0.511887                                       | $+4.00 \pm 1.4$           | $311 \pm 210$          | $971 \pm 135$     |
| GM-168  | Bleida basalt                       | 743      | 3.510 | 11.41 | 0.1860                            | $0.512821 \pm 22$                 | 0.511915                                       | $+4.55 \pm 1.4$           | undef                  | $1241 \pm 316$    |
| RTM-117 | Plagiogranite (Nqob ophiolite)      | 743      | 0.557 | 2.664 | 0.1264                            | $0.512563 \pm 59$                 | 0.511947                                       | $+5.19 \pm 1.4$           | $167 \pm 216$          | $879 \pm 136$     |

older rocks of the Bleïda Group (from the ophiolites, the Iriiri Migmatite and a continental-margin basalt) as these rocks represent the earliest stages of the development of the Anti-Atlas Orogen. The Sm–Nd whole-rock data are provided in Table 3. Values of  $\epsilon_{\text{Nd}}$  are all positive: ranging from within-error of zero to +7.3; indicating that these igneous rock units were derived from sources having time-integrated depletions in the LREE relative to Bulk Earth (CHUR). For this reason, meaningless model  $T_{\text{CHUR}}$  ages are recovered (i.e.  $T_{\text{CHUR}} < T_{\text{formation}}$ ) and  $T_{\text{DM}}$  are more meaningful. In the older, 743 Ma, sample group (Bleïda rocks)  $T_{\text{DM}}$  ages range from 947 to 1364 Ma with sample CBM 100 (quartz keratophyre) having a  $T_{\text{DM}}$  which is lower than its crystallisation age. This simply indicates that CBM 100 has an  $^{143}\text{Nd}/^{144}\text{Nd}$  value which was lower than that of the Depleted Mantle model used. These results preclude the involvement of substantial proportions of ancient continental crustal material in their genesis. The data support derivation from mixtures of a depleted mantle source (asthenosphere?) and juvenile crustal material less than 1300 Ma in age. In other words, the rocks are not derived from, or contain significant quantities of, reworked Zenaga Complex material. The quartz keratophyre (CBM 100) was generated exclusively from the depleted source.

### 3.2.3. Depositional setting and geochemistry of the Bleïda Group

The *Taghdout Subgroup* comprises clastic and chemical platform sediments deposited on the cratonward (southern) side of a sedimentary basin. Clauer (1976) has suggested a minimum age of  $788 \pm 9$  Ma for the deposition of the equivalent of the Bleïda sedimentary group elsewhere in the Anti-Atlas. Stromatolites, cross-bedding (locally herringbone) indicate that the dolomite and interbedded shale of the Tirsal Formation were deposited in shallow marine environments with wave reworking of oolitic carbonate deposits. The cross-bedded, upward-fining brown quartzites have fluvial characteristics while interference ripples and mud-cracks indicate standing water which was occasionally exposed to subaerial dessication and rain-pitting. The consistent longitudinal rip-

ples developed in the pure, mature Mimount quartzite indicates a shallow marine environment. The jaspilitic rocks and cherts represent chemical precipitation, in a marine environment, of volcanogenic fluids probably rising along active rift faults at the extended craton margin. The basalt/basaltic andesite composition of the Agouniy Formation (Serv. Geol. Maroc., 1990) may indicate that the basin was relatively close to an immature oceanic arc. This is supported by the shallow marine nature of the sediments and the dearth of typical rift clastic rocks.

The Agouniy Formation volcanic rocks straddle the sub-alkaline/alkaline boundary on the TAS diagram and have basaltic to basaltic trachyandesite compositions (Fig. 10a). The relatively high Fe contents indicate that they form part of a tholeiitic chemical series (Fig. 10b). The Tachoukacht schists and the Iriiri migmatites are both sub-alkaline and exhibit similar ranges in  $\text{SiO}_2$  contents equivalent to andesite–dacite–rhyolite volcanic rocks. The Iriiri migmatites are slightly more alkalic overlapping into the fields of trachyandesite and trachy–dacite (Fig. 10c). Both these units are calc-alkaline (Fig. 10d).

Analyses of components of the Tasriwine and Nqob ophiolites are depicted on TAS and FMA plots in Fig. 10e and f. The Tasriwine metabasites form two compositional groups: a low– $\text{SiO}_2$  group of tholeiitic basalts and a group of calc-alkaline andesites and dacites. The Nqob rocks are tholeiitic basalts (one basaltic andesite) with indications of slight alkaline affinity in some analyses. Variations between Mg and some major and trace elements are depicted in Fig. 10g. Reasonably coherent linear variations are noted between MgO,  $\text{SiO}_2$  and the compatible trace elements Cr and Ni but the differences within the Tasriwine metabasites become apparent in the alkalis and  $\text{Fe}_2\text{O}_3$  plots. Rapid depletion in V with decreasing MgO, at low MgO values, indicates the fractionation of magnetite.

The geochemical ‘tectonic discrimination’ plots derived by Pearce and Cann (1973) provide a convenient way of comparing the trace element composition of basaltic rocks. In Fig. 10h the Ti, Zr and Y compositions of the Agouniy basalts, the basaltic components of the Tasriwine ophiolite

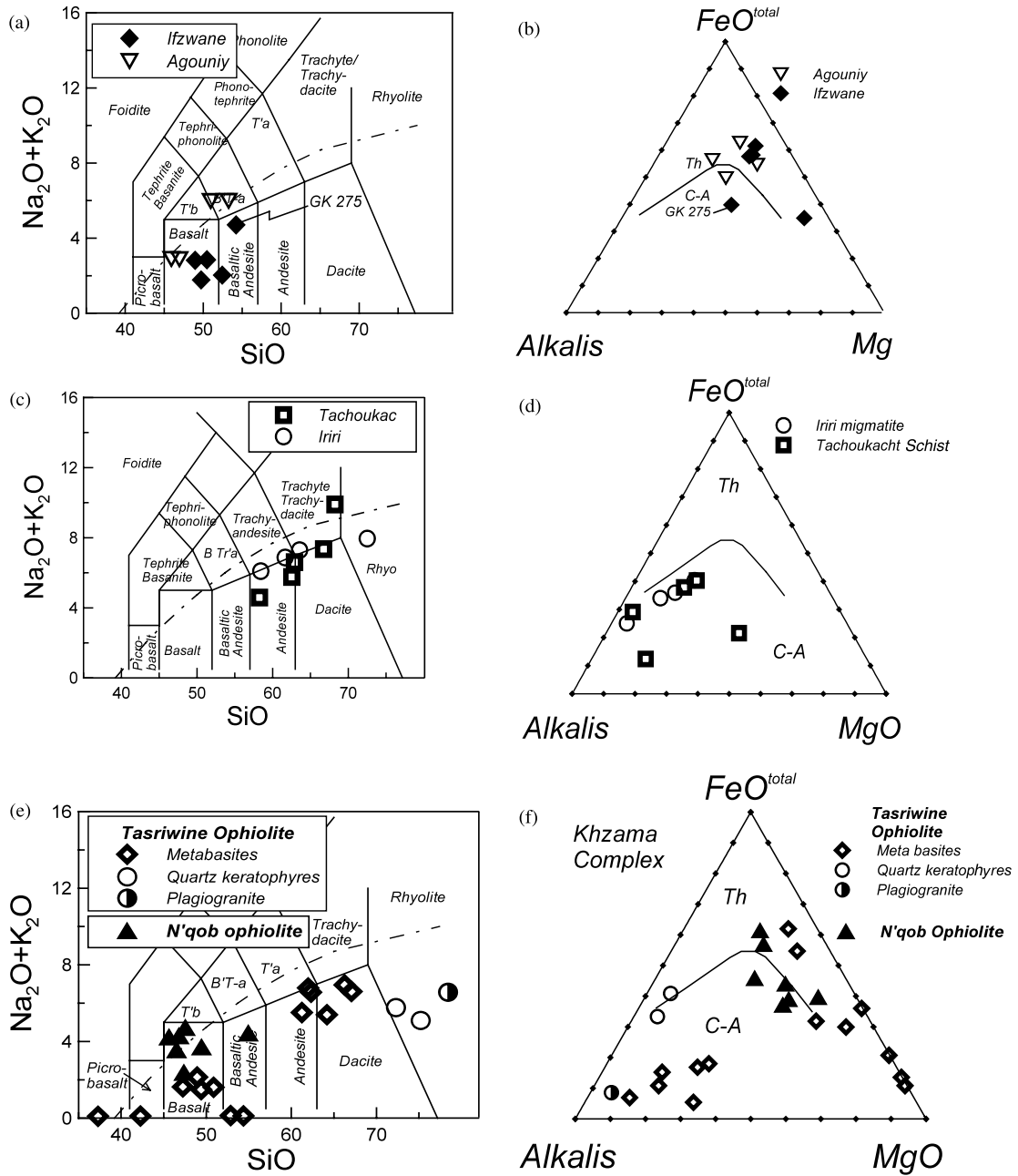


Fig. 10. Geochemical plots of chemical analyses of units of the Bleida Group. (a) TAS and (b) FMA plots comparing Agouiniy Formation volcanics and Ifzwane Suite dolerites; (c) TAS and (d) FMA plots comparing Tachoukacht schists and Iri migmatites; (e) TAS and (f) FMA plots of the ophiolites; (g) plot showing the compositional variation of selected major and trace elements versus MgO in analyses of Khzama Complex rocks; (h) tectonic discrimination plot (Pearce and Cann, 1973) for analyses of Tasriwine, Agouiniy and Tachoukacht rocks. Classification fields in (a), (c) and (e) are those of Le Maitre et al. (1989); discrimination curve in (b), (d) and (f) is from Irvine and Barager (1971).

and the Tachoukacht schists are compared. The Agouniy basalts are distinct in having elevated Ti compositions equivalent to those found in within-plate basalts. By contrast, the basaltic components of the Tasriwine ophiolite have lower Ti and Zr but higher Y and are compositionally similar to island arc tholeiites. The Tachoukacht schists have very high Zr values and were probably from evolved arc volcanics.

### 3.3. Ifzwane Suite dolerites

The *Ifzwane Suite* comprises an extensive dolerite dyke swarm, with larger, irregular and sill-like bodies which intrude the Zenaga Complex and the lower part of the Taghdout Subgroup (up to the Tirsal Formation). The dolerite numerous bodies form an interlinked intrusive network, with three main trends apparent—NNE, NW and E–W (Fig. 3). The rocks vary from coarse-grained gabbros to medium- and fine-grained dolerites, dark grey when fresh, but commonly reddened due to extensive secondary ferruginisation. Primary igneous mineralogy and texture are typically preserved, with lamellar plagioclase and larger clinopyroxene grains in an ophitic to sub-ophitic relationship, with accessory opaque mineral (often skeletal to embayed ilmenite). Granophyric quartz–K-feldspar mesostasis is locally seen, suggesting tholeiitic composition.

On the total alkalis–SiO<sub>2</sub> diagram (Fig. 10a) the rocks are sub-alkaline with compositions equivalent to basalt to basaltic andesite with SiO<sub>2</sub> contents of 49–52%. The tholeiitic nature of the dolerites is confirmed in the ternary plot in Fig. 10b. The one anomalous value in each plot (GK 275) has the highest LOI and alkali contents suggesting that it suffered alkali addition during alteration.

The *Ifzwane Suite* has given Rb–Sr dates which indicate that they may have intruded at about 800 Ma (Cahen et al., 1984). This corresponds broadly to the field relationships and emplacement during an early Pan-African extensional event associated with Neoproterozoic rifting of the West African Craton (Zenaga Complex).

### 3.4. Sarhro Group

The *Sarhro Group* represents a very thick succession of deformed, low-grade volcano-sedimentary rocks that comprise the basin-fill deposits of the Anti-Atlas Orogen in the Sirwa Window (Fig. 11). In broad terms, the lower part is a greywacke–turbidite flysch-like sequence with subordinate volcanic rocks, while upper units are dominated by arkosic and conglomeratic clastic rocks. Historically the sequence was known as the ‘Serie de Sirwa-Sarhro’ (or ‘Siroua-Saghro’; Choubert, 1963). The Sarhro Group of the Sirwa Window has been subdivided into seven formations and a number of members. Several kilometres of strata are present, although the exact amount cannot be ascertained due to the fragmentary nature of the outcrop (caused by cover, tectonic and intrusive boundaries) and the unknown degree of tectonic repetition. Neither the base nor the top of the Sarhro Group is anywhere exposed in the Sirwa Window. These problems, combined with the probable presence of major tectonic discontinuities within the exposed area, mean that the precise stratigraphic integrity of the various units is unknown.

The lowermost, E–W striking Tittalt Formation, is only exposed in the central-western part of the area (Fig. 11). It is immediately bounded in the north by two formations (Aghtim and Tizoula), which are similar to the Imghi Formation in the south. Despite intense folding, the facing directions of the Sarhro Group are generally north to the north of the Tittalt Formation ‘axis’ and south to the south of it, so that progressively younger strata are exposed both to the north and south, away from the Tittalt Formation which may lie in the core of a major anticlinorium. In the south, the Imghi Formation is overlain by two, predominantly clastic formations (Azarwas and Tafiat) which are missing in the north. Furthermore, in the north of the Sirwa Window, a large area in the High Atlas is underlain by another unit (Timichcha Formation) which has similarities with the Tittalt, Aghtim and Tizoula Formations. Moreover, the Imghi Formation in the south may be the approximate equivalents of the Aghtim, Tizoula and Timichcha Formations. These complications

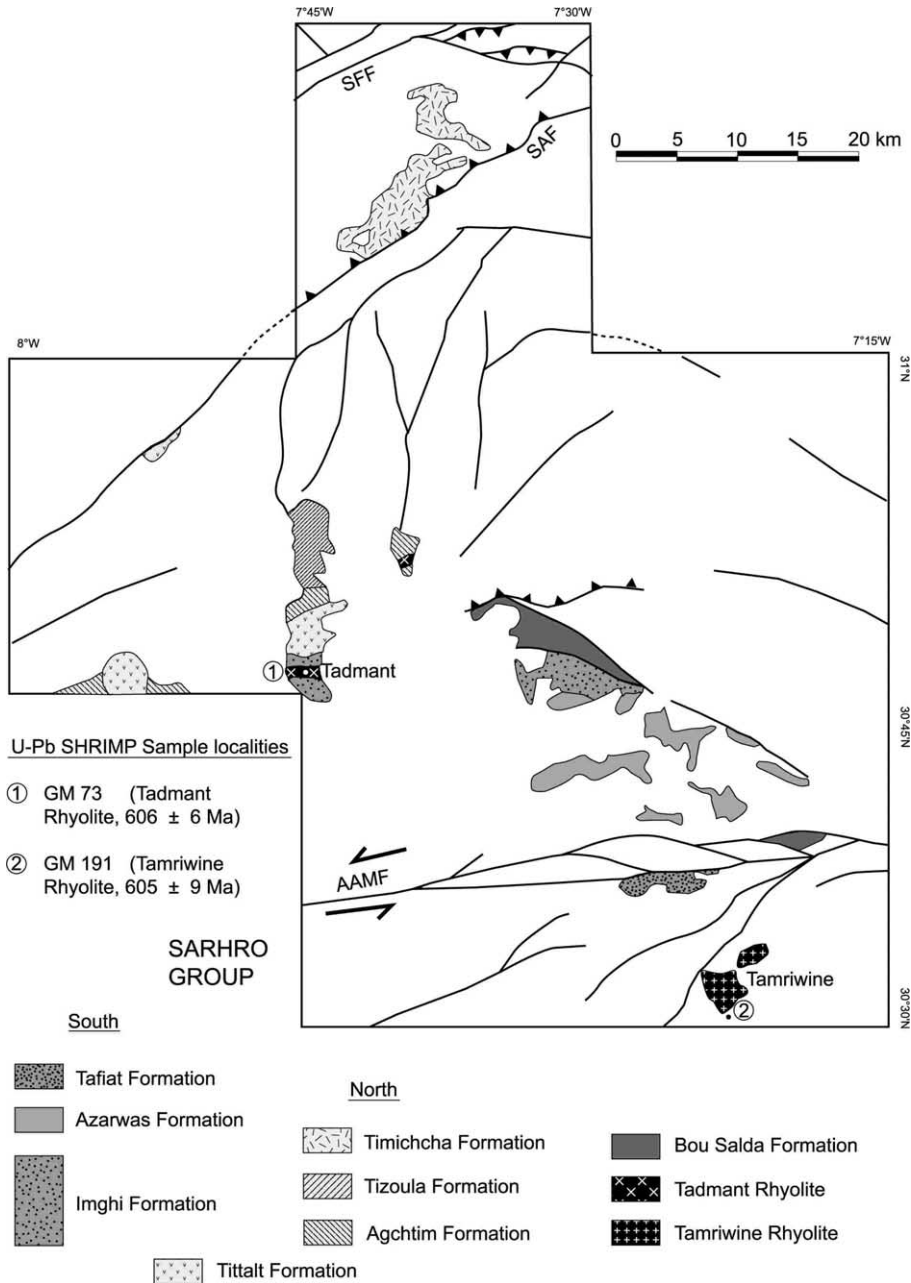


Fig. 11. Distribution of the Sarhro Group, the Bou Salda Formation and associated Tadmant and Tamriwine Rhyolites.

probably reflect not only primary facies variation proximal to (south) and distal from (north) the Craton margin, but also record the effects of major structural discontinuities and folds which do not crop out. A generalised stratigraphic section

through the Sarhro Group, showing the main elements of the north and south areas is presented in Fig. 12. For detailed measured sections, the reader is directed to the seven sheet explanations referred to earlier.

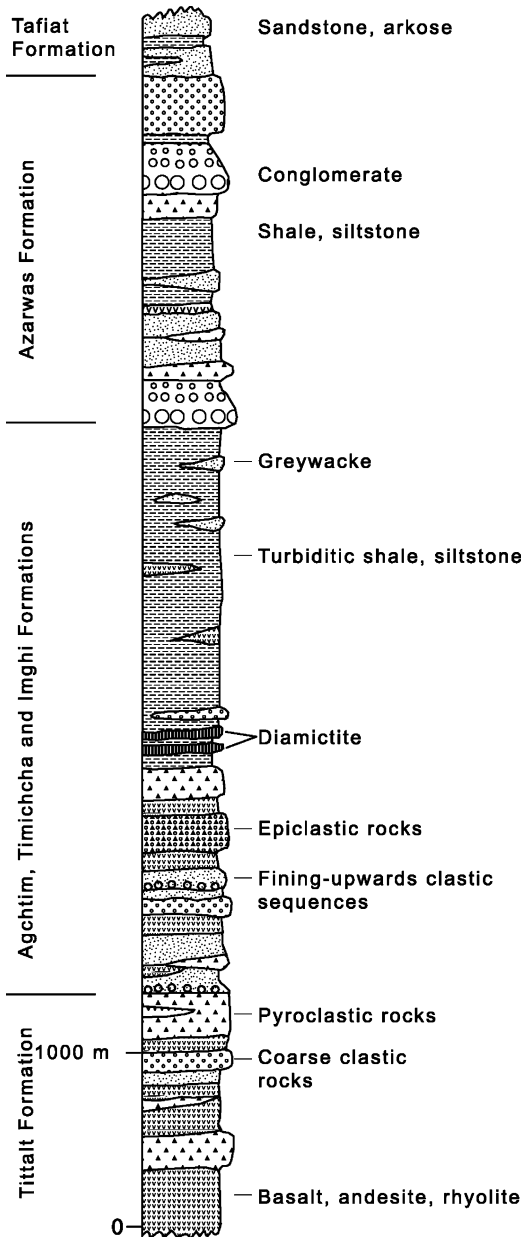


Fig. 12. Idealised composite stratigraphic section through the Sarhro Group.

### 3.4.1. Northern Sarhro Group outcrops

The lowermost *Tittalt Formation* is predominantly composed of volcanic rocks of basaltic, andesitic and andesitic to trachytic composition

and pyroclastic rocks with subordinate sedimentary intercalations. Locally, several cycles of interbedded rhyolitic pyroclastic rocks and poorly-bedded porphyritic basaltic andesite flows occur. At the very top of the sequence, conglomerate, feldspathic quartzite and shale are locally overlain by a porphyritic andesitic agglomerate. Most of the volcanic rocks are strongly retrogressed. The rocks are strongly folded and cleaved, so way-up criteria are sparse.

North of the *Tittalt Formation*, the tectonically-overlying (thrust) *Agchtim Formation* comprises two lower predominantly detrital members, each about 220 m thick, and two overlying members each about 400 m thick. The basal member is composed of matrix-supported conglomerate with interbedded basalt/rhyolitic lava. The conglomerate contains well-rounded clasts, up to 35 cm in diameter, composed of white quartzite, andesite, dacite and rhyolite with rare granite and gneiss (Zenaga Complex?) in a volcanoclastic matrix. It grades upwards into a sequence of conglomeratic sandstone, sandstone (greyish-green, fine-grained feldspathic greywacke), arkose, gritstone, finely-laminated turbiditic siltstone and purple shale. The sandstone beds are 5–20 cm thick with internal alternating dark and light laminations of 1–5 mm thickness. Depositional units usually show a vertical gradation from parallel lamination at the base to ripple cross-lamination at the top. Small interference ripples are common, along with ball-and-pillow compaction structures. Units of light yellow-green chert, up to 2 m thick occur within the sandy part of the succession.

The second member comprises steeply-dipping, cyclic, upward-fining successions up to 75 cm thick basal conglomerate grading upward to purplish grey arkose and, locally, black shale. The conglomerates are matrix supported, with pebbles (dacite, andesite, rare quartzite, granite) usually less than 4 cm in size, but occasionally up to 10–12 cm. Pebble size decreases as roundness increases upwards in each cycle. The next member is comprised of shales and fine-grained greywacke sandstones with interbedded volcanic rocks. Finally, the upper member is predominantly composed of rhyolitic and andesitic volcanic breccias and ashfall tuffs.

The overlying *Tizoula Formation* comprises a package of folded and cleaved volcanoclastic slates and phyllites which crop out in the west-central part of the Sirwa Window. The principal lithology comprises a thick monotonous sequence of dark grey turbidites (shales and siltstones) with interbedded greenish–grey impure greywacke sandstones and pale green ash (cineritic) layers. Dips are typically  $\sim 70^\circ$  S, such that in some sections >6000 m of strata are apparently exposed. While this is not a true stratigraphic thickness and the amount of tectonic duplication cannot be easily ascertained, the repetition of some conglomerate/greywacke units due to folding suggests that the *Tizoula Formation* may be 1–2 km thick. Where way-up criteria can be ascertained, the facing directions vary from north to south, demonstrating the presence of tight to isoclinal folds. The prominent steep fabric in most of the *Tizoula Formation* is a pervasive cleavage ( $S_1$ ), axial planar to tight to isoclinal upright folds. Bedding lies at a high angle to the slaty cleavage ( $S_0$ ) in fold closures. Very thinly-bedded (cm-scale) original sandstone layers are represented by deformed and dismembered granular epidote–quartz pods, while interbedded shales are represented by fine-grained, cordierite-rich black phyllite. A second phase of deformation is locally apparent, where the  $S_1$  fabric and deformed  $S_0$  bedding, are together folded by tight angular/chevron folds with steeply-dipping axes, possibly associated with a later strike–slip event. In the contact metamorphic aureole of the Askaoun Granodiorite, biotite–magnetite hornfels and pinnitised cordierite hornfels developed from these greywackes and meta-pelites.

A number of semi-autochthonous, uplifted masses of hornfelsic Sarhro Group rocks occur in the High Atlas as tectonically bounded slivers or as huge xenoliths and roof pendants within later intrusive granitoids. These rocks cannot be readily correlated with the main Sarhro succession and have been grouped within a separate unit, the *Timichcha Formation*. It consists of approximately 1500 m of folded cherts, turbiditic greywackes, shales and associated acid to intermediate volcanic and volcanoclastic rocks. Reconstruction of the stratigraphy of the *Timichcha Formation* is diffi-

cult due to the deformation of the sequence and intrusive fragmentation (rafting) by the granitoids. Our suggested stratigraphic succession recognised in the High Atlas comprises, from bottom to top: micaceous quartzite, chert, greywacke, rhyolite, tuff, trachyte, chert, greywacke, arkosic quartzite, andesite, rhyolite, trachyte, tuff and agglomerate, thus differing somewhat from that of Vogel et al. (1980).

#### 3.4.2. Southern Sarhro Group outcrops

Lying above, and to the south, of the Tittalt Formation, the *Imghi Formation* contains elements of both the Aghim and *Tizoula Formations*. The main lithology consists of poorly graded, thick-bedded greywacke composed mainly of stacked fine- to very fine-grained sandstone beds and greyish-green, well bedded, graded turbidites. The greywacke is locally hornfelsed (with spotting) adjacent to the Askaoun Granodiorite and heavily fractured as a result of the Miocene Sirwa volcanic eruption. Fine-grained beds display ripple cross-lamination, linguoid as well as straight-crested ripples and thin yellowish calcareous interbeds. These Tce turbidites (Bouma, 1962), display WSW–ENE palaeocurrent directions. Several folded diamictite beds that vary from less than 1 to 30 m in thickness were mapped. These units have abrupt lower contacts and consists of polymictic, unsorted, cobble- and pebble-diamictite near the base and unsorted, angular, matrix-supported diamictite near the top. Quartzite cobbles in the diamictite and greywacke matrix are generally well-rounded and represent re-sedimented, second or third cycle clasts. The clasts are locally faceted and striated and display sets of parallel slip-fractures which possibly originated from ice-shear in glaciers. Coarse-grained, cross-bedded subarkosic sandstone and quartz-pebble conglomerate interbedded with yellow and green chert (volcanic ash) appears towards the top of the succession, along with volcanic breccia and lapilli tuff. Conglomerates derived from Bleida Group quartzites become prominent towards the south, near the source region. In the eastern part of the Sirwa Window, the *Imghi Formation* comprises at least 2000 m of greywackes, impure sandstones,

turbiditic shales and diamictites. No diamictites were recorded from the northern area.

The preceding formations correspond to the lower, flysch sediments and volcanic rocks of the Sarhro Group. The upper part, only exposed in the south and commencing with the *Azarwas Formation*, comprises the upper, coarse clastic part of the group. It is widely distributed over the Sirwa Window, consisting mainly of arkosic to pebbly sandstone with intercalated beds of conglomerate and rare volcanic rocks. The lower member is a massive basal diamictite horizon, some 30–40 m thick, composed of angular fragments and rounded cobbles of quartzite, vein quartz, granite and lava in a fine-grained, purple mud matrix that oversteps onto the Imghi Formation in the eastern part of the area. The overlying bulk of the Azarwas Formation consists of repeated upward-fining cycles of arkosic sandstone, gritstone and conglomerate. However, the overall trend is coarsening-up and the uppermost exposed cycle ends in a thick, very coarse pebble-to-boulder, clast-supported conglomerate containing poorly sorted, well-rounded chert, quartzite and granite clasts and subangular to subrounded shale, feldspar and volcanic clasts. The conglomerates are the most notable feature of the Azarwas Formation, with massive quartz boulder conglomerates, some with mafic volcanic clasts and at least one coarse, angular palaeosclerite deposit.

The uppermost member comprises a sequence of greyish–green arkosic greywackes, brown cross-bedded arkosic sandstones, whitish arkose and thin interbedded yellowish-weathering siltstone with subordinate shale, rare conglomerate and feldspathic microconglomerate and some intercalated basalt–andesite–rhyolitic volcanic rocks. Over most of the Sirwa Window, the Azarwas Formation forms the highest part of the exposed Sarhro Group. However, in the vicinity of the Sirwa volcano, higher beds, of black, dark olive-green and purple fine-grained siltstone and shale are exposed, termed the *Tafiat Formation*.

#### 3.4.3. Age, depositional setting and geochemistry of the Sarhro Group

The flysch-like basin fill sedimentary rocks of the lower Sarhro Group do not contain units

which can be easily dated. However, as noted above, the group contains glaciogenic diamictites, providing indirect evidence for the age of the Sarhro Group. World wide glaciations in the Neoproterozoic occurred at about 750–700 Ma (Sturtian glaciation) and 625–580 Ma (Varangian glaciation; Meert and Van der Voo, 1994). The deformation and metamorphism affecting the Sarhro Group is associated with the Anti-Atlas orogeny which has been dated at  $663 \pm 13$  Ma (Section 3.2.3). Consequently, the diamictites cannot be Varangian and so must correlate, if at all, with the older, Sturtian event ( $\sim 700$  Ma), an age entirely consistent with the field relationships.

The Sarhro Group occurs across the entire Anti-Atlas belt and forms the main flysch fill of the oceanic basins that developed between the West African Craton and a northern continent. The basal formations of this group are not exposed. As such, the Sarhro Group represents a late, deep water (distal) equivalent of the Bleida Group which was deposited on continental crust along the rifted continental margin to the south.

Eight analyses of Sarhro Group volcanic rocks were made which show sub-alkaline characteristics and a compositional range from basaltic andesite to dacite (Fig. 13a). The calc-alkaline nature of the volcanic rocks are indicated on the FMA plot in Fig. 13b. Some previous workers have suggested that the Sarhro Group was deposited in a back-arc basin that developed Craton-ward of the Tasriwine–Tachoukacht arc complex (Huch, 1988; Brabers, 1988), while others suggested a fore-arc basin setting (Saquaque et al., 1992; Hefferan et al., 1992; Ennih and Liégeois, 2001). The geochemistry of the rocks is not diagnostic of either setting. Concentrations of Ti, Zr and Y in the Sarhro volcanics are comparable to those which characterise arc-derived calc-alkaline basalts (Fig. 13c) supporting the inference that the Sarhro volcanism was related to arc formation during the early stages of fore-arc basin development.

There is a clear gradation from volcanic and distal turbidite deposits in the lower part of the Sarhro Group to coarse-grained arkosic sandstones, gritstones and conglomerate (Azarwas Formation) in the upper part of the basin fill

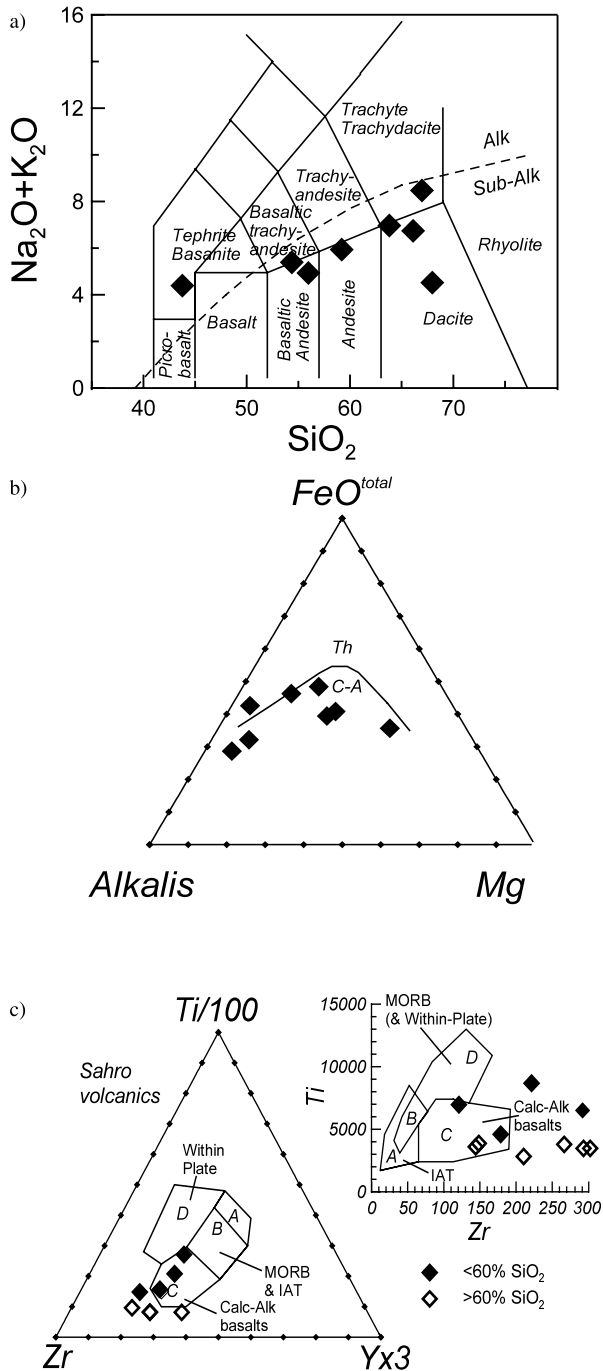


Fig. 13. Geochemical plots of the volcanic rocks of the Sarho Group. (a) Silica-alkalis (TAS) plot of Sarho Group analyses; (b) FMA plot; (c) Tectonic discrimination diagrams for basalts proposed by Pearce and Cann (1973).

succession, signifying aggradation and more proximal sedimentation. This is interpreted as indicating that the Azarwas Formation was deposited after reversal from spreading to basin contraction, when feldspar-bearing volcanic and intrusive rocks in the island arc complex were being elevated and eroded. In this scenario the lower part represents the spreading phase and the Azarwas Formation the contractional phase of basin development.

Diamictites in the Sarhro Group are interpreted as containing re-sedimented, glacial-derived clasts that were transported into the deeper parts of the basin by turbidity currents that originated on the unstable, uplifted rift-margins of the Anti-Atlas basin. Soft-sediment folding in the greywacke at the base of some of the diamictite beds suggests deposition on an unstable slope, rapid deposition and/or sediment shear before consolidation.

### 3.5. Bou Salda Formation and the Tadmant and Tamriwine rhyolites

The *Bou Salda Formation* is a volcano-sedimentary sequence which is in many respects transitional between the Sarhro and overlying Ouarzazate Groups. The relationship between the Bou Salda Formation and adjacent strata is always tectonic or intrusive, such that direct field relationships cannot be observed. The formation is usually preserved in narrow, fault-bounded troughs,  $< 1$  km across (Fig. 11). In some outcrop areas, these troughs trend regionally discordantly to the adjacent rocks (for example in the Bou Salda hills south of Tachoukacht), whereas in others, the rifts are parallel with the regional structure (for example in the thick deposits occupying E–W rifts in the AAMF tectonic zone).

The Bou Salda Formation is made up of three distinct lithological packages which have been given formal member status. At the base, a thick volcanic member is composed predominately of amygdaloidal basalt, with subordinate andesite and rhyolite. Basalts consist of fine-grained plagioclase, amphibole, titanomagnetite and chlorite, with relicts of clinopyroxene. Altered andesites contain  $\sim 3$  mm phenocrysts of plagioclase in a fine crystalline plagioclase-rich groundmass with up to 30% opaque minerals, epidote and chlorite.

The acid lavas are layered and flow-banded. The volcanic rocks are overlain by a predominantly sedimentary member, comprising massive lenticular conglomerates, arkosic gritstones and sandstones with an appreciable amount of purplish lithic grains as well as interbedded greywackes, shales, tuffs, basalts (locally spilitic) and chert. The conglomerates commonly contain massive cobble and boulders (up to 2 m diameter) of rounded to sub-rounded quartzite clasts.

In the grabens within the AAMF, the Bou Salda Formation is thicker (several hundreds of metres thick) and four members are recognised. The basal volcanic unit here includes andesitic agglomerate and vesicular basalt flows, while the sedimentary member contains conglomerates up to 150 m thick with quartzite and granite boulders over 1 m in diameter. Overlying the clastic rocks in this region is a volcanic unit made up of over 1000 m of red rhyolitic ignimbrite and minor ash-fall tuff, overlain by massive grey amygdaloidal basalts with epidote-filled vesicles and intercalations of acid tuff, in turn succeeded by lenses of brown dolomite. Finally, the uppermost unit contains over 2000 m of purple shale and an upper green quartzite. This unit is strongly deformed (cleavage in the shale, folding in the quartzite) due to movement along the AAMF.

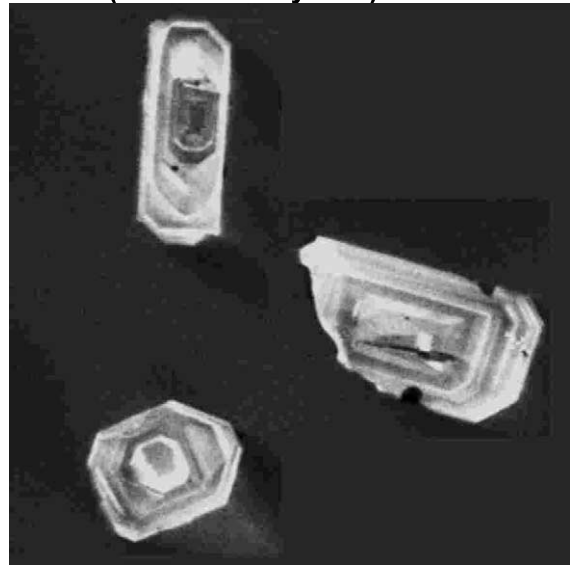
Two rhyolitic units, the *Tamriwine* and *Tadmant Rhyolites* occupy the same stratigraphic position, time interval and spatial distribution as the Bou Salda Formation, being intrusive into, but interleaved with the Sarhro Group, but overlain by the Ouarzazate Group (Fig. 11). It is possible that they are related to Bou Salda magmatism and are thus considered here.

The *Tamriwine Rhyolite*, composed of rhyolite, volcanic breccia, tuff and ignimbrite, has been thrust over the northern margin of the Zenaga Complex. The formation is unconformably overlain by the Ouarzazate Group, which it closely resembles lithologically. Brabers (1988), who first noted this age relationship, proposed that the Tamriwine rhyolites represent a phase of continental volcanism related to rifting at the onset of Bleïda Group deposition and thus represents a continental volcanic facies of the rifted margin sediments of the Taghdout Subgroup. The base

consist of a ~3-m thick volcanic breccia grading up into ignimbrite and rhyolite. Owing to repeated southeast-vergent thrusting, the succession is often repeated and apparently inverted with basement slivers lying structurally above the basal agglomerate.

No field relationships are seen between the Tamriwine Formation and the Sarhro Group, but identical rhyolitic rocks are interlayered with greywackes of the Sarhro Group in the Zgounder silver mine area. These rocks form a 400–1000 m thick unit known as the *Tadmant Rhyolite*. While the contacts are broadly parallel with the bedding

### GM 73 (Tadmant Rhyolite)



### GM 191 (Tamriwine Rhyolite)



Fig. 14. CL images of zircons from the Tadmant and Tamriwine Rhyolites.

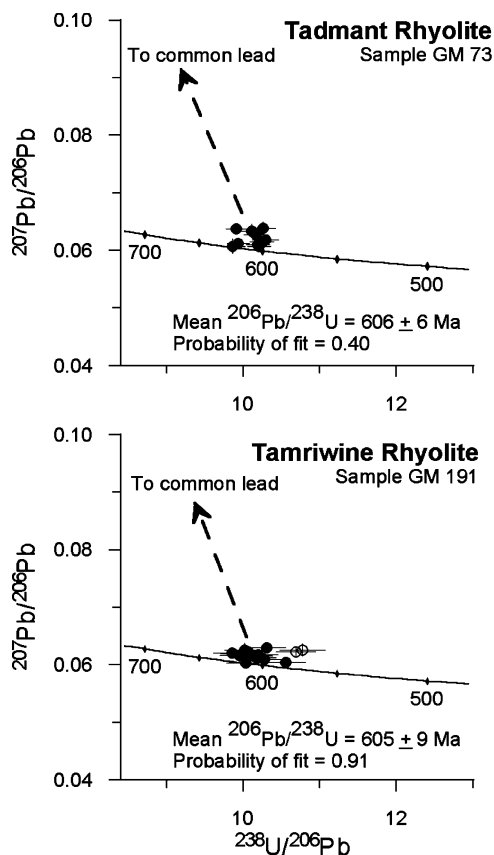


Fig. 15. Tera-Wasserberg plots of SHRIMP data from the Tadmant and Tamriwine Rhyolites.

of the Sarhro Group, local cross-cutting relationships show that the rhyolite is intrusive into the sedimentary rocks and the entire body takes the form of overlapping rhyolite domes with ignimbritic phases (see also Zemouri and Rjimati, 1995). The lithology varies from pink rhyolite porphyry to flow-banded rhyolite, ignimbrite and tuff.

### 3.5.1. Geochronology, geochemistry and depositional setting of the Bou Salda Formation

The age of the Bou Salda Formation has not directly been determined, but the closely associated Tadmant and Tamriwine Rhyolites were dated. Zircon morphologies are described in Table 2 and CL images given in Fig. 14. The rhyolites gave statistically identical SHRIMP dates of  $605 \pm 9$  and  $606 \pm 6$  Ma respectively (Fig. 15). These

dates are taken as the age of crystallisation of the rhyolites and provide the best estimate of the age of the Bou Salda Formation.

Representative geochemical analyses of basaltic rocks from the Bou Salda Formation and the Tadmant Rhyolite show that, compared to the basalts of the Tasriwine ophiolite, the Bou Salda basalts are enriched in  $K_2O$ ,  $TiO_2$ , Rb, Ba, Zr, Nb, Pb, Th and U and can be classified as arc basalts (see also Schermerhorn et al., 1986). Thus the sedimentary and volcanic composition of the Bou Salda Formation suggests it represents arc-derived clastic and volcanic rocks that were deposited in narrow fault-bound troughs as the fore-arc basin was contracting and the arc complex was being uplifted and eroded. It thus forms part of a syn-collisional, proximal and progradational, subarkosic to arkosic volcanoclastic succession above the Azarwas Formation.

Both in its stratigraphic position and composition, the Bou Salda Formation may resemble the Tidiline Formation of the Bou Azzer region (e.g. Hefferan et al., 1992) and the Azarwas Formation of the Sarhro Group. The Tidiline Formation has also been interpreted to represent syn-collisional molasse deposits derived from an uplifted and dissected arc (Hefferan et al., 1992).

### 3.6. Post-Sarhro Group plutonism (Assarag Suite)

Deformation of rocks older than the Sarhro Group was followed by an important period of plutonism during which massive batholiths and plutons of the late- to post-tectonic *Assarag Suite* were emplaced. The most important of these is a vast polyphase intrusion known as the *Askaoun batholith* which covers over  $800 \text{ km}^2$  in the NW part of the Sirwa Window (Fig. 16). In addition to 'normal' Askaoun Granodiorite, the suite in the High Atlas region includes other older and younger granitoids, some of which form the composite *Ida-ou-Ilouen batholith*. They are discussed in chronological order, as established from cross-cutting relationships, below.

#### 3.6.1. Askaoun batholith

The *Amlouggui Tonalite* appears to be the oldest phase of the Assarag Suite. It is a coarse- even-

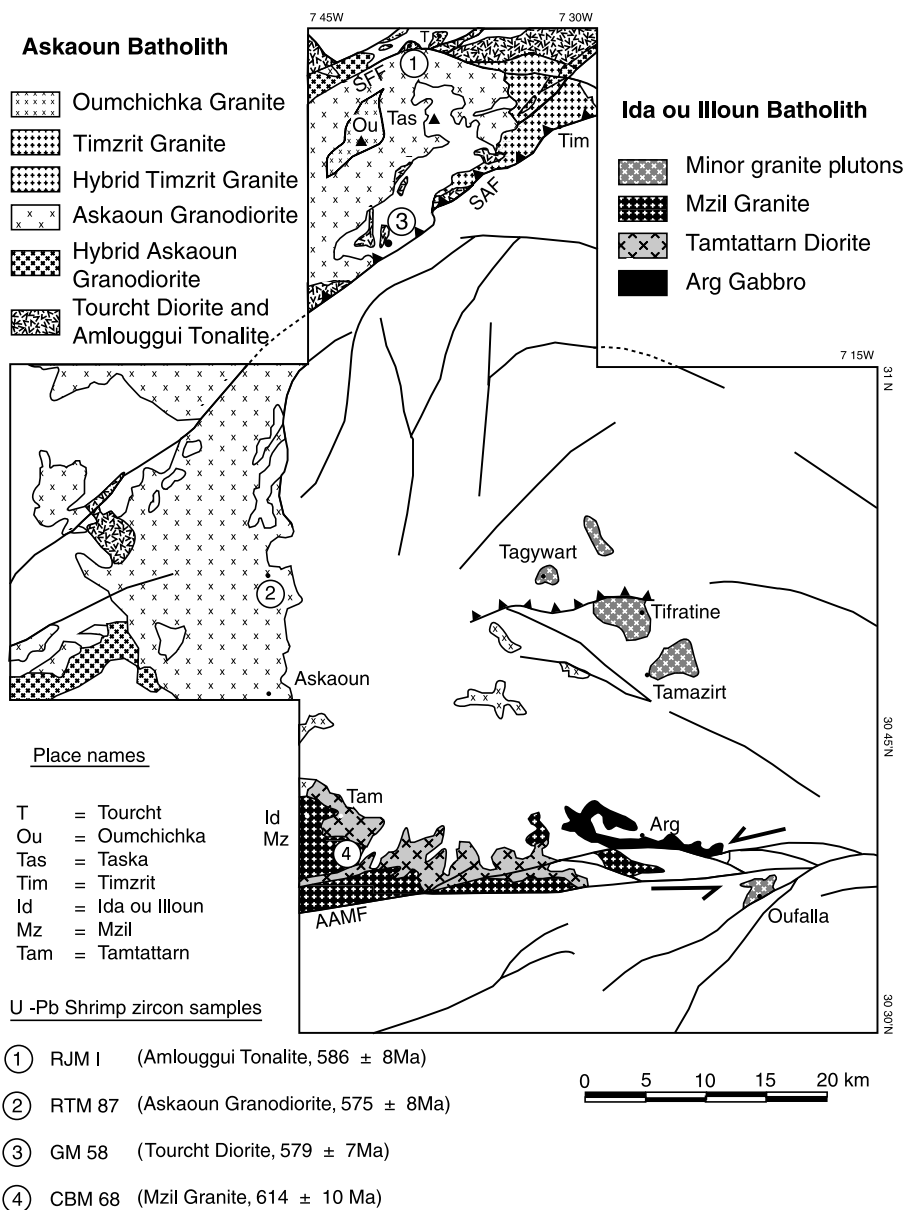


Fig. 16. Distribution of the Assarag Suite.

grained (average grain size 2–4 mm), foliated, homogenous mesocratic granitoid which appears to intrude the gneisses of the Ourika Complex and has a tectonic foliation parallel to that of the gneisses. In the field, the structural and fabric parallelism between the Amlougui Tonalite and the Ourika Complex suggested that the former

might be an intrusive phase of the Ourika Complex. The Tonalite is made up of quartz (~15%), sericitised plagioclase (55%), poikiloblastic hornblende (25%) and subordinate biotite (5%), with accessory opaque mineral, zircon and apatite. The gneissic texture is defined mainly by parallel preferred orientation of amphibole and mica.

The *Tourcht Diorite* is also one of the older intrusive phases of the Assarag Suite. In the High Atlas, the diorite intrudes the Sarhro Group rocks as irregular plutons, sheets and vein networks of anastomosing apophyses. The diorite complex is heterogeneous, ranging from fine- to medium-grained, dark grey microdiorite to medium-grained (1–2 mm), ocellar and porphyritic types. The diorite is typically complexly mixed, veined and intermingled with the Askaoun Granodiorite. Contacts of the various components of these igneous mélanges range from sharp to diffuse. Porphyritic diorites contain plagioclase phenocrysts measuring up to  $3 \times 5$  mm in size and constituting up to 20% of the rock. ‘Typical’ *Tourcht Diorite* contains altered hornblende (55–65%, often with clinopyroxene cores), sericitised/saussuritised plagioclase (andesine to albite) with  $\sim 5$ –10% quartz and accessory titanite, zircon and ore minerals. The *Tourcht Diorite* develops into a hybrid phase where it has been intruded by the Askaoun Granodiorite and other granites. The contacts of the hybrid phases are usually continuously gradational, suggesting penecontemporaneity and magma mixing processes. Locally this hybrid mixture develops a ductile foliation comprising decimeter-scale layers of diorite with parallel bands of granitic material. This ductile banding is gradationally replaced by sets of sub-parallel brittle shears, especially near tectonic contacts with the Ourika Complex. Such features suggest that the deeper root of the Askaoun batholith exposed here is late syntectonic with respect to Pan-African deformation, unlike the unfoliated, post-tectonic relationships seen at higher levels to the south.

The coarse-grained (2–5 mm average grain size), non-porphyritic, unfoliated, grey, *Askaoun Granodiorite* covers in excess of 600 km<sup>2</sup> in the west of the area, where it gives rise to extremely rugged topography. The *Askaoun Granodiorite* is demonstrably intrusive across folds and cleavage in the Sarhro Group, which is hornfelsed in a  $\sim 1$ -km wide contact aureole. The granodiorite is made up of quartz, andesine, subordinate K-spar, brown biotite and green hornblende (with rare relict augite), together with accessory opaque mineral, apatite, and zircon  $\pm$  titanite in mafic aggregates.

Zircon typology studies on the Askaoun Granodiorite by Regragui (1997) suggest a calc-alkaline parentage. This typical mineralogy varies in proportions such that a complete spectrum of compositions from quartz diorite ( $\sim 10\%$  quartz), through to leucocratic granodiorite ( $\sim 30\%$  quartz) are represented. Thus, in some areas, a melanocratic, quartz dioritic phase occurs which has the same mineralogy as the main phase, but the proportion of biotite and hornblende is higher (Colour Index 30–40%). Local increases in K-feldspar content give rise to monzogranitic varieties.

A younger, dark-grey, slightly finer-grained phase (and slightly more mafic than the main phase) was recorded from a number of localities in the western parts of the batholith. The fine-grained phase has plagioclase and hornblende phenocrysts in a fine grained ( $\sim 2$  mm) matrix. The granite has a slightly heterogeneous, contaminated/hybridised appearance. It is composed of quartz, plagioclase (often zoned and variably sericitised), K-spar (+ some myrmekite), hornblende, biotite, opaque mineral and apatite. Secondary epidote is commonly observed.

Rounded plagioclase–porphyroblastic dioritic enclaves (autoliths and/or *Tourcht Diorite*), in the 10–50 cm size range, are common in the Askaoun Granodiorite, tending to occur in certain well-defined zones. In some of these, the host rock is so heavily contaminated that a ‘hybrid phase’ of the pluton has been mapped (*Hybrid Askaoun Granodiorite* on Fig. 16). Such zones occur in the SW part of the batholith and in the High Atlas Mountains, where the Askaoun Granodiorite locally forms the high watershed. In these zones, blocks and screens of diorite (and more scarce xenoliths of other lithologies such as basalt, amphibolite and ultramafic country rocks), up to hundreds of metres in size, are intimately admixed with the granodiorite. The enclaves seen in the granodiorite in the Askaoun area were studied in detail by Regragui (1997), who recorded both monzodioritic and quartz dioritic compositions. These large blocks are themselves extensively veined by the host Askaoun Granodiorite, giving rise to a complex igneous mélange of granodiorite and diorite or other exotic lithologies in which

there is a general age progression from mafic (older) to felsic (younger). This picture is rendered still more complex by the ubiquitous presence of mafic dykes. In the western Ourika Valley (High Atlas) the hybrid granodiorite is complexly mixed with a range of amphibolitic and ultramafic rock types suggesting that this region exposes a deeper part of the pluton where magma mingling of acid and mafic phases occurred. In this zone, dense concentrations of subangular to sub-rounded amphibolitic and dioritic clasts (typically 20–40 cm long, but up to several metres in size) showing marked parallel orientation and partial, peripheral digestion.

The Askaoun Granodiorite is transected by fractured zones of pervasive fluid alteration. These zones are up to more than 1 km wide, characterised by sericitisation and saussuritisation with green–grey plagioclase and pink K-feldspar; and sporadically formed spots and fracture-filled veinlets of epidote.

In the northern part of the Sirwa Window, upthrust masses of the Askaoun batholith form an extensive part of the High Atlas range between Taska Mountain and the Tizi-n-Tichka pass (~20 km of watershed). The batholith in this region is a complex mélange of associated polyphase plutons and igneous facies. Some of these are mafic in composition, whilst others show a weak tectonic fabric suggesting that the outcrops may represent the uplifted roots of the batholith.

The *Oumchichka Granite* forms a large massif which intrudes the Askaoun Granodiorite in the High Atlas. It is a coarse-grained, pink, unfoliated leucogranite with characteristic purple quartz, pink micropertthitic K-spar, plagioclase, ~2–5% chlorite after biotite and accessory opaque mineral, zircon and apatite. The *Timzrit Granite* is a white-weathering, pale grey leucogranite containing large rounded quartz grains up to 1 cm across. It crops out along the south flank of the High Atlas where it intrudes the Askaoun Granodiorite. The granite is typically highly weathered and crushed, having in many localities been involved in the South Atlas thrust front where it is intruded by a swarm of altered dolerite dykes. It is typically composed of large quartz aggregates (35%), partly saussuritised albite (up to 60%)

with sericitised microcline (~15%), dark green biotite partly altered to chlorite (~5%) ± hornblende, zircon, apatite and ore. The Timzrit Granite locally interfingers complexly with Tourcht Diorite. A mappable contaminated/hybrid phase is recognised (*Hybrid Timzrit Granite* on Fig. 16).

### 3.6.2. *Ida-ou-Illoun batholith*

South of the Miocene Sirwa volcano, a large plutonic body, the *Ida-ou-Illoun batholith* consists of an association of gabbro, diorite, granodiorite, porphyritic to microporphyritic monzogranite and leucogranite (Jouider, 1997), which are here grouped with the Assarag Suite on grounds of their post-tectonic relationship towards the Sarhro Group. The most mafic unit, the *Arg Gabbro* is exposed in the central part of the Sirwa Window, mainly within the AAMF, where it occurs as stacked thrust slices and tectonic fragments intruding the Bleïda and Sarhro Groups. The gabbros are dark grey coarse-grained rocks with cumulate olivine, idiomorphic clinopyroxene (partly retrogressed to tremolite) and plagioclase ± orthopyroxene. In thrust zones the gabbros are converted progressively to foliated amphibolites, with uralitised and epidotised pyroxene and the growth of metamorphic biotite.

A number of plutonic units of intermediate composition are represented in the Assarag Suite. The *Tamtattarn Diorite* is an unfoliated, mesocratic diorite in which two phases are recognised, one coarse-, the other fine-grained. The diorite intrudes the *Arg Gabbro* with diffuse contacts, indicating penecontemporaneity, which has led to well-developed hybrid/magma-mixing textures. The diorite is unfoliated, meso- to melanocratic and greyish, locally with white idiomorphic, zoned plagioclase phenocrysts in an even-grained matrix. It consists of hornblende, plagioclase, minor quartz and accessory titanite with secondary chlorite, biotite, sericite, muscovite, epidote and calcite.

The most acid phase of the *Ida-ou-Illoun batholith* is the porphyritic *Mzil Granite*, a light grey to pinkish granite with equant K-spar phenocrysts (~1 × 1 cm<sup>2</sup>–5 cm), set in a matrix of coarse-grained quartz and feldspar with subhedral grains

of biotite and hornblende. Phenocryst alignment, which was observed, represents an igneous fabric. The granite intrudes the Arg Gabbro and Tamattarn Diorite.

### 3.6.3. Minor granite plutons

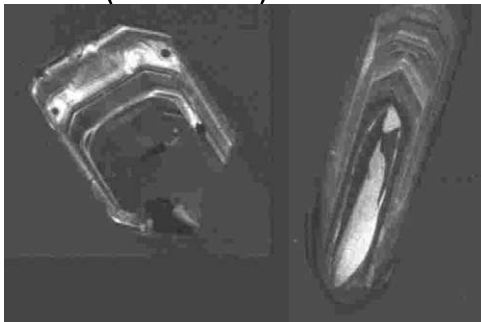
Four *Minor granite plutons* of the Assarag Suite also occur in the central part of the Sirwa Window (Fig. 16). The *Tagaywart Tonalite* is a equigranular rock composed of plagioclase and quartz with chloritised biotite, epidote, zircon, apatite and tourmaline. The *Tifratine* and *Tamazirt Granites* are medium-grained, pink granites containing hypidiomorphic, equigranular albite/oligoclase,

quartz, chloritized biotite and K-feldspar with accessory titanite, apatite, zircon, monazite, tourmaline, magnetite and hematite. They crop out in the central-east parts of the Sirwa Window and may be connected at depth. The unfoliated *Oufalla Granite* in the AAMF is a medium- to coarse-, even-grained, white to pale, pink K-spar-rich leucogranite, which contains xenoliths of deformed Bleida Group rocks and Arg Gabbro.

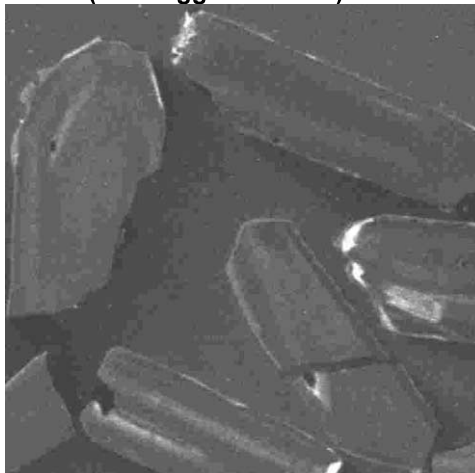
### 3.6.4. Geochronology of the Assarag Suite

Zircons from four units of the Assarag Suite were dated. Zircon morphologies are described in Table 2 and CL images of typical grains shown in

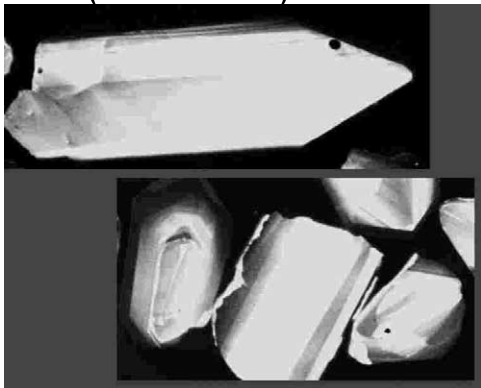
**CBM 68 (Mzil Granite)**



**RJM 1 (Amlouggui Tonalite)**



**GM 58 (Tourcht Diorite)**



**RTM 87 (Askaoun Granodiorite)**

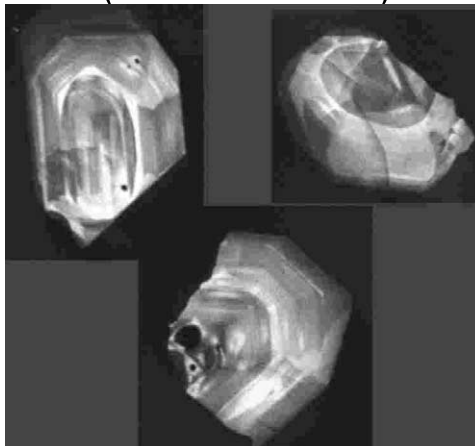


Fig. 17. CL images of zircons from the Assarag Suite.

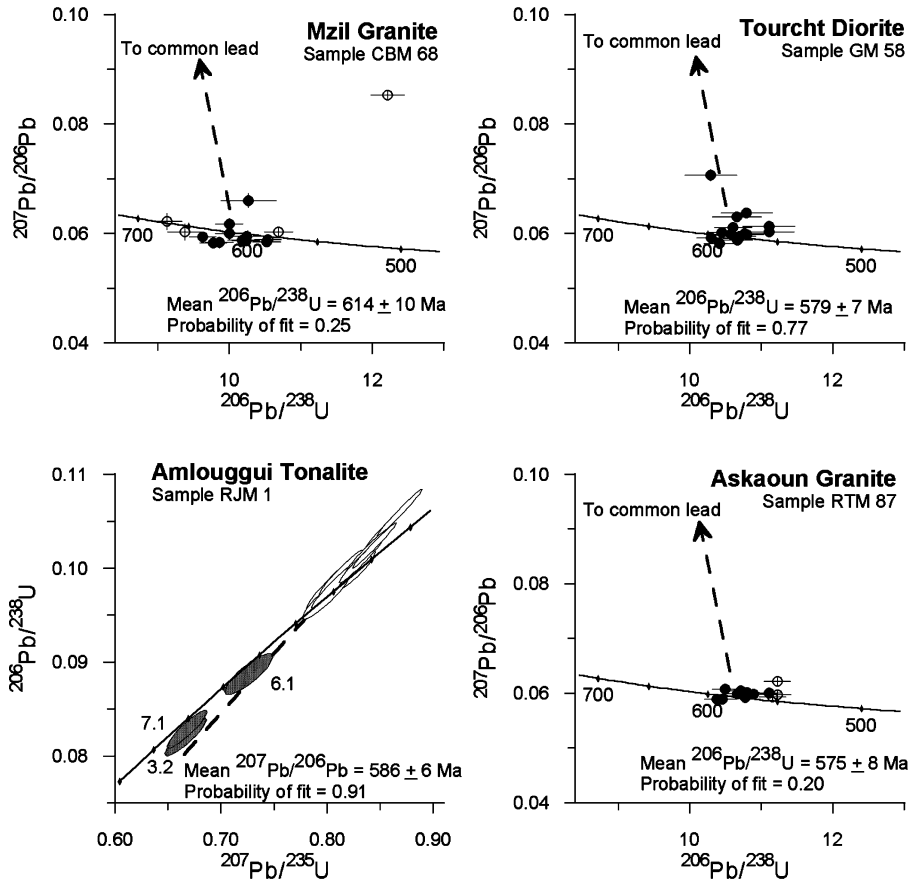


Fig. 18. Tera-Wasserberg plots of SHRIMP data from the Assarag Suite.

Fig. 17 and plotted on Fig. 18. The zircon SHRIMP analyses of zircons from the Mzil Granite indicate a crystallisation age of  $614 \pm 10$  Ma. An older, inherited component yielded a date of  $660 \pm 10$  Ma, which is thought to relate to zircons formed during the main Anti-Atlas tectonothermal event at the same times as the growth of metamorphic rims of zircons in the Irii Migmatite (Section 3.2.3). The Mzil Granite, and by implication the Ida-ou-Iloun batholith, represents the oldest dated component of the Assarag Suite, the other units dated yielding ages of  $586 \pm 8$  Ma for the *Amlougui Tonalite*,  $579 \pm 7$  Ma for the *Tourcht Diorite* and  $575 \pm 8$  Ma for the *Askaoun Granodiorite*. Aït Malek et al. (1998) have reported similar dates for the Tarcouate granodiorite

( $584 \pm 14 / -8$  Ma), Tarcouate gabbro–diorite ( $575 \pm 2$  Ma) and the Taourgha granite  $560 \pm 2$  Ma, units from the Bas Draa and Kerdous Inliers, SW of the Sirwa Window.

Biotite-whole-rock Rb–Sr dates were obtained from two samples of these Neoproterozoic granites (CBM 68, Mzil Granite; RTM 86 Askaoun Granodiorite). The data give Pan-African dates of  $582 \pm 10$  Ma and  $559 \pm 8$  Ma respectively (Table 4), 20–50 Ma younger than the corresponding SHRIMP dates. These are interpreted as dating cooling of the crust in this area below a temperature of approximately 300 °C. These data confirm earlier work summarised by Charlot (1976) and Cahen et al. (1984) indicating that, unlike some of the Precambrian windows further west in the Anti-

Table 4  
Rb–Sr mica data from various lithologies of the Sirwa Window

| Sample                 | $^{87}\text{Rb}/^{86}\text{Sr}$ | $^{87}\text{Sr}/^{86}\text{Sr}$ | Date (Ma) $\pm$ 95%    |
|------------------------|---------------------------------|---------------------------------|------------------------|
| CBM 226<br>(feldspar)  | 16.79                           | 0.946667 $\pm$ 38               | 1006 $\pm$ 16<br>model |
| CBM 226<br>(muscovite) | 23.18                           | 1.100135 $\pm$ 44               | 1190 $\pm$ 19<br>model |
| CBM 68<br>(biotite)    | 6.733                           | 0.761172 $\pm$ 32               | 582 $\pm$ 10           |
| CBM 68                 | 0.9714                          | 0.713361 $\pm$ 16               |                        |
| GM 220<br>(biotite)    | 2.912                           | 0.730189 $\pm$ 75               | 525 $\pm$ 12           |
| GM 220                 | 1.041                           | 0.716190 $\pm$ 19               |                        |
| GM 242<br>(muscovite)  | 820                             | 20.9613 $\pm$ 3                 | 1718 $\pm$ 27<br>model |
| RTM 86<br>(biotite)    | 2.801                           | 0.728627 $\pm$ 21               | 559 $\pm$ 8            |
| RTM 86                 | 0.2858                          | 0.708598 $\pm$ 14               |                        |

$^{87}\text{Rb}/^{86}\text{Sr}$  values quoted are relative to a mean value of  $0.710331 \pm 20$  (1 sigma on 11 analyses) for NIST 987 strontium standard. Model dates for minerals calculated for assumed  $^{87}\text{Sr}/^{86}\text{Sr}$  of 0.705. Where possible, mica dates have been calculated on the basis of mineral–whole rock pairs. Analytical uncertainties are 0.8% for  $^{87}\text{Rb}/^{86}\text{Sr}$ , 0.01% for  $^{87}\text{Sr}/^{86}\text{Sr}$ . Error correlations of 0.76 and 0.50 have been assumed for mica and feldspar respectively and 0.00 for all other samples.

Atlas, the Sirwa Window was not significantly thermally overprinted by the Hercynian or younger orogenesis.

### 3.6.5. Geochemistry of the Assarag Suite

The wide chemical variability of the components of the Assarag Suite is apparent on the TAS and FMA plots in Fig. 19a and b, where the sub-alkaline/calc-alkaline magmatic character is demonstrated. ASI increases with  $\text{SiO}_2$  content and all the granitic members are markedly peraluminous in character. Members of the suite become markedly more potassic ( $\text{K}_2\text{O}/\text{Na}_2\text{O}$  ratios increase) with increasing silica but some degree of alkali mobilisation is apparent in the granitic units with more than 70%  $\text{SiO}_2$ . Thus they are classed as High-K calc-alkaline granitoids (e.g. Ennih and Liégeois, 2001). Among the trace elements Ba and Rb show a fivefold increase in concentration over

the  $\text{SiO}_2$  range of 45–65% but are both variable in the granites. The variations in alkali oxides, Rb and Ba in the high- $\text{SiO}_2$  granitic components are consistent with late-stage albitisation.

Field relationships indicate a clear post-tectonic setting for the Assarag Suite intrusives. The mafic component of the Ida-ou-Ilou batholith, the Arg Gabbro, plots within the fields anticipated for MORB-related magmas on the Pearce and Cann (1973) discrimination diagrams (Fig. 19c) whereas the felsic components of the Assarag Suite (including the remainder of the Ida-ou-Ilou components) have trace element signatures more consistent with granitoids derived from volcanic arc settings (Fig. 19d) as defined by Pearce et al. (1984). Only the Imaghoudene granite has a within-plate granite signature. Such inconsistencies between field/geological constraints and geochemical signature are not uncommon (e.g. see papers in Weaver and Johnson, 1987). Pearce (1996) showed that granites derived through processes operating in post-collisional tectonic settings have trace element signatures that overlap those generally found in granites generated in arc, within-plate and syn-collisional settings. Significantly, all the Assarag granitoids fall within this field in Fig. 19d.

### 3.7. Ouarzazate Group

The Ouarzazate Group constitutes the thickest and most extensive sequence of the Anti-Atlas Supergroup, covering nearly 50% of the surface area of the Sirwa Window (Fig. 20). It is a highly complex post-orogenic volcanic/volcaniclastic succession with subordinate clastic–epiclastic sediments that unconformably overlie the Bleïda and Sarhro Groups and the post-tectonic granitoids. Throughout the Sirwa Window, the products of five volcanic centres, each with its own stratigraphic succession, have been identified. Only one of these centres is demonstrably situated within the window itself. These aspects, together with extreme basement topography variations, makes geological mapping and unraveling of the stratigraphy difficult. The separate volcanic complexes have been defined on the basis of their internal geometry, distribution and stratigraphy as well

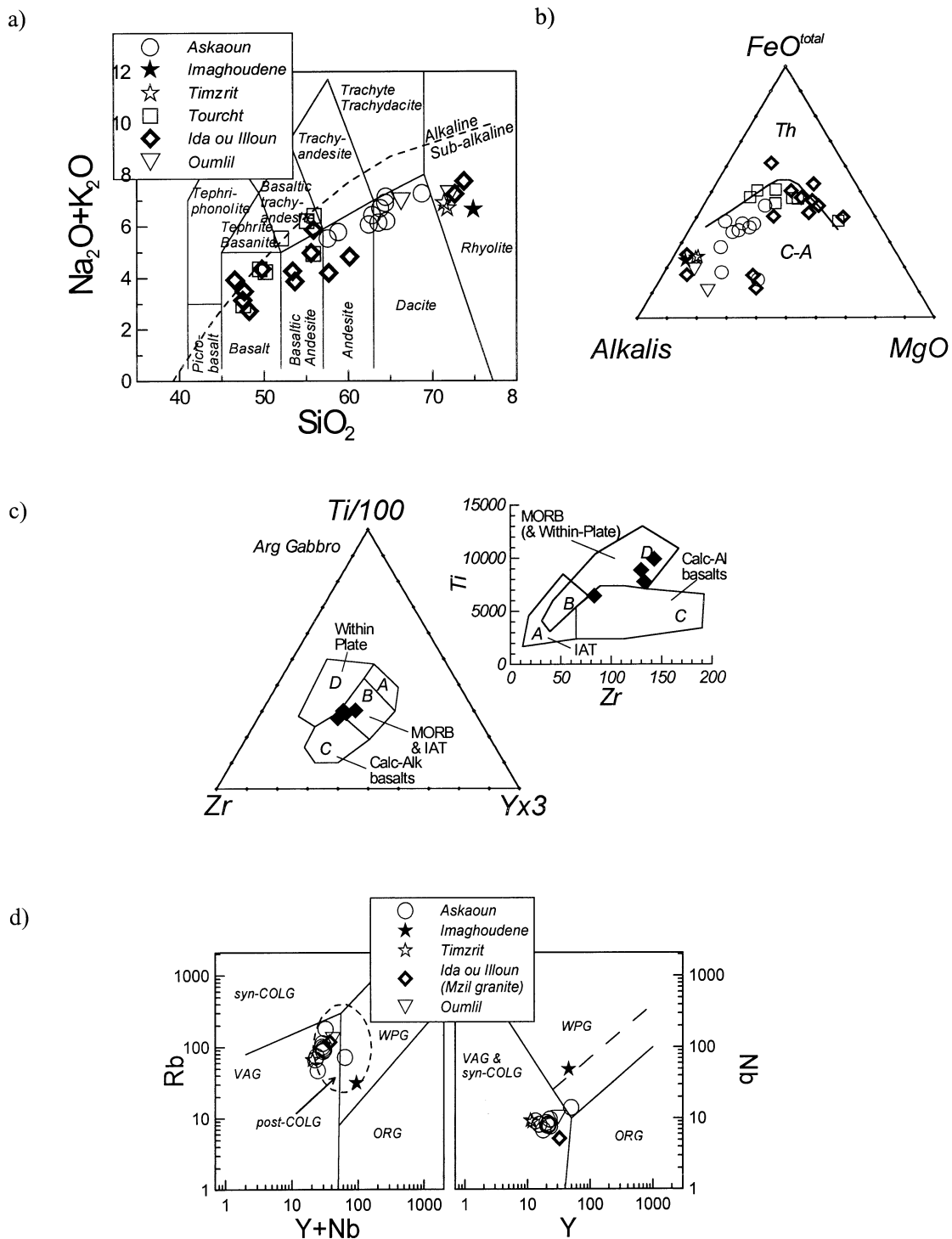


Fig. 19. Geochemical plots of the plutonic rocks of the Assarag Suite. (a) Silica-alkalis (TAS) plot, (b) FMA plot, (c) Arg gabbro (Ida-ou-Illoun batholith) plotted on the Pearce and Cann (1973) diagram; (d) granitoids plotted on Pearce et al. (1984) diagrams, with field for post-collision granites (post-COLG) from Pearce (1996).



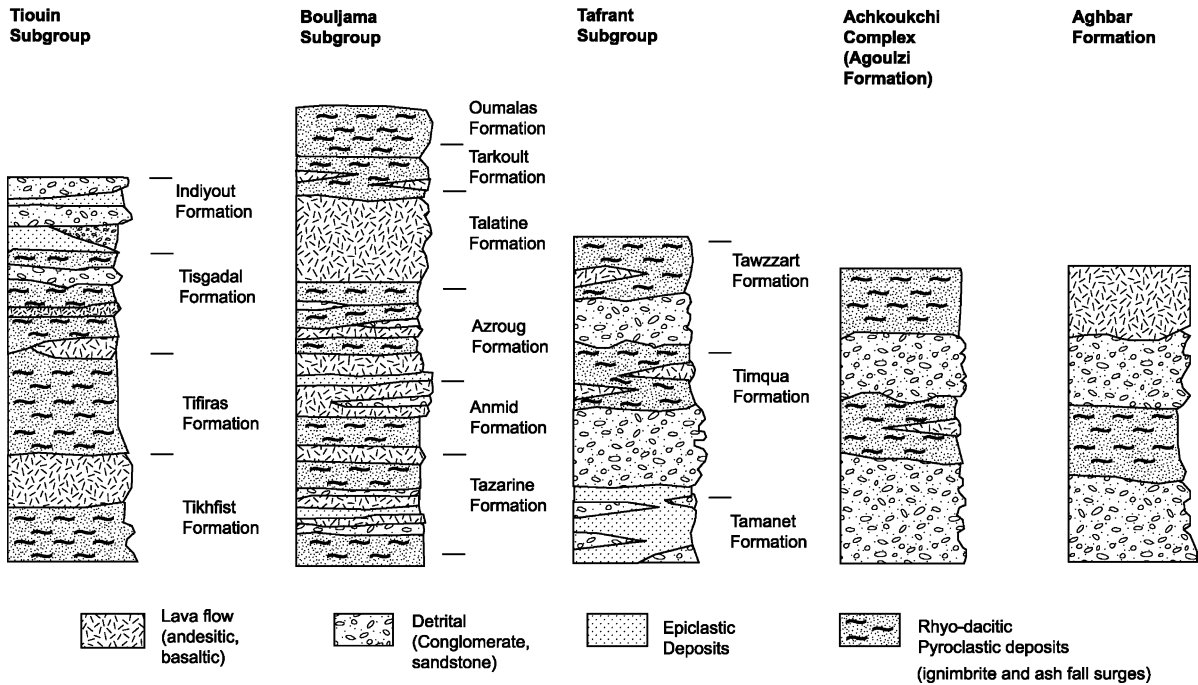


Fig. 21. Schematic stratigraphic logs through the five major units of the Ouarzazate Group (not to scale).

inter-relationships between conformable packages. The term ‘Subgroup’ was applied to layered successions of volcanic, volcanoclastic and sedimentary rocks whereas the term ‘Complex’ refer to successions that also contain a subvolcanic intrusive phase. In broad stratigraphic order, the *Tiouin*, *Bouljama* and *Tafrant Subgroups* and the *Achkougchi Complex* are recognised, whilst the *Aghbar Formation* is the thinner, distal product of a more remote volcanic centre. The stratigraphy of the various volcanic centres is schematically illustrated in Fig. 21.

### 3.7.1. Volcano-sedimentary rocks

3.7.1.1. *Tiouin Subgroup*. Four formations are recognised within the *Tiouin Subgroup*, each predominantly composed of volcanic rocks, with volcano-sedimentary and epiclastic rocks becoming more important towards the top (Fig. 21). The basal *Tikhfist Formation* is made up of three members, commencing with a basal sedimentary succession containing red epiclastic sandstones, shales and conglomerates with minor columnar-

jointed andesites, rhyolites and tuffs and rare stromatolitic limestone lenses. It is succeeded by volcanic rocks of rhyolitic to dacitic composition with minor andesites. The massive rhyolites are composed of spectacularly flow-banded units with accretionary lapilli tuffs. The uppermost member is composed of massive pyroclastic deposits and purple porphyritic andesites and dacites. Local green mudstones with thin chert beds occur.

The overlying *Tifiras Formation* is entirely pyroclastic and has been sub-divided into two members. The lowermost is predominantly comprised of massive rhyolites (often ignimbritic), agglomerates and tuffs, followed by an upper tuffaceous member. The succeeding *Tisgadal Formation* comprises a well-stratified package of volcanic and pyroclastic rocks. It is subdivided into three members made up of basal tuffs and volcanic breccias with rare basalt, a middle dacite-rhyolite unit with a 10 m thick basal conglomerate and an upper andesitic unit overlain by repeated cycles of lapilli tuff and layered ignimbrite.

The highest exposed stratigraphic unit in the *Tiouin Subgroup* is known as the *Indiyout Forma-*

tion. It is predominantly an epiclastic sedimentary succession comprising a basal package of coarse clastic, conglomeratic rocks (mainly volcanic clasts), a middle red volcanoclastic member (almost 300 m of agglomeratic, conglomeratic and tuffaceous rocks), topped by fining-up conglomerate-epiclastic gritstone-tuffaceous cross-bedded sandstone cycles. The uppermost, acid volcanic member, is composed of ignimbrites and lapilli tuffs and a prominent rhyolite horizon.

**3.7.1.2. Bouljama Subgroup.** The Bouljama Subgroup occupies the NW part of the Sirwa Window, but it is not certain where the main centre is situated. It contains thick volcanic deposits with subordinate detrital rocks, subdivided into six formations, not all of which are developed in any one place. In addition, each unit is marked by massive, local facies variations (Fig. 21).

The *Tazarine Formation* comprises four members. The lowermost unit comprises andesitic agglomerate, tuff, volcanic breccia and ignimbrite with minor rhyolite and andesite layers. Towards the top, gritty, arkosic sandstone and cobble-conglomerate occur interbedded with massive ignimbritic rhyolite. The subsequent member is composed mainly of andesitic to rhyolitic rocks, massive agglomerate and thin, well-bedded, epiclastic beds containing quartzite clasts, along with feldspar porphyry flows. Above this lies a series of fine-grained porphyritic andesite, tuff and agglomerate, as well as green rhyo-porphyry and rhyolitic ignimbrite, with a prominent conglomerate locally developed at the base. Finally, an uppermost member of strongly altered, dark green–grey andesite is sporadically developed.

The lowermost *Anmid Formation* has a basal member consisting of a thick succession of volcanic breccia and rhyolitic ignimbrite with interbedded tuffs, andesites and massive grey plagioclase–porphyritic dacitic to trachyandesitic and andesitic/basaltic andesitic lavas. It is overlain by a highly altered coarse porphyritic basaltic to andesitic lava with feldspar glomero-porphyritic phenocrysts up to 3 cm in length. The lavas are often vesicular with amygdales filled with quartz, calcite, chlorite and oxides which display complex zonation (Zahour, 1990). This member is overlain

by volcanic breccia and a layered succession of andesite, dacite, rhyolite and basalt with cyclic interbedded tuff, breccia, ignimbrite and minor sandstone. The uppermost member consists of red shales, sandstones and tuffs.

The overlying *Talatine Formation* consists of lava flows. It has been subdivided into a lower member made up of massive, structureless feldspar porphyritic felsic lava and an upper succession of andesite. The lower member is overlain by a sequence of massive lavas with variable composition from purple and grey andesites to light grey flow-banded trachytes and minor black flinty, feldspar porphyritic rhyolites/dacites. Red-weathering ignimbrites with relatively minor agglomeratic lenticles appear near the top.

The overlying *Azroug Formation* commences with a very prominent rhyolite flow, overlain by a well-layered volcanic succession comprising volcanic breccia, agglomerate, basalt, andesite, dacite, ignimbrite and sandstone. In general the entire formation is characterized by repeated cycles of andesite-agglomerate/tuff/sandstone–rhyolitic/dacitic ignimbrite.

The *Tarkoult Formation* conformably overlies the Azroug Formation and is composed mainly of yellow-weathering rhyolitic ignimbrite and rhyolite with tuffs, lapilli-tuffs and agglomerate. Mafic andesitic and basaltic lenses occur in places. The *Oumalas Formation* is a well stratified succession of trachy–andesite, andesite and pyroclastic tuffs, contained within a semi-circular depression, possibly a caldera. On the eastern side of the structure, thick feeder dykes have been intruded parallel to its boundary. It contains a lower unit of flat-lying trachy-andesitic lava flows with phenocrysts of sanidine and clinopyroxene. Overlying porphyritic andesite flows are steeply dragged down against one of the feeder dykes in the east, whereas the flows gently dip inward ( $10^\circ$ ) in the western parts of the structure. The centre of the structure is occupied by pyroclastic rocks with alternating air fall deposits, surge deposits, crystal and ash flows and pumice and ash flows. Other facies, corresponding to plinian eruptions, consist of layered deposits with millimetre-scale glass shards, xenoliths, small pumices, autoclasts and fine ash.

**3.7.1.3. Tafrant Subgroup.** The Tafrant Subgroup occurs south of the AAMF and is restricted to the southeastern parts of the Sirwa Window. It is a predominantly detrital unit with subordinate volcanic deposits (Fig. 21). It is made up of three formations, one of which is only exposed in the far south, south of a highstand in the Zenaga Complex basement. This subgroup displays extreme facies variation, in some measure due to the irregularity of the Zenaga Complex floor upon which it was deposited. Many low-angle intraformational unconformities are present in the succession.

The lowermost *Tamanet Formation* primarily consists of epiclastic sedimentary rocks with varying proportions of brown fining-upward sequences of small-pebble conglomerate, gritstone, sandstone and shale with interbedded tuff and agglomerate. A lenticular, angular scree-conglomerate, up to 15 m thick, sporadically occurs along the basal unconformity surface. Another distinctive and laterally continuous, highly chaotic fan-conglomerate unit in the middle part of the formation, with volcanic and quartzite clasts up to 1.5 m in size in a purplish–red matrix, has been afforded member status. Some regionally extensive sheets of maroon porphyritic rhyolite occur towards the top of the formation.

The base of the succeeding *Timqa Formation* is defined by a conglomerate member up to 100 m thick. It consists of poorly-sorted pebble- (10 mm diameter) to cobble-sized (100 mm diameter), subangular to subrounded clasts of andesite, rhyolite, quartzite, granite and various epiclastic/pyroclastic fragments. The rest of the unit comprises several identical cycles of greenish to reddish rhyolitic air-fall, lapilli-tuffs grading upward into reworked greywacke, ending in red mudstones with desiccation cracks. This cyclic sequence of ~100 m thick is discordantly overlain by a 3–5 m thick volcanic avalanche breccia member, comprising angular volcanic fragments embedded in a lapilli-ash matrix.

South of a basement high of the Zenaga Complex known as the Kourkda High, the Tafrant Sub-group is represented by the *Tawzzart Formation*. At the base, a coarse-grained boulder conglomerate is sporadically developed, overlain by a

mixed volcanoclastic sequence of tuffs and pyroclastic breccias, with fine-grained green andesite flows. A prominent, thick but laterally discontinuous greenish rhyolite unit has been named the Aguin Member and was selected for SHRIMP dating (see below).

**3.7.1.4. Achkougchi Complex.** The *Achkougchi Complex* occupies a central position within the Sirwa Window lying directly beneath the Neogene Sirwa volcano (Fig. 20). Intrusive and extrusive members of this complex have a circular exposure pattern probably reflecting its original caldera outline, with the core occupied by subvolcanic granitic/granophyric intrusions. The same Neoproterozoic volcanic centre was reactivated in the Neogene during the Sirwa event.

The volcano-sedimentary component of the complex is represented by the *Agoulzi Formation*, comprising a basal red conglomerate, sandstone and shale member, composed entirely of reworked volcanic material, succeeded by an andesitic member with lavas, tuffs and ignimbrites and an upper conglomerate/breccia topped by a columnar-jointed rhyolite–ignimbrite member. The plutonic component of the complex (e.g. the Amassine granite, grading locally into rhyolite) is described in the intrusive section, below.

**3.7.1.5. Aghbar Formation.** A distinct, relatively thin Ouarzazate Group volcano-sedimentary sequence crops out in the extreme western part of the Sirwa Window (Fig. 20). As it is so much thinner than the other subgroups, it has been afforded Formation status. The *Aghbar Formation* begins with a basal conglomerate member, consisting of rounded to sub-rounded granite cobbles and boulders, overlain by a well-bedded purple, epiclastic sandstone/shale unit (Fig. 21). The conformably overlying rocks are ash-fall tuffs and agglomerates, overlain by fine-grained greywacke, with some interbedded chert units. A third member is a clastic sedimentary and epiclastic sequence composed of grey and pinkish cross-bedded arkosic sandstones and grits, interbedded with tuffaceous layers and thin layers and lenticles of cream-coloured cinerite up to a few centimetres thick. The uppermost unit is composed of massive to

weakly-stratified micro-porphyrific lavas of rhyolitic to andesitic composition. Certain zones within this unit have been extensively pyrophyllitised. The pyrophyllite forms white to pale-green, irregular, lenticular, stratiform and locally transgressive bodies, which are developed in the vicinity of faults and, in some places small acid dykes. The rocks have been described in Caia et al. (1968), who recognised conversion of the volcanic rocks into three main types of pyrophyllite–kaolinite–quartz rocks, contemporaneous with the extrusion of the country rocks and related to the action of terminal-volcanic hydrothermal fluids. The rocks of the Aghbar Formation are viewed as the distal deposits of a fifth volcanic centre, located well to the west of the exposed Sirwa Window.

### 3.7.2. *Syn-Ouarzazate Group intrusive rocks*

As noted, the Ouarzazate Group is intimately associated with coeval high-level granites and a large number of acid (and minor basic) intrusions. For simplicity, these are broadly grouped together into the *Toufghrane Suite* (Fig. 20). While some of the granites can be linked to specific Ouarzazate Group volcanic centres, many cannot. Some plutons are simple, others polyphase. Some granites are coarse-grained, others fine-grained and grade into quartz porphyries. Yet others are associated with minor intrusions such as plugs, necks and dyke swarms. While it would be repetitive to discuss all the granites and associated rocks that have been identified, they can be grouped into a number of different types and associations, each of which, with some examples are described below.

**3.7.2.1. Coarse-grained, simple plutons.** In the western and northern part of the Sirwa Window, large bodies of a coarse-grained pink granite known as the *Imourkhsane Granite* are conspicuous (Fig. 20). This granite is typical of those not obviously associated with any particular volcanic centre. It is a homogenous, pink coarse-grained (3–5 mm average grain size), homophaneous alkali leucogranite with red K-spar, subordinate turbid greenish cream coloured plagioclase and sparse flecks of greenish chlorite. Quartz grains are typically rounded and graphic texture common.

Well-rounded xenoliths of medium-grained diorite occur. The granite is pervasively hydrothermally altered and associated with disseminated molybdenite flakes.

**3.7.2.2. Polyphase plutons.** One of the best examples of a syn-Ouarzazate Group polyphase pluton is the *Tilsakht Granite*, intruded into the northern part of the Zenaga Complex (Fig. 20). This pluton takes the form of a ring complex with a diameter of some 6 km. Zenaga Complex gneisses are exposed in the core. The intrusion comprises three phases. The oldest is a fine-grained, greenish, sub-granophyric microgranite/microgranodiorite which forms the central outcrops. The microgranite is intruded by a grey, fine-grained microgranite with scattered, small plagioclase phenocrysts up to 1 cm in size. Both these phases are intruded by a coarse-grained, pink K-spar rich biotite leucogranite which constitutes by far the volumetrically most important phase and makes up the ring of prominent mountains which rise from the Zenaga plains. The granite shows extensive subsolidus alteration (hydrothermal?), with kaolinisation of K-spar, sericitisation of plagioclase and partial to total pseudomorphing of mafic minerals by chlorite, epidote and opaque minerals. Cracks infilled with haematite are common and much of the red colouration of the granite (mainly in K-spar) results from pervasive haematisation.

The *Tidzi Granite* which crops out in the NE part of the Sirwa Window is a two-phase intrusion. It contains a medium- to coarse-grained, orange- to pink-weathering K-spar-rich leucogranite and a finer grained dark phase which is locally dioritic to monzonitic in composition. Xenoliths of Ouarzazate Group volcanic rocks were observed within the pluton. The granite is hydrothermally altered and is occasionally cross-cut by centimeter-thick veins of brecciated acid volcanic material and barite-calcite-specular hematite crystals.

**3.7.2.3. Fine-grained granites, associated with minor intrusive phases.** The *Ongougane Granite* includes large (< 1 km strike-length), fine-grained leucogranitic and felsic porphyry bodies taking the form of elongate masses and irregular plutons and a major felsic dyke swarm in the NW part of the

area around Assarag. Many of the dykes in the swarm are composite, with basaltic cores and flow-banded rhyolite margins. Some individual dykes can be traced for over 15 km. Locally the dykes form dense swarms, some of which have been named in the literature (e.g. the ‘Daroufarnou dykes’ of Huch, 1988 near Tachoukacht). The dykes intrude the lower part of the Ouarzazate Group, so presumably fed the upper parts of the volcanic pile. The felsic dykes are fine-grained (~0.5 mm average groundmass grain size), granoblastic rocks with granophyric textures locally developed (locally in small quartz–feldspar rosettes), and composed of quartz–feldspar–minor opaque mineral (pyrite or magnetite) ± zircon and secondary chlorite. They usually contain 1–2 mm sized microphenocrysts of sericitised plagioclase or microcline and rarer rounded quartz microphenocrysts with embayment (resorption) textures. The Ongougane Granite forms fairly substantial elongate, lensoid, but dyke-like bodies. The larger masses of Ongougane Granite tend to be very irregular in shape and form. At the margins, these bodies form a ramifying network of anastomosing dykes and veins. Some of these apophyses continue for several kilometres into the country rocks as well-defined dykes, which also locally split into smaller dyke networks and in turn coalesce into more substantial irregular bodies. The *Ighrem Granite* crops out in extreme NW part of the area, as a locally flow-foliated, fine- to medium-grained granite, with a surface area of some 25 km<sup>2</sup>.

**3.7.2.4. Granites genetically associated with specific volcanic centres.** Granitic rocks associated with a specific volcanic centre occur beneath the massive Miocene volcano of Sirwa in the centre of the window (Fig. 20). The *Amassine Granites* lies in the central caldera of the Achkougchi Complex volcanic assemblage. It encompasses a number of alkali feldspar granites. The *Boutazart pluton* is an unfoliated medium-grained leucogranite with K-spar, some albite and quartz, and with minor biotite, zircon and opaques. It contains characteristic ~4 mm sized round quartz grains and K-spar

microphenocrysts set in a fine-grained (locally cryptocrystalline) groundmass. It grades laterally into rhyolite. The granite is associated with acid (quartz–feldspar porphyry, texturally similar to the granite) and mafic (basalt and dolerite) dyke swarms which can be shown to have been emplaced both simultaneous with, and after the Achkougchi Complex. The *Boutazart granite* grades laterally into rhyolite towards the edge of the volcanic centre. The volcanic centre straddles the AAMF and is obscured beneath the much younger (Miocene) deposits of Sirwa volcano. Clearly, this zone has been subject to repeated volcanism over time. In addition to the *Boutazart Granite*, the Achkougchi centre is associated with the *Tikitar Granite*, a quartz–feldspar porphyritic leucogranite and the *Tazoult Quartz Porphyry*, a pink sheet-like intrusion with large (5 mm) rounded, resorbed quartz and brick-red euhedral K-spar phenocrysts.

**3.7.2.5. Acid and basic minor intrusions.** In addition to the dykes visibly associated with certain granites, the whole Sirwa Window abounds with minor intrusions lithologically identical to the Ouarzazate Group. For example, in addition to the *Tilsakht Granite*, the *Zenaga Complex* is intruded by a number of rhyolitic domes, necks and felsite dykes of Ouarzazate Group age. These rocks doubtless formed the feeders for the extrusive rocks of the Ouarzazate Group, now eroded away from the roof of the *Zenaga plains*. *Rhyolitic domes* and *necks* occur throughout the *Zenaga Complex*, forming prominent rocky hillocks which rise up to over 150 m above the plains (Fig. 20). Most are a few tens to hundreds of metres across, with the biggest massif of Adghagh measuring 2 × 0.5 km<sup>2</sup>. The latter body has a border facies of explosive volcanic breccia comprised of rhyolite and country rock clasts (schist, granite) set in a tuffaceous matrix. Many of the smaller bodies are sub-circular in form and made up of pinkish rhyolite with concentric flow-banding sub-parallel to the margins. Some are made up of massive, white scoriaceous, vesicular quartz–feldspar porphyry. Yet other bodies are composed entirely of

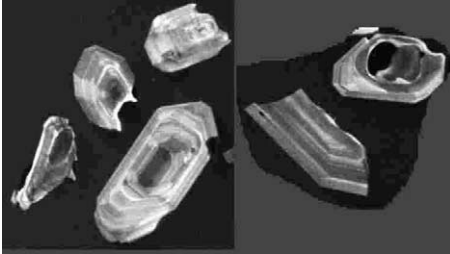
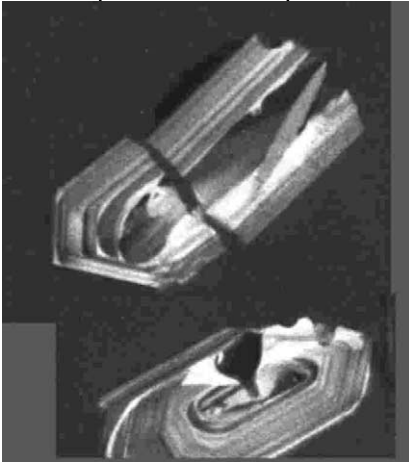
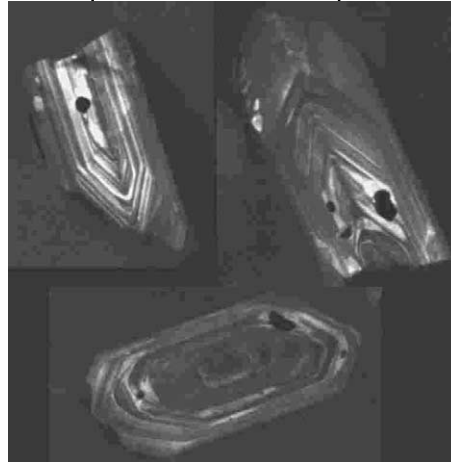
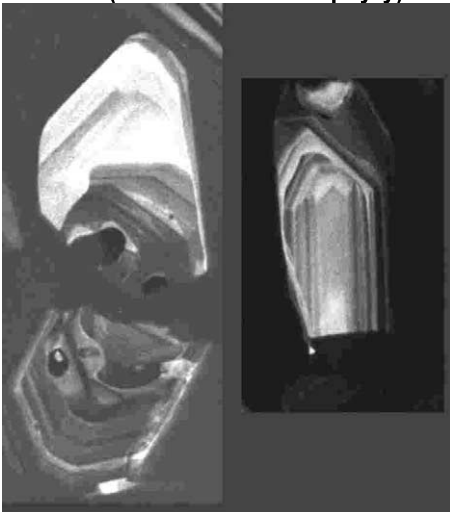
**CM 7 (Tawzzart Formation)****GK 313 (Tikhfist Formation)****GM 220 (Tilsakht Granite)****GM 51 (Imourkhsane Granite)****RTM 154 (Tazoult Quartz Porphyry)**

Fig. 22. CL images from two Ouarzazate Group rhyolites and three syn-Ouarzazate Group granites.

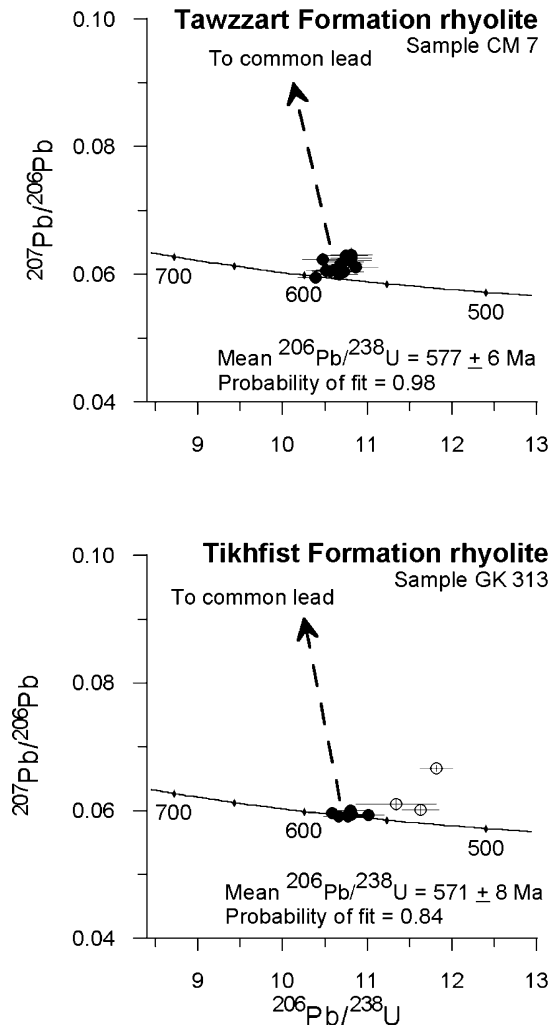


Fig. 23. Tera-Wasserberg plots of the Ouarzazate Group rhyolites.

vent breccia. A number of flow-banded rhyolite dykes intrude the Zenaga Complex. Most are only a few metres in width and can be followed for a few tens or hundreds of metres along strike.

The Ouarzazate Group rocks are invariably strongly ferruginised and have caused extensive reddening and purpling of the Zenaga Complex country rocks. Indeed, the generally purplish- to brown-weathered nature of most outcrops of the

Zenaga Complex is probably due to the hydrothermal/deuteric alteration effects of the passage of felsic Ouarzazate Group age magmatism and by their covering with the hot volcanic pile during late Neoproterozoic times. The strongly ferruginous nature of this alteration is probably the source for the myriad small specular haematite deposits which are found throughout the Zenaga plains.

Whilst the minor intrusive rocks of the Zenaga Plains are easy to identify, on account of their huge lithological contrast with the basement gneisses, such intrusions within the Ouarzazate Group itself are harder to recognise. However, in the central parts of the Sirwa Window, a number of dyke-like intrusions and small stocks of the *Tourirt Granite* are intrusive in the Ouarzazate Group volcanic rocks. The granite is composed of even-grained, leucocratic pink granite which intrudes a greenish-grey microgranitic phase.

The Ouarzazate Group is associated with a number of *dyke swarms* (Fig. 20). The most dense swarm, in the NW, has broadly SSW–NNE trend over a width of several kilometres and a strike-length of more than 50 km, where dykes constitute up to 10% of the total rock mass. The most prominent swarms intrude the Askaoun batholith. The mafic dykes range from apophyses and stringers, a few centimetres wide, up to substantial bodies up to 25 m in width. It is common to find several phases of dyke intruded along the same fracture, leading to composite dykes. Some dolerite dykes transect the lower formations of the Ouarzazate Group and are thus post-Ouarzazate in age, but it is probable that pre-Ouarzazate Group mafic dykes are also present.

The mafic dykes show variability, with a large range in grain sizes apparent. Some dykes are plagioclase-phyric whilst others are aphyric. In the former, some dykes contain small plagioclase phenocrysts (~1 mm). Others, of more andesitic composition, contain large (up to 1 cm in length) ‘feathery’ plagioclase phenocrysts which are identical in lithology to flows in the Anmid Formation and thus probably represent feeders. Despite the field variability in grain size and phenocryst content, less variability in the mineralogy is seen.

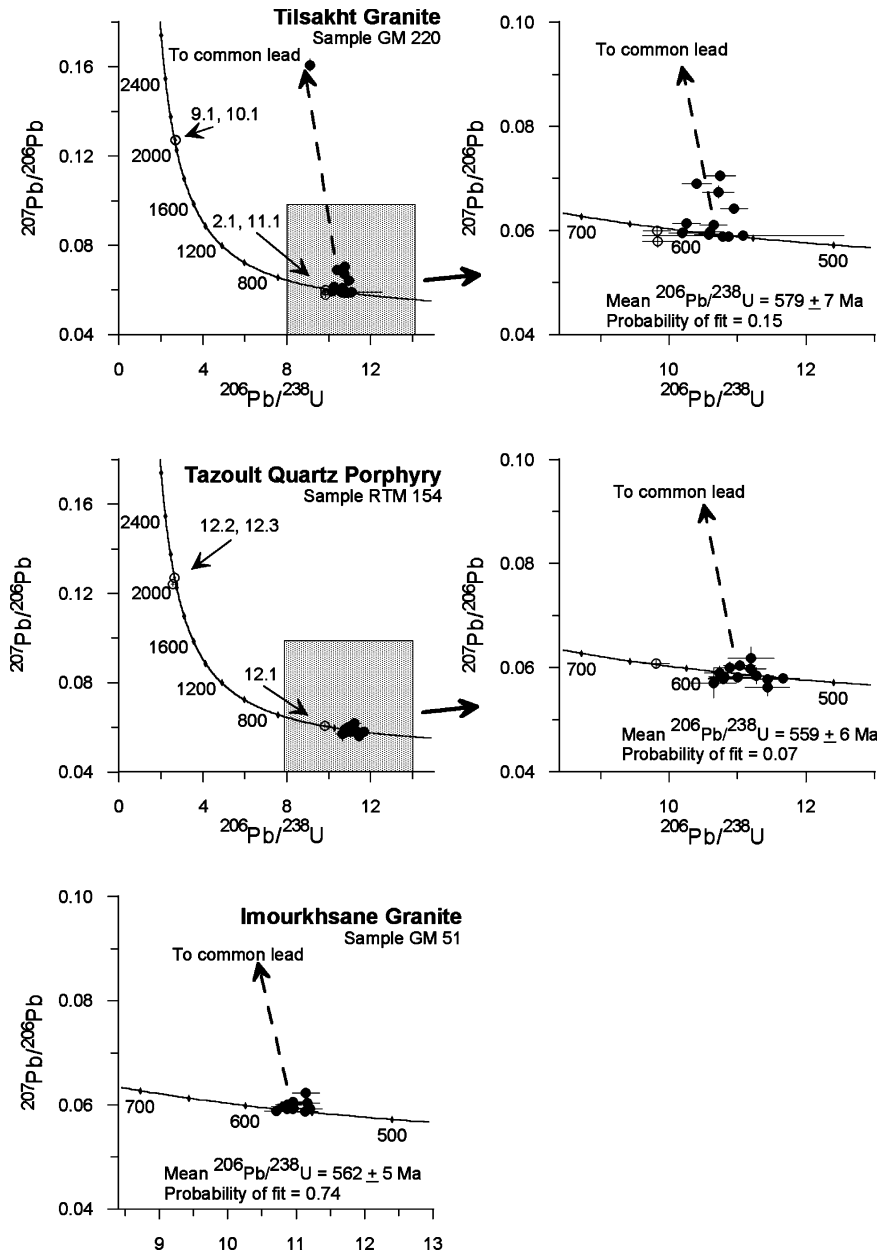


Fig. 24. Tera-Wasserberg plots of the syn-Ouarzazate Group granites.

The mafic dykes of all swarms are almost uniformly composed of plagioclase in sub-ophitic relationship with pale pink titaniferous augite, abundant ilmenite, accessory apatite and interstitial secondary chlorite and epidote. Phenocrysts

tend to be totally replaced by fibrous sericite, whilst groundmass plagioclase is less altered. A few fine-grained, basaltic, dykes appear to be amygdaloidal, with small ( $\sim 1\text{--}2 \text{ mm}$ ) vesicles filled with dolomite, and/or chlorite and epidote.

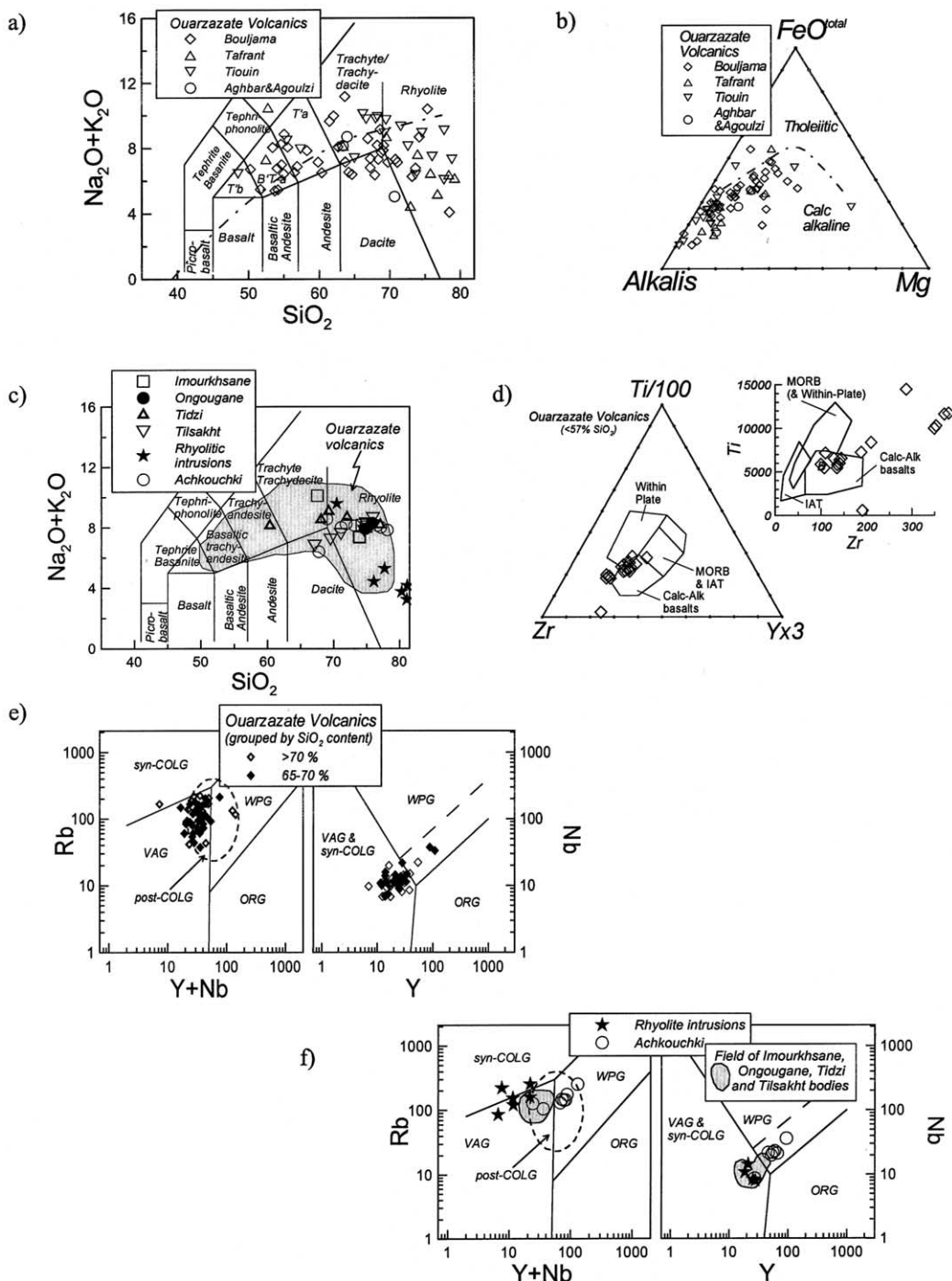


Fig. 25. Geochemical plots of the volcanic rocks of the Ouarzazate Group: (a) Silica-alkalis (TAS) plot; (b) FM A plot; (c) silica-alkalis (TAS) plot of Syn-Ouarzazate Group intrusive rocks; (d) Pearce and Cann (1973) plot for volcanics with < 57% SiO<sub>2</sub>; (e) Pearce et al. (1984) plots for volcanics with > 65% SiO<sub>2</sub>; (f) Pearce et al. (1984) plot for syn-Ouarzazate Group intrusives. Field for post-collision granites (post-COLG) is from Pearce (1996).

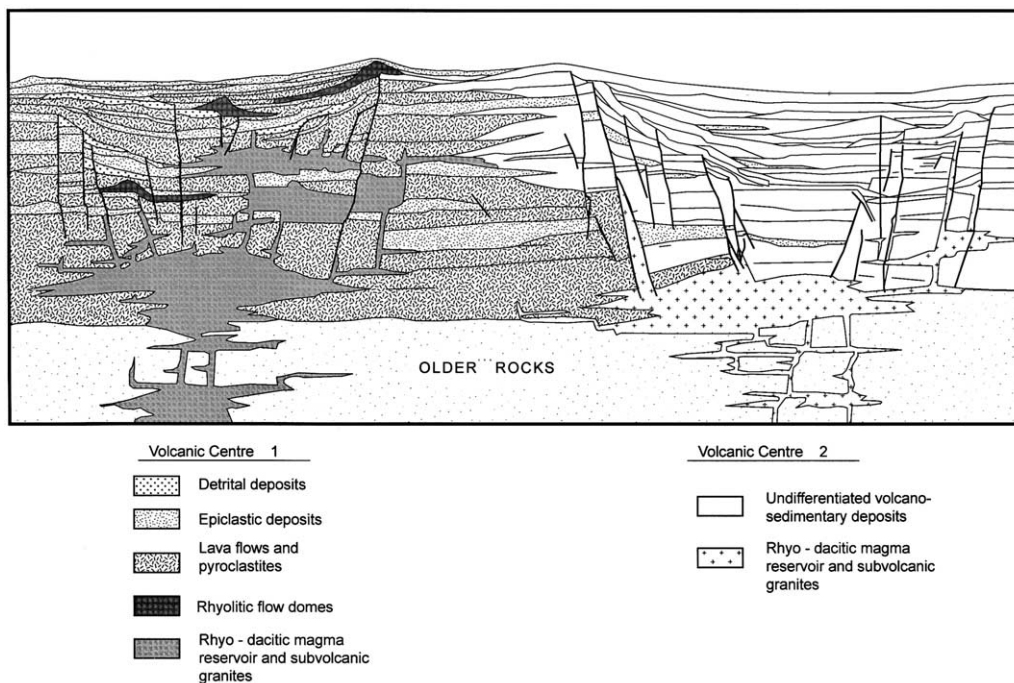


Fig. 26. Idealised cross-section part of the Ouarzazate Group illustrating the interdigitation of separate volcanic centres, growth faults and rapid facies variation.

### 3.7.3. Geochronology of the Ouarzazate Group and coeval intrusive rocks

Two rhyolite samples from two different volcanic centres, north and south of the AAMF, were dated. Zircon morphologies are outlined in Table 2 and CL images given in Fig. 22. The rhyolites gave identical SHRIMP ages: Tiffist Formation (Tiouin Subgroup)  $571 \pm 8$  Ma and the *Tawzzart Formation* (Aguins Member, Tafrant Subgroup)  $577 \pm 6$  Ma (Fig. 23).

The volcanic centres are marked by collapsed calderas with coeval sub-volcanic granite plutons. Three examples of granites, from slightly different settings were dated and gave statistically identical ages. The polyphase ring-like *Tilsakht Granite* (not obviously spatially associated with volcanic rocks) yielded an age of  $579 \pm 7$  Ma (Fig. 25). This granite intrudes the Zenaga Complex supracrustal schists

and the zircon population includes inherited components with a date of  $2060 \pm 10$  Ma, similar to the inherited dates obtained from the Zenaga granitoids. These dates probably relate to the precursor rocks to the Zenaga schists. The *Imourkhsane Granite* is also not obviously associated with volcanic rocks, but intrudes the lower part of the Ouarzazate Group. A SHRIMP date of  $562 \pm 5$  Ma was obtained which is younger than the ages of the *Tilsakht Granite* and the volcanic rocks (Fig. 24). Finally, the *Tazoult Quartz Porphyry* (Achekouchi Complex) gave an identical date of  $559 \pm 6$  Ma. (Fig. 24), suggesting that the Achekouchi Complex, with the *Imourkhsane granite*, are the youngest components of the Ouarzazate Group. The sample of *Tazoult Quartz Porphyry* contains inherited zircon components of  $\sim 2045$  Ma, again probably inherited from the Zenaga

Complex. Two of the granites had zircon components with dates of  $\sim 625$  Ma, which does not correlate with any obvious known event, but may derive from unexposed, or unidentified, late-tectonic source rocks.

The dates reported here are similar to those reported by Mifdal and Peucat (1985) from rhyolites and ignimbrites of the Jebel Bachkoun-Tiouine areas in the Sirwa window. Recalculated dates (allowing for scatter in the data) are:  $577 \pm 10/-4$  Ma (rhyolite);  $586 \pm 323/-24$  Ma (ignimbrite) and  $562 \pm 4/-3$  Ma.

A biotite-whole-rock Rb–Sr date of  $525 \pm 12$  Ma was obtained from samples GM 220 of the Tilsakht Granite, some 50 Ma younger than the corresponding SHRIMP date. This date represents the time of cooling of the crust in the Zenaga area below a temperature of approximately 300 °C, again showing that the Sirwa Window was not significantly thermally overprinted by Hercynian or younger orogenies.

Two samples of Ouarzazate rhyolites and one of the Tazoult Quartz Porphyry were analysed for Sm and Nd isotopes (Table 3). The volcanics yield statistically identical  $\epsilon_{\text{Nd}}$  of  $+1.98 \pm 1.4$  (lower) and  $+2.87 \pm 1.4$  (upper) with  $T_{\text{DM}}$  dates of 837 and 1029 Ma respectively. The granite sample has a  $\epsilon_{\text{Nd}}$  within error of zero ( $+0.37 \pm 1.4$ ) and  $T_{\text{DM}}$  of 1100 Ma. These data argue that these siliceous magmatic rocks were derived from relatively juvenile crust, crust generated in a similar fashion to the 743 Ma TTG gneiss (Iriru Migmatite-GM 119) and plagiogranite (TRM 117).

#### 3.7.4. Geochemistry and depositional setting of the Ouarzazate Group and coeval intrusive rocks

A large number of volcanic rocks from all five volcanic centres have been analysed for major and trace elements. On standard TAS and FMA plots (Fig. 25a and b) the volcanic rocks define a compositionally diverse calc-alkaline series which straddles the alkaline/sub-alkaline divide.

The coeval intrusive rocks are compositionally similar to the more siliceous members of the Ouarzazate volcanic rocks as demonstrated on the TAS plot (Fig. 25e). Most of the intrusives are markedly peraluminous in character—ASI indices of 1.0–1.2 being characteristic.

In broad terms, similar evolutionary trends can be seen in each of the subgroups, each grades from basaltic or andesitic volcanic rocks at the base to dacitic–rhyolitic volcanic rocks in the middle and an upper acid volcanoclastic-dominated sequence (cf. also Bajja et al., 1998; Ben Chra, 1997). As noted before, there is a clear distinction between Ouarzazate Group deposits north of the E–W trending AAMF tectonic zone, with predominantly volcanic rocks in the north and dominantly clastic rocks to the south. This fault zone is interpreted as a rejuvenated rift-initiation fault belonging to the post-collisional extensional molasse basin that eventually evolved into a marine foreland basin in the Cambrian. To explain the extrusion of the Ouarzazate Group volcanic rocks in the Bou Azzer–Bleïda region, Azizi Samir et al. (1990) postulated a NW–SE extensional event with synvolcanic sinistral WNW–ESE and NE–SW faulting. The orientation of these faults was doubtless determined by older structures and differ from area to area. As noted before, the Ouarzazate Group rocks which crop out in the Sirwa Window were the products of coeval, separate, but inter-fingering volcanic centres in the manner illustrated conceptually in Fig. 26.

Previously published geochemical studies (e.g. Bajja et al., 1998; Ben Chra, 1997) interpret the lower andesitic Ouarzazate volcanic rocks as the products of a calc-alkaline, subduction-related, volcanic-arc complex, and the upper rhyolitic volcanic rocks as late-orogenic and post-tectonic acidic volcanism. Bajja et al. (1998) used this argument to propose a redefinition of the Ouarzazate as referring only to the upper acid phase and relocating the lower andesitic portion to the Sarhro Group. Stratigraphically, structurally and sedimentologically, however, this interpretation is untenable as the traditionally-defined Ouarzazate Group (followed here) is without question a single stratigraphic group, less deformed than, and unconformably overlying, the older deformed successions such as the Sarhro Group. Nevertheless, the andesitic, calc-alkaline nature of the lower volcanic rocks, apparently anomalous in the extensional rift environment envisaged for the Ouarzazate Group (which is typically characterised by bimodal volcanism) then has to be explained.

Ouarzazate volcanic rocks are plotted on the tectonic discrimination diagrams of Pearce and Cann (1973; less than 55% SiO<sub>2</sub>), Pearce et al. (1984) and Pearce (1996), for more siliceous volcanics, in Fig. 25c and d, respectively. The less siliceous Ouarzazate volcanics plot in the compositional field of island arc calc-alkaline basalts whereas the more siliceous volcanics have compositions equivalent to those found in granitic rocks generated in volcanic arcs or in post-collisional settings. Analyses of the syn-Ouarzazate granitoid intrusives plot mostly within the volcanic arc/syn-collision granite field in (Fig. 25f). The Achkouchki granite, however, has higher Nb and Y compositions-comparable to those found in within-plate granitoids whereas the rhyolitic intrusions have lower Nb concentrations which cause them to plot outside the field of post-collision granitoids.

Field relationships in the Sirwa region clearly shows that even the lowermost Ouarzazate formations post-date post-tectonic intrusions such as the Askaoun Granodiorite, themselves emplaced after subduction, collisional deformation and uplift of the arc had occurred (e.g. Gresse et al., 1998). To a large degree the chemistry of the siliceous volcanics and several of the granitoid intrusions are consistent with such a rifted, post-collisional setting. It is proposed that the apparent arc-related chemical signature of the volcanic rocks of the lower half of the Ouarzazate Group is a continued reflection of the composition of the preceding, subducted arc rocks from which they were sourced.

### 3.8. Tata Group

The late Neoproterozoic to Cambrian sedimentary rocks of the Tata Group crop out over large areas of the periphery of the Sirwa Window, often preserved in the cores of fault-bounded synclines. Over much of the area the Tata Group lies unconformably/para-unconformably on the Ouarzazate Group, often with an angular discordance of up to 20°.

The Tata Group typically commences with a brown to reddish-brown, upward-coarsening basal conglomerate, the *Tamallakout Formation*. This

coarse clastic unit is up to 100 m thick, but in other places, particularly over local basement highs, it is very thin or absent. It is everywhere overlain by a succession of well-bedded light brown colour, pinkish brown to grey dolomites known as the *Adoudou Formation*. Towards the top, the dolomite, which is typically 200 to over 350 m thick, is interbedded with maroon, red and purple shales, mudstones and interbedded sandstones of the overlying *Taliwine Formation* (= Lie-de-Vin Formation).

Deposition of the Tata Group followed the post-orogenic molasse volcanoclastic rocks of the Ouarzazate Group. With continued extension in the late Vendian this molasse basin developed into a marine foreland basin in which the Tata Group was deposited, with transgressive, shallow marine carbonate deposition followed by marginal continental red-beds deposited during a regressive event. Stable oxygen isotope study of Margaritz et al. (1991), and the U–Pb zircon geochronology of Compston et al. (1992) and Landing et al. (1998), suggest that the Cambrian–Precambrian boundary at ~540 Ma lies near the base of the Tata Group, somewhere in the Adoudou–Taliwine Formations (see also Geyer and Landing, 1995). The succeeding Cambrian and younger sedimentary rocks of the upper part of the Tata Group (including the second major dolomite unit, the *Igoudin Formation*) are widespread over the Anti-Atlas and the Sirwa Window and will not be considered further.

## 4. Structural and metamorphic features

The main structural and metamorphic features of the rocks of the Sirwa Window have been described in the foregoing account of the lithostratigraphy. It is outside the scope of this article to give a detailed structural analysis and a complete account of all the metamorphic assemblages in this large area of complex geology—such detailed information is given in the seven sheet explanations cited in Section 1 and in other references in the text. It is however necessary to reiterate the main structural and metamorphic features in chronolo-

gical order to set the scene for the concluding section.

#### 4.1. Palaeoproterozoic basement

The *Zenaga Complex* is composed entirely of metamorphic rocks. The oldest gneisses and schists show polyphase ductile folding and shearing and were metamorphosed to amphibolite grade as shown by: garnet–sillimanite assemblages in metapelites; hornblende–plagioclase assemblages in metabasites; and garnet–epidote–plagioclase assemblages in calc-silicate rocks. Partial melting occurred to produce widespread migmatite development in the more aluminous rocks. The schists were intruded by various plutonic rocks, mainly granites with ductile fabrics which parallel those of the older gneisses. It is clear that the granites were intruded at a syntectonic stage during the ductile deformation and metamorphism of the country rocks. In general the main penetrative fabric in the *Zenaga Complex* is steep (sub-vertical) and trends SW–NE, but this is by no means consistent. It has long been assumed that the igneous, metamorphic and tectonic history of the *Zenaga Complex* is Palaeoproterozoic (Eburnean) in age (Charlot, 1976). The U–Pb data presented here confirm that supposition.

Rb–Sr muscovite data provide additional constraints on the lower-temperature ( $\sim 500$  °C) cooling history of the *Zenaga* rocks. A feldspar–muscovite two-point line from CBM 226 (Tamazzarra Granite pegmatite) gave a date of  $1671 \pm 117$  Ma. Muscovite from GM 242, which is very radiogenic, gave a model date of  $1718 \pm 27$  Ma, similar to those from the *Zenaga Complex*, interpreted as both igneous emplacement dates and cooling ages by different authors (e.g. Charlot, 1976; Cahen et al., 1984). Our SHRIMP data rule out the former, and are probably too young for the latter ( $\sim 300$  Ma after emplacement), so the effects of some later thermal episode is the most likely explanation.

Obviously, the *Zenaga Complex* underwent subsequent Neoproterozoic orogenesis but, as the basement acted by then as a rigid cratonic block, most of the Pan-African deformation was partitioned into the Neoproterozoic rocks, above

regional basement-cover detachments. It is thus unclear which structures in the basement (e.g. later folds and faults) are of Pan-African age. The imbricate basement slivers that are included in the AAMF were emplaced during the Pan-African. Probably also, rare thrusts in the basement (e.g. those which transport *Zenaga* basement over younger rocks, see Thomas et al., 2001), may also be Pan-African, but these could equally be the result of Hercynian or Alpine tectonics.

#### 4.2. Pan-African Anti-Atlas Orogeny

After cessation of all tectonic activity associated with the formation of the *Zenaga Complex*, a long time ensued, before an important extensional event affected the *Zenaga Complex* in the mid Neoproterozoic. This event, which heralds the major rift event at the beginning of the Pan-African cycle, evidenced by the depositional setting of the Taghdout Sub-Group is also manifested in the *Zenaga Complex* by the intrusion of dolerite sheets and dykes known as the *Ifzwane Suite*. The dykes form a prominent major swarm across the *Zenaga* plains. The age of the *Ifzwane Suite* is poorly constrained by a Rb–Sr isochron date of  $787 \pm 10$  Ma (Cahen et al., 1984).

The rift event which heralded the eventual break-up of the northern margin of the *Zenaga Complex* is manifested in the continental margin facies of the Bleida Group as syn-sedimentary faulting, along which exhalative deposits were introduced. The intensity and style of deformation and metamorphism in the Bleida Group is variable in the same way as the lithological associations, which are in turn dependant on position relative to the Craton. The Taghdout Subgroup adjacent to the Craton margin is unmetamorphosed but strongly tectonised in a brittle fashion, manifest mainly in faults and S-verging thrusts and associated folds. In the east, the entire succession is sub-vertical in attitude, but generally not folded. Further northwards, in the sinistral AAMF, the Taghdout Subgroup, along with Nqob Ophiolitic rocks are at amphibolite facies and strongly imbricated and folded, with a southerly vergence. The AAMF represents a rejuvenated, but allochthonous part of the suture zone, being a  $\sim 2$

km-wide, E–W trending zone of intense polyphase imbrication. Brabers (1988) suggested that the zone has a major strike-slip component.

In inliers further north, the Bleïda Group rocks are metamorphosed to amphibolite grade and possess a polyphase ductile foliation (e.g. Tachoukacht Schist) or, in some thrust slices, a migmatitic fabric caused by upper amphibolite facies conditions with partial anatexis (e.g. the Irimi Migmatite). In all cases, the sense of tectonic transport is north-over-south, although local changes from back-thrusting and folding are apparent. Saquaque et al. (1992) considered that the compression vectors of basin closure were NW–SE. The same tectonic episodes can be recognised in the greenschist grade Sarhro Group, the deposition of which partially overlaps, timewise with part of the Taghdout Subgroup of the Bleïda Group. This is manifested as refolded folds and cleavages as described in Section 3.4.1.

The majority of exposures of the post-Sarhro Group intrusive plutonic rocks of the Assarag Suite are essentially undeformed and post-tectonic to the Anti-Atlas orogen, although later faults abound. In some of the upfaulted blocks in the High Atlas, deeper, hybridised parts of the Askaoun batholith are exposed and a ductile fabric is locally apparent. The Askaoun granodiorite cross-cuts folds and cleavage in the Sarhro Group and has produced a ~1 km wide contact metamorphic aureole, manifest as cordierite–biotite hornfels in phyllitic turbidites of, for example, the Tizoula Formation. The Ouarzazate Group and its intrusive equivalents, along with the Tata Group has undergone (often syn-depositional) faulting and block tilting during the Pan-African orogeny.

#### 4.3. Younger events

The Anti-Atlas Orogen has undergone Hercynian (Palaeozoic) and Alpine (Cenozoic) deformation. Hercynian and/or Alpine cross-folding gave rise to the ‘Boutonières’ (windows) of which the Sirwa Window is an example, and produced spectacular disharmonic folds in the Late Neoproterozoic–Lower Cambrian dolomites of the Tata Group, above major décollements, themselves usually representing reactivated older basement

structures such as the AAMF. The Alpine deformation was responsible for the elevation of the deeper parts of the Askaoun batholith in the High Atlas mountains. Major basement structures such as the AAMF have been repeatedly reactivated through time and associated deep crustal weaknesses have been used as volcanic conduits in Precambrian to Tertiary times. The Tertiary Sirwa Volcano is situated directly on the same site as a Neoproterozoic volcanic centre (Achkoukchi Complex of the Ouarzazate Group) which is itself positioned over the site of the AAMF, the zone of preservation of tectonic fragments of ophiolite fragments and pre-Ouarzazate Group rifting.

Biotite-whole-rock mineral Rb–Sr dates for the granites of Sirwa (Mzil, Askaoun, Tilsakht intrusions-see above) are in the range 582–525 Ma, slightly younger than the corresponding emplacement (SHRIMP) ages. The dates are interpreted as cooling of the crust to below ~300 °C, and are consistent with older work (e.g. Charlot, 1976; Cahen et al., 1984), indicating that, unlike the Precambrian windows to the west, the Sirwa window was not thermally overprinted to >300 °C during the Hercynian or Alpine Orogenies.

## 5. Precambrian metallogeny of the Sirwa Window

During the Precambrian, eight main episodes of mineralising hydrothermal activity have been recognised in the Sirwa Window. To provide some insight into the Precambrian metallogenic evolution of the area, these are briefly described below in chronological order.

### 5.1. Syn-orogenic Eburnean gold veins

Auriferous gold veins are common in the Zenaga Complex, hosted in mica schists and the syn-tectonic granites. Structural and textural observations indicate that most of them formed during the main to late phases of the Eburnean Orogeny. The hydrothermal solutions were probably generated at depth by metamorphic dewatering, or emanated from the syntectonic granites. This mineralisation is comparable to the gold

deposits which are very common in the Archean to Palaeoproterozoic basement complexes elsewhere in the world.

### 5.2. Late orogenic Eburnean pegmatites

Numerous lenticular and vein-like pegmatites associated with the Tamazzarra Granite occur in all the lithologies of the Zenaga Complex (Bouladon et al., 1950). They are younger than the gold veins and tend to be undeformed, but are typically zoned exhibiting (from country rock to core): (1) tourmalinised mica schist, (2) mica-rich pegmatite, (3) graphic alkaline feldspar–quartz, (4) core of quartz. Rare element minerals reported include beryl and, rarely, triphylite and columbo-tantalite. The pegmatites were deposited at the end of the Eburnean Orogeny from pervasive residual Tamazzarra Granitic fluids, generated at depth.

### 5.3. Late Pan-African Ag–Cu–U–Co–Au mineralisation

A number of epigenetic deposits are known, probably the result of hydrothermal activity linked to granites of the Assarag Suite. The most characteristic assemblage is the Ag±Cu–U deposit of Zgounder (Petruk 1975). The deposit occurs as lenticular bodies of mineralised, pre-Askaoun Granodiorite veinlets and disseminations along a broad shear zone in greywackes of the Sarhro Group. The mineralisation process started with high-T development of skarn, followed by the introduction of the metals. Other significant mineralisation which may belong to this category are Inki (Cu–Co–Mo), which forms veins in Sarhro Group sandstone (Viland, 1988), and Tafrent (Au), consisting of disseminations in the Nqob Ophiolite.

### 5.4. Late Pan-African Mo-porphyry

In the Assarag Valley, the Imourkhsane Granite contains disseminated molybdenite in quartz veinlets and small pegmatites, forming a type of

mineralisation which appears to be unique in the region.

### 5.5. Post-orogenic, syn-Ouarzazate Group manganese

In the NE part of the Sirwa Window, a large number of syn-depositional Mn oxide-barite occurrences are hosted in volcanic rocks and red clastic sediments of the Ouarzazate Group (Jouravsky, 1963). The mineralisation, which forms small veins and some more important stratiform deposits, is of a low-T epithermal nature, with Mn and Ba having precipitated by oxidation of solutions close to the palaeosurface. The stratiform deposits are probably derived from subsurface impregnations in gravel and subaerial deposition of aprons. The hydrothermal circulations were probably associated with rift faults and not necessarily with volcanic activity. The deposits underwent mild Hercynian burial metamorphism, evidenced by the transformation of the primary Mn oxides into mosaic-textured braunite, by recrystallisation of the botryoidal textures and by the formation of piedmontite. In the northern part of the Sirwa Window a similar Mn–Ba event was repeated during the Upper Cretaceous, with the formation of the Aglagal veins and of the important stratiform deposit of Imini (Lalaloui et al. 1991). The metals were also leached from the pre-Cretaceous basement by circulation along basinal faults, without the influence of intrusions, and without metamorphic overprinting.

### 5.6. Post-orogenic, syn-Ouarzazate epithermal pyrophyllite

In the NW part of the Sirwa Window, irregular stratiform bodies of white pyrophyllite are developed in an 8 km-wide zone in association with faults (Caña et al. 1968). The pyrophyllite resulted from advanced argillic alteration of the Ouarzazate Group volcanoclastics by coeval hydrothermal solutions which reached the surface during deposition. These fluids became highly acidic by oxidation of sulphide and leached most of the original elements in the volcanic rocks, apart from Al and Si. Traces of cinnabar are associated with the

Table 5  
Summary of SHRIMP dates obtained

| Unit   | Sample  | Emplacement date<br>(Ma $\pm$ 95% confidence) | Inheritance (i) and metamorphic<br>(m) dates ( $\pm$ 95% conf.) |
|--|---------|---|---|
| <i>Syn-Ouarzazate Group granites</i>                     |         |   |   |
| Tazoult Quartz Porphyry                                  | RTM 154 | 559 $\pm$ 6                                   | 625 $\pm$ 12 (i)<br>2045 $\pm$ 10 (i)                           |
| Imourkhsane Granite                                      | GM 51   | 562 $\pm$ 5                                   |   |
| Tilsakht Granite   | GM 220  | 579 $\pm$ 7                                   | 625 $\pm$ 8 (i)<br>2060 $\pm$ 10 (i)                            |
| <i>Ouarzazate Group rhyolites</i>                        |         |   |   |
| Tikhfist Formation rhyolite                              | GK 313  | 571 $\pm$ 8                                   |   |
| Tawzzart Formation rhyolite                              | CM 7    | 577 $\pm$ 6                                   |   |
| <i>Post Sarhro Group intrusive rocks</i>                 |         |   |   |
| Askaoun Granodiorite                                     | RTM 87  | 575 $\pm$ 8                                   |   |
| Amlouggui Tonalite                                       | RJM 1   | 586 $\pm$ 8                                   |   |
| Tourcht Diorite  | GM 58   | 579 $\pm$ 7                                   |   |
| Mzil Granite   | CBM 68  | 614 $\pm$ 10                                  | 660 $\pm$ 10 (i)  |
| <i>Rhyolites associated with the Bou Salda Formation</i> |         |   |   |
| Tamriwine Rhyolite                                       | GM 191  | 605 $\pm$ 9                                   |   |
| Tadmant Rhyolite   | GM 73   | 606 $\pm$ 6                                   |   |
| <i>Island-arc related rocks</i>                          |         |   |   |
| Irii Migmatite   | GM 119  | 743 $\pm$ 14                                  | 663 $\pm$ 13 (m)  |
| <i>Zenaga Complex granites</i>                           |         |   |   |
| Azguemerzi Granodiorite                                  | RTM 247 | 2032 $\pm$ 5                                  | ~ 2170 (i)  |
| Assourg Tonalite   | RJM 48  | 2037 $\pm$ 7                                  |   |
| Tamazzarra Granite                                       | GK 230  | 2037 $\pm$ 9                                  | ~ 2170 (i)  |

pyrophyllite, along with minerals typical of advance argillic alteration such as occasional barite, alunite and zunyite.

#### 5.7. Post-orogenic, syn-to late Ouarzazate Cu ( $\pm$ Pb, Ag, Au)

A large number of occurrences and small deposits of this type are known (Viland, 1988). They consist of veins and disseminations along shear zones, typically in andesites, of chalcopyrite, bornite and chalcocite in a gangue of quartz  $\pm$  carbonate. Lead, silver and gold may occasionally occur. The metals may have been deposited by hydrothermal circulations penecontemporaneously

with the deposition of the Ouarzazate Group which were generated by syn-to-late Ouarzazate intrusions, such as the Tidzi Granite. In many cases, however, it is not possible to ascertain the precise age of deposition, which could be much younger. Reworking of Ouarzazate-age mineralisation during later orogenic events has often been proposed.

#### 5.8. Post-orogenic stratabound copper in the Tata Group

In the SW part of the Sirwa Window, minor disseminations and veins of copper occur in conglomerate, gritstone and dolomite of the Ta-

mallakout and Adoudou Formations. This type of mineralisation is well-known west and south of the Sirwa Window, where sizeable deposits are known (Viland, 1988). Copper seems to have been deposited by hydrothermal solutions rising through the pre-Tata Group basement and then spreading into the still-porous sedimentary cover synchronously with deposition.

## 6. An evolutionary model for the development of the Anti-Atlas Orogen from the Sirwa Window

The Sirwa Window is one of the best exposures of the Pan-African Anti-Atlas belt, including the northern margin of the Palaeoproterozoic West African Craton. The Anti-Atlas Orogen developed during the construction of Gondwana in the late Neoproterozoic. From our study of the lithostratigraphy, petrography, geochemistry and radiometric dating of the Sirwa Window, the geological history can be summarised in a five-stage evolutionary model (Fig. 27). The timing of events can be seen from the summary of the U–Pb SHRIMP zircon results in Table 5, and the probability histogram of Fig. 28.

### 6.1. The Palaeoproterozoic basement ( ~ 2035 Ma)

The Zenaga Complex comprises supracrustal semi-pelitic schists, gneisses and migmatites, inter-layered with psammitic and calc-silicate gneisses and muscovite-rich gneisses. The rocks are interpreted as a sequence of metasedimentary rocks which are the time-equivalents of the Birrimian rocks of West Africa. The ~2170 Ma SHRIMP dates from cores of zircons in the dated granites possibly reflect the protolith ages of the Zenaga schists. The schists and gneisses were intruded by various granitoids at  $2032 \pm 5$  to  $2037 \pm 9$  Ma. These include pre- to syntectonic megacrystic granite (augen gneiss) and Tonalite orthogneiss, metabasites and foliated syntectonic muscovite leucogranite. The dates obtained also probably quite closely date peak conditions of the Eburnean Orogeny in this part of the West African Craton.

Younger Rb–Sr dates may represent slow cooling or a younger thermal event at ~1700 Ma.

### 6.2. Stage 1—Neoproterozoic extension, rifting of West African Craton and early arc formation (possibly ~800–750 Ma)

The Neoproterozoic successions of the Sirwa Window show evidence for a rift–drift phase and subsequent arc accretion Orogen along the northern margin of the Craton. An early Neoproterozoic rift succession of quartzites, dolomites, jaspilites, shales and basalts, known as the Bleida Group was deposited in rift grabens along the northern margin of the Craton. In addition, a suite of tholeiitic dolerite dykes and sills (Ifzwane Suite) intruded the Zenaga Complex and the lower part of the Bleida Group (Fig. 27), possibly at ~800 Ma (Cahen et al., 1984). This rifting event may be related to the break-up of the Mesoproterozoic supercontinent of Rodinia at ~750 Ma (e.g. Powell et al., 1993), an age in accord with the emplacement of the Ifzwane Suite dolerites.

The rifting eventually led to break-up of the West African Craton and an oceanic basin of unknown dimensions developed between the southern remnant of the West African Craton and the northern fragment (unknown continent).

### 6.3. Stage 2—subduction, island arc growth, flysch basin development and infill ( ~ 750–700 Ma)

At some stage after, ocean basin formation, northerly subduction of oceanic crust (e.g. Hefferan et al., 1992; Saquaque et al., 1992) was initiated somewhere offshore (north) of the West African Craton, led to the development of an island arc-fore-arc basin complex (Fig. 27). In the central part of the Sirwa Window, medium to high-grade metamorphic rocks comprising tonalitic and amphibolitic gneisses with minor inter-layered garnetiferous migmatites, represent all that is exposed of the roots of the arc complex. These rocks gave a SHRIMP zircon date of  $743 \pm 14$  Ma which is the best estimate of the time of formation of the arc.

The thick, predominantly greywacke/turbidite and calc-alkaline, andesitic volcanogenic succes-

sion of the lower part of the Sarhro Group was deposited in the fore-arc basin. The Sarhro Group, which comprises two major coarsening-upward cycles which both contain important volcanoclastic deposits, records the reversal in plate movements from extension to contraction. The lower part of the Sarhro Group (which probably overlaps time-wise with part of the Bleïda Group), includes the andesitic arc volcanic rocks interlayered with the turbidite sequences, whereas the upper part contains coarse clastic, arkosic deposits derived from uplift and erosion of the arc complex during closing of the fore-arc basin. If the diamictites in the Sarhro Group can be correlated with world-wide Sturtian glacial event at  $\sim 700$  Ma, this is consistent with the age of the arc as defined in the Iriiri Migmatite.

*6.4. Stage 3—basin closure, arc-continent collision, ophiolite emplacement, precursor molasse basins and post-tectonic granitoid magmatism (660–580 Ma)*

The Sarhro and Bleïda Groups show evidence of low-grade regional metamorphism and deformation (cleavage and folding). Both were locally deformed and metamorphosed up to amphibolite grade in high strain zones such as the Nqob and Tasriwine ophiolite belts (Khzama Complex).

Continued closure of the oceanic basin to the north of the island arc complex, and of the intervening fore-arc basin, during the late Precambrian resulted in south-directed arc-continent collision, evidence of which is preserved today in the central parts of the Sirwa Window, in the AAMF and the Khzama ophiolite belt. Tectonic remnants of the ocean-floor sequences are preserved as thrust-bounded ophiolitic fragments at Khzama and Nqob (Fig. 27). The ophiolites comprise deformed amphibolite grade sequences of mafic and ultramafic rocks, in which primary structures, such as pillow basalts, are rarely preserved. The best estimate of the timing of this collision is the  $663 \pm 14$  Ma SHRIMP date from metamorphic rims on the zircons of the Iriiri migmatite.

The Iriiri migmatite (remnants of the arc) are tectonically juxtaposed to the south against a

series of retrogressed biotite–muscovite–amphibole (predominantly andesitic) schists (higher levels of the volcanic arc), in turn overthrust by slivers of oceanic crust (Tasriwine ophiolite) to the north. The southern Nqob zone is represented by an E–W trending, tectonic *mélange*, with an oblique sinistral sense of movement, in which rocks of the Bleïda and Sarhro Groups, slivers of oceanic crust (Nqob Ophiolite), island-arc remnants and various pre- and syntectonic plutonic rocks are highly deformed together in an extremely complex, 6-km wide, south-verging, amphibolite grade, allochthonous oblique sinistral thrust-nappe zone. The latest, mainly lateral movements of the AAMF probably brought the Nqob ophiolite into its present position. It is probably Pan-African movement vectors in these zones have been extensively overprinted by later Hercynian and Alpine movements.

An initial precursor phase of post-orogenic extension is represented by the volcanic and clastic sedimentary rocks of the Bou Salda Formation and associated intrusive rhyolites, along with the Mzil Granite. The Mzil Granite was intruded at 614 Ma, while the rhyolites crystallised around 605 Ma (Tadmant and Tamriwine Rhyolites) in, and adjacent to, narrow, fault-bounded proto-rifts on the site of the older suture zones of Khzama and Nqob.

Post-collision, calc-alkaline magmatism is manifested as multiple plutonic intrusions (mainly granitoids) forming vast batholithic bodies in excess of 500 km<sup>2</sup>. These granitoids are typically High-K calc-alkaline I-types, with coeval gabbro–diorite–granodiorite–granite complexes showing complex magma-mixing and hybridisation phenomena. The age of this magmatism is given by dates at around 586–575 Ma obtained on members of the Assarag Suite.

*6.5. Stage 4—post-orogenic collapse, extension and molasse basin formation/infill (580–550 Ma)*

Soon after collision and suturing, extensive post-orogenic uplift and subsequent collapse led to the extensional regime which resulted in the formation of faulted molasse basins into which the thick volcanic-clastic sedimentary succession of

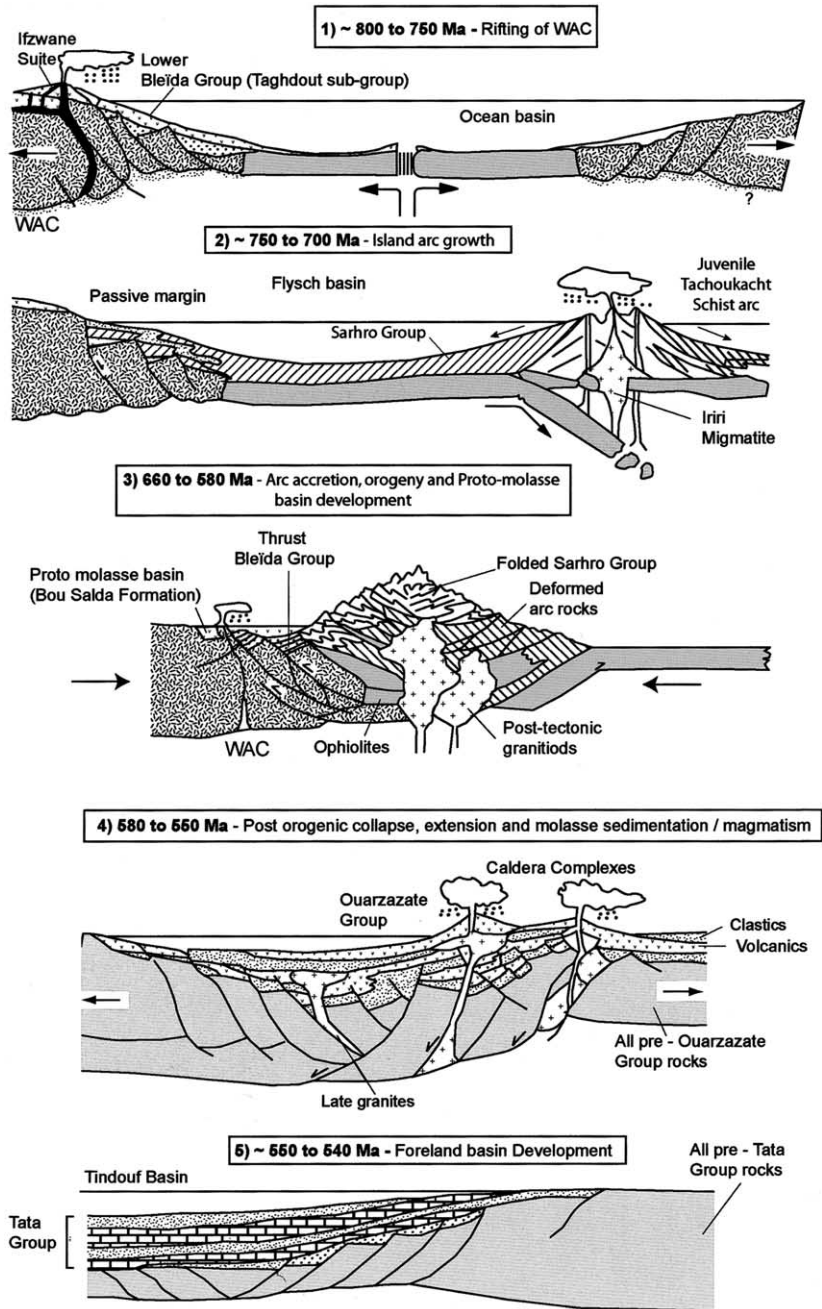


Fig. 27. Sketch 5-stage evolutionary model for the Anti-Atlas Orogen. (1) ~ 800–750 Ma: rifting and break-up of the West African Craton (WAC) and northward drift of North Moroccan Craton (NMC). Intrusion of Ifzwane Suite, deposition/extrusion of lower Bleida Group; (2) 750–700 Ma: subduction, growth of island-arc (Tachoukacht Schists), Iriri Migmatite emplacement (743 Ma), deposition of lower Sarhro Group (flysch phase) in fore-arc flysch basin; (3) 660–580 Ma: reversal of plate movement vector (deposition of upper clastic part of Sarhro Group), fore-arc basin closure, arc-continent collision (arc-accretion), ophiolite obduction, deformation and metamorphism, early post-tectonic magmatism (Assarag Suite), proto-molasse basins in foreland (Bou Salda Formation, rhyolites); (4) 580–550 Ma: Post-tectonic molasse sedimentation and magmatism (Ouarzazate Group and coeval acid rocks); (5) 550–540 Ma and younger: Marine foreland basin development (Tata Group and up into Palaeozoic strata).

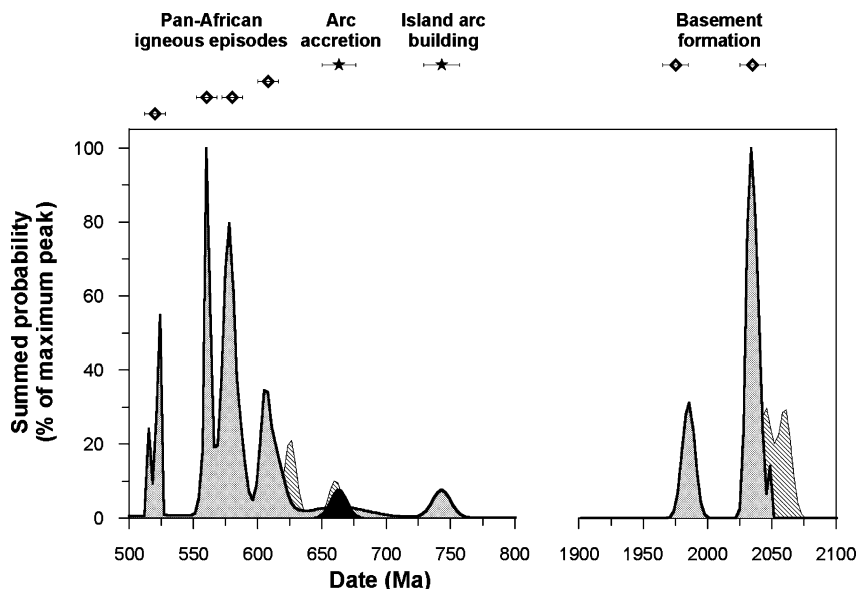


Fig. 28. Normalised probability diagram for zircon dates from the Anti-Atlas region of Morocco. Data from this paper and published literature (Ducrot and Lancelot, 1977; Ducrot, 1979; Compston et al., 1992; Landing et al., 1998; Ait Malek et al., 1998). Light stipple represents dates for igneous domains in the zircons, medium stipple = inherited domains and very dense stipple = dates from metamorphic rims.

the Ouarzazate Group was deposited unconformably on the older rocks in both the Orogen and the foreland (Fig. 27). The thick and extensive Ouarzazate Group outcrops in the Sirwa Window are the result of explosive volcanic activity and rapid clastic sedimentation from five separate volcanic centres, probably controlled by active rift faults. The importance of faulting can be gauged by noting that the various Ouarzazate Group basins are fundamentally different in character north and south of the AAMF, suggesting that this zone represents an underlying, post-collisional, crustal-scale rift zone. To the south, the Ouarzazate Group contains repeated thick, basement-derived conglomerate wedges interbedded with finer grained clastic red beds and volcanoclastic rocks, whereas to the north the succession is typified by a vast thickness of mainly acid volcanic/volcanoclastic rocks with a substantially lower proportion of clastic sedimentary rocks. Despite this difference Ouarzazate Group volcanism was coeval on either side of the AAMF, as shown by the age of the Ouarzazate volcanic rocks to the north and south.

The Ouarzazate Group, apart from rift clastics and volcanic rocks, contains numerous associated sub-volcanic granitic plutons, dyke swarms and some rhyolitic caldera complexes. Four of these have been dated, showing a range of dates from  $579 \pm 7$  Ma (Tilsakht and Tidzi Granites), to 560 Ma (Bou Tazoult Quartz Porphyry; Imourkhsane Granite). This span of some 20 Ma shows the long-lived nature of the major post-tectonic magmatism of the Anti-Atlas Orogen.

#### 6.6. Stage 6—foreland basin development ( $\sim 550$ to Cambrian and younger)

The uppermost acid volcanic and volcano-sedimentary rocks of the Ouarzazate Group are conformably to disconformably overlain by a typical foreland basin succession, the Tata Group (Fig. 27). This succession commences locally with a coarse-grained, immature conglomerate-clastic unit which is overlain by two marine carbonate cycles interbedded with red shales. Stable isotope studies have indicated that the base of the Cam-

brian Era ( $\sim 544$  Ma) lies within the lower part of the sequence (Margaritz et al., 1991). Extensional deposition continued through the Cambrian and Ordovician into the Silurian as the proto-Atlantic Ocean was established.

## Acknowledgements

The authors would like to thank all their colleagues and friends in Morocco who made the fieldwork so pleasant and productive. In particular, we thank Hassan Rehioui of Tecmaris and our field assistants, Abdullah, Samir, Brahim, Hassan, Mustapha, Youssef, Ali, Said and Lahcen. Messrs M. Dahmani, M. Labriki, C. Rjimati, Ms Zamourri, Dr M. Boutaleb (of DG-MEM), Dr Abdallah Moutaqqi, and Professor El Boukkari are thanked for valuable discussions during the two field workshops that were held in the Sirwa Window. Elijah Nkosi is thanked for performing mineral separations and Belinda Oosthuizen for drafting the maps. The paper was greatly improved by the comments of the referees, Jean-Paul Liégeois and Kevin Hefferan and their input is gratefully acknowledged.

## References

- Aït Malek, H., Gasquet, D., Bertrand, J.M., Leterrier, J., 1998. Géochronologie U–Pb sur zircon de granitoides éburnéens et panafricains dans les boutonnières protérozoïques d'Igherm, du Kerdous et du Bas Drâa (Anti-Atlas occidental, Maroc). *C.R. Acad. Sci. Paris* 327, 819–826.
- Azizi Samir, M.R., Ferrandini, J., Tane, J.L., 1990. Tectonique et volcanisme tardi-Pan Africains (580–560 Ma) dans l'Anti-Atlas Central (Maroc): interprétation géodynamique à l'échelle du NW de l'Afrique. *J. Afr. Earth Sci.* 10, 549–563.
- Bajja, A., Greiling, R.O., Rocci, G., 1998. Pan-African andesites and dacites in the eastern Anti-Atlas: syn-subduction or post-collisional? *Z. Dt. Geol. Ges.* 149, 1–12.
- Bassias, Y., Wallbrecher, E., Willgallia, A., 1988. Tectonothermal evolution of the late Panafrican Orogeny in the central Anti-Atlas; southern Morocco. In: *The Atlas system of Morocco, studies on its geodynamic evolution. Lecture Notes Earth Sci.* 15, 43–60.
- Ben Chra, M., 1997. Etude du volcanisme du Néo-Protérozoïque terminal de la boutonnière d'Aguerzoula-Bachkoune, Anti-Atlas central (Maroc). Lithostratigraphie, pétrographie, géochimie et géodynamiques. These Ph.D. 3 Cycle, Univ. Cadi Ayyad, Marrakech, 231.
- Bouladon, J., Journavsky, G., Morin, P., 1950. Etude préliminaire des pegmatites à muscovite, béryl et tantalite de la région de Tazenakht. *Notes et Mém. Serv. Géol. Maroc* 3, 207–235.
- Bouma, A.H., 1962. *Sedimentology of Some Flysch Deposits*. Elsevier, Amsterdam, p. 168.
- Brabers, P.M., 1988. A plate tectonic model for the Pan-African Orogeny in the Anti-Atlas, Morocco. In: Jacobshagen, V.H. (Ed.), *The Atlas System of Morocco Lecture Notes in the Earth Sciences*, vol. 15. Springer, Berlin, pp. 61–80.
- Cahen, L., Snelling, N.J., Delhal, J., Vail, J.R., 1984. *The Geochronology and Evolution of Africa*. Clarendon Press, Oxford, p. 512.
- Caïa, J., Dietrich, J.-E., Mazéas, J.-P., 1968. Etude de gîtes et occurrences de roches à pyrophyllite du Maroc. *Notes Serv. Géol. Maroc* 28 (211), 37–81.
- Chabane, A., 1991. Les roches vertes du Proterozoïque supérieur de Khzama (Siroua, Anti-Atlas central, Maroc), un exemple Précambrien d'ophiolite d'avant arc formée en contexte transformante. Ph.D. Thesis, Univ. Cadi Ayyad, Marrakech.
- Charlot, R., 1976. The Precambrian of the Anti-Atlas (Morocco); a geochronological synthesis. *Precambrian Res.* 3, 273–299.
- Chevallier, L.P., Gresse, P.G., Macey, P.H., Thomas, R.J., Martini, J.E.J., Harmer, R.E., Armstrong, R.A., Eglinton, B.M., 2001. Notice Explicative de la Carte Géologique du Maroc au 1/50 000 feuille Douar Cour. *Notes et Mémoires Serv. Geol. Maroc* 421, 178.
- Choubert, G., 1963. Histoire géologique du Précambrien de l'Anti-Atlas. *Notes Mém. Serv. Géol. Maroc* 162, 352.
- Claoue-Long, J.C., Compston, W., Roberts, J., Fanning, C.M., 1995. Two carboniferous ages: a comparison of SHRIMP zircon dating with conventional zircon ages and  $40\text{Ar}/39\text{Ar}$  analysis, 3–21. In: *Geochronology time scales and global stratigraphic correlation*, SEPM Special publication, 54, SEPM.
- Clauer, N., 1976. Géochimie isotopique du strontium des milieux sédimentaires. Application à la géochronologie du Craton ouest africain. Thèse Univ. Strasbourg, France, 227.
- Compston, W., Williams, I.S., Kirschvink, J.L., Zhang, Z., Ma, G., 1992. Zircon U–Pb ages for the early Cambrian time-scale. *J. Geol. Soc. Lond.* 149, 171–184.
- Compston, W., Williams, I.S., Meyer, C., 1984. U–Pb geochronology of zircons from lunar breccia 73217 using a sensitive high mass-resolution ion microprobe. *J. Geophys. Res.* 89, B525–534.
- De Beer, C.H., Chevallier, L.P., De Kock, G.S., Gresse, P.G., Thomas, R.J., 2000. Notice Explicative de la Carte Géologique du Maroc au 1/50 000 feuille Sirwa. *Notes et Mémoires Serv. Geol. Maroc* 395, 86.
- De Kock, G.S., De Beer, C.H., Chevallier, L.P., Gresse, P.G., Thomas, R.J., 2000. Notice Explicative de la Carte Géologique du Maroc au 1/50 000 feuille Taghdout. *Notes et Mémoires Serv. Geol. Maroc* 396, 142.

- Ducrot, J., 1979. Datation a 615 Ma de la granodiorite de Bleida et consequences sur la chronologie des phases tectoniques, metamorphiques et magmatiques pan-africaines dans l'Anti-Atlas marocain. *Bull. Soc. Geol. France* 21, 495–499.
- Ducrot, J., Lancelot, J.R., 1977. Probleme de la limite Precambrien-Cambrien; etude radiochronologique par la methode U–Pb sur zircons du volcan du Jbel Boho (Anti-Atlas marocain). *Can. J. Earth Sci.* 14, 2771–2777.
- Eglington, B.M., Harmer, R.E., 1999. *GEODATE* for Windows version 1: Isotope regression and modeling software. Council for Geoscience Open File Report, 1999-0206-O, 51.
- El Boukhari, A., Chabane, A., Rocci, G., Tane, J.-L., 1991. Le volcanisme de la région de N'Kob (SE du Siroua, Anti-Atlas Marocain) témoin de l'existence d'un rift au Protérozoïque supérieur, à la marge NE du Craton ouest africain. *C.R. Acad. Sci. Paris* 312 (Série II), 735–738.
- Ennih, N., Liégeois, J.P., 2001. The Moroccan Anti-Atlas: the West African Craton passive margin with limited Pan-African activity. Implications for the northern limit of the Craton. *Precambrian Res.* 112, 291–304.
- Fekkek, A., Boualoul, M., Badra, L., Amenzou, M., Saquaque, A., El Imrani, I.E., 1999. Origine et contexte géotectonique des dépôts détritiques du Groupe néoproterozoïque inférieur de Kelaat Mgouna (Anti-Atlas oriental, Maroc). *J. Afr. Earth Sci.* 30, 295–311.
- Geyer, G., Landing, E., 1995. Morocco '95, the Lower-Middle Cambrian standard of Western Gondwana (Special Issue 2). *Berineria, Würzburg*, p. 268.
- Gresse, P.G., Thomas, R.J., De Beer, C.H., De Kock, G.S., 1998. The development of the Anti-Atlas Orogen, Morocco: parallels with the Pan-African belts of southern Africa and South America. *J. Afr. Earth Sci.* 27, 92–93.
- Gresse, P.G., De Beer, C.H., Chevallier, L.P., De Kock, G.S., Thomas, R.J., 2000. Notice Explicative de la Carte Géologique du Maroc au 1/500 000 feuille Tachoukacht. *Notes et Mémoires Serv. Geol. Maroc* 393, 106.
- Harmer, R.E., Lee, C.A., Eglington, B.M., 1998. A deep mantle source for carbonatite magmatism: evidence from the nephelinites and carbonatites of the Buhera district, SE Zimbabwe. *Earth Planetary Sci. Lett.* 158, 131–142.
- Hefferan, K.P., Karson, J.A., Saquaque, A., 1992. Proterozoic collisional basins in a Pan-African suture zone, Anti-Atlas mountains, Morocco. *Precambrian Res.* 54, 295–319.
- Hefferan, K.P., Admou, H., Karson, J.A., Saquaque, A., 2000. Anti-Atlas (Morocco) role in Neoproterozoic Western Gondwana reconstruction. *Precambrian Res.* 103, 89–96.
- Hoffmeister, H., 1988. Geologische und geochemische untersuchungen an Präkambrischen und Paläozoischen gesteinen im gebiet östlich Amassine (Anti-Atlas, Marokko). *Dipl. Freien Univ, Berlin*.
- Huch, K.M., Die Panafrikanische Khzama-geosutur im zentralen Anti-Atlas, Marokko. *Ph.D. Thesis, Freie Univ., Berlin*, 172, unpublished.
- Irvine, T.N., Barager, W.R.A., 1971. A guide to the chemical classification of the common volcanic rocks. *Can. J. Earth Sci.* 8, 523–548.
- Jouider, A., 1997. Etude des Granitoides du Proterozoïque Supérieur du Massif D'Ida-ou-Iloum (Siroua, S.W., Anti-Atlas Central, Maroc): Petrographie, Geochimie, typologie des zircons et sites geodynamiques. *Diploma Thesis, 3 Cycle, University Cadi Ayyad, Faculty of Science, Semailia, Marrakech*, 209.
- Jouravsky, G., 1963. Filons de manganèse dans les formations volcaniques du Précambrien III de l'Anti-Atlas. *Etude minéralogique. Notes Serv. Géol. Maroc* 22 (170), 81–92.
- Lalaloui, M.-D., Beauchamp, J., Sagon, J.-P., 1991. Le gisement de manganèse de l'Imini (Maroc): un dépôt sédimentaire sur la ligne de rivage. *Chron. Rech. Min.* 502, 23–36.
- Landing, E., Bowring, S.A., Davidek, K.L., Westrop, S.R., Geyer, G., Heldmaier, W., 1998. Duration of the Early Cambrian: U–Pb ages of volcanic ashes from Avalon and Gondwana. *Can. J. Earth Sci.* 35, 329–338.
- Leblanc, M., 1981. Ophiolites précambriennes et gîtes arsénisés de cobalt (Bou-Azzer, Maroc). *Notes Mém. Serv. Géol. Maroc* 280, 306.
- Le Maitre, R.W., Bateman, P., Dudek, A., Keller, J., Lameyre, J., Le Bas, M.J., Sabine, P.A., Schmid, R., Sorensen, H., Streckeisen, A., Woolley, A.R., Zanettin, B., 1989. A classification of igneous rocks and glossary of terms. In: *Recommendations of the International Union of Geological Sciences on the Systematics of Igneous Rocks*. Blackwell, p. 193.
- Ludwig, K.R., 1999. *User's Manual for Isoplot/Ex Version 2.06: a Geochronological Toolkit for Microsoft Excel*, vol. 1a (Special Publication). *Geochronology Center, Berkeley*, pp. 1–49.
- Margaritz, M., Kirschvink, J.L., Latham, A.J., Zhuravlev, A.Y., Rozanov, A.Y., 1991. Precambrian/Cambrian boundary problem: Carbon isotope correlations for Vendian and Tommotian time between Siberia and Morocco. *Geology* 19, 847–850.
- Meert, J.G., Van der Voo, R., 1994. The Neoproterozoic (1000–540 Ma) glacial intervals: no more snowball earth? *Earth Planet. Sci. Lett.* 123, 1–13.
- Michard, A., Gurriet, P., Soudant, M., Albarede, F., 1985. Nd isotopes in French Pahaerozoic shales: external vs. internal aspects of crustal evolution. *Geochem. Et Cosmochim Acta* 49, 601–610.
- Mifdal, A., Peucat, J.J., 1985. Datations U–Pb et Rb–Sr du volcanisme acide de l'Anti-Atlas marocain et du socle sous-jacent dans la region de Ouarzazate; apport au probleme de la limite Precambrien–Cambrien. *Sciences Geologiques (Bulletin)* 38, 185–200.
- Nefly, M., 1998. Le Massif cristallophyllien Précambrien de L'Ourika (Haut-Atlas de Marrakech, Maroc). *These 3 Cycle, Univ. Cadi Ayyad, Marrakech*, 166.
- Paces, J.B., Miller, J.D., 1993. Precise U–Pb ages of Duluth Complex and related mafic intrusions, northeastern Minnesota: geochronological insights to physical, petrogenetic, paleomagnetic, and tectonomagmatic processes associated with the 1.1 Ga midcontinent rift system. *J. Geophys. Res.* 98, 13997–14013.

- Pearce, J.A., Cann, J.R., 1973. Tectonic setting of basic volcanic rocks using trace element analyses. *Earth Sci. Planet Lett.* 19, 290–300.
- Pearce, J.A., Harris, N.B.W., Tindle, A.G., 1984. Trace element discrimination diagrams for the tectonic interpretation of granitic rocks. *J. Petrol* 25, 956–983.
- Pearce, J.A., 1996. Sources and settings of granitic rocks. *Episodes* 19, 120–125.
- Petruk, W., 1975. Mineralogy and geology of the Zgounder silver deposit in Morocco. *Can. Miner* 13, 43–54.
- Powell, C.McA., McElhinny, M.W., Li, Z.X., Meert, J.G., Park, J.K., 1993. Paleomagnetic constraints on timing of the Neoproterozoic breakup of Rodinia and the Cambrian formation of Gondwana. *Geology* 21, 889–892.
- Proust, F., 1973. Etude stratigraphique, pétrographique et structurale du Bloc Oriental du Massif ancien du haut Atlas (Maroc). *Notes et Mém. Serv. Géol. Maroc* 34 (254), 15–53.
- Regragui, M., 1997. L'étude lithostratigraphique et pétrographique des formations précambriennes du secteur d'Askaou (Siroua ouest Anti-Atlas central). *Mem. C.E.A., Univ. Cadi Ayyad, Marrakech*, 81.
- Saquaque, A., Beharree, M., Abia, H., Nrini, Z., Reuber, I., Karson, J.A., 1992. Evidence for a Pan-African volcanic arc and wrench fault tectonics in the Jbel Saghro, Anti-Atlas, Morocco. *Geol. Rundsch.* 81, 1–13.
- Schermerhorn, L.J.G., Wallbrecher, E., Huch, K.M., 1986. Der subduktionskomplex, granitplutonismus und schertektonik im grundgebirge des Sirwa-Doms (Anti-Atlas, Marokko). *Berlin Geowiss. Abh.* 66, 301–332.
- Serv. Geol. Maroc., 1990. Carte Géologique de la Taliwine. *Notes and Mem. Serv. Geol. Maroc.*, 352.
- Steiger, R.H., Jäger, E., 1977. Subcommission on geochronology: convention on the use of decay constants in geo- and cosmochronology. *Earth Planet Sci. Lett.* 36, 359–362.
- Tera, F., Wasserburg, G.J., 1972. U–Th–Pb systematics in three Apollo 14 basalts and the problem of initial Pb in lunar rocks. *Earth Planet Sci. Lett.* 14, 281–304.
- Thomas, R.J., De Beer, C.H., Chevallier, L.P., De Kock, G.S., Gresse, P.G., 2000a. Notice Explicative de la Carte Géologique du Maroc au 1/50 000 feuille Assarag. *Notes et Mémoires Serv. Geol. Maroc* 392, 84.
- Thomas, R.J., De Beer, C.H., Chevallier, L.P., De Kock, G.S., Gresse, P.G., 2000b. Notice Explicative de la Carte Géologique du Maroc au 1/50 000 feuille Tamallakout. *Notes et Mémoires Serv. Geol. Maroc* 394, 90.
- Thomas, R.J., de Beer, C.H., Ingram, B., Martini, J.E.J., Harmer, R.E., Armstrong, R.A., Eglington, B.M., 2001. Notice Explicative de la Carte Géologique du Maroc au 1/50 000 feuille Aqdif. *Notes et Mémoires Serv. Geol. Maroc* 420, 143.
- Viland, J.-C., 1988. Le cuivre et les métaux associés de l'Anti-Atlas marocain. *Notes Serv. Géol. Maroc* 44 (334), 127–213.
- Villeneuve, M., Corneé, J.-J., 1991. Evolution paléogéographique de la marge nord-ouest de l'Afrique du Cambrien à la fin du Carbonifère (du Maroc au Libéria). *Can. J. Earth Sci.* 28, 1121–1130.
- Vogel, D.E., Missotten, R., Desutter, F., 1980. Carte Géologique du Maroc au 1/100 000 Feuille Ouikaïmeden-Toubkal. Notice Explicative. *Katholieke Univ, Leuven*, p. 121.
- Wallbrecher, E., 1988. The Anti-Atlas system; an overview. In: *The Atlas system of Morocco; studies on its geodynamic evolution. Lecture Notes Earth Sci.* 15, 13–17.
- Weaver, S.D., Johnson, R.W., (Eds.), 1987. Tectonic controls on magma chemistry. *Journal of Volcanology and Geothermal Research* 32, 285.
- Williams, I.S., Claesson, S., 1987. Isotopic evidence for the Precambrian provenance and Caledonian metamorphism of high grade paragneisses from the Seve Nappes, Scandinavian Caledonides. II. Ion microprobe zircon U–Th–Pb. *Contrib. Mineral Petrol* 97, 205–217.
- Zahour, G., 1990. Etude du volcanisme Précambrien terminal de la région d'Ait-Maghlif-Siroua nord-est. Anti-Atlas central, Maroc-Lithostratigraphie-pétrographie-géochimie. *These 3 Cycle, Univ. Cadi Ayyad, Marrakech*, 236.
- Zemouri, A., Rjimati, E., 1995. Carte géologique de la Boutonnière de Zgounder. *Serv. Geol. Maroc*.